GLT-1 DYSFUNCTION AS AN UNDERLYING CAUSE OF CEREBRAL PALSY

A Dissertation
Submitted to
the Temple University Graduate Board

In Partial Fulfillment
of the Requirements for the Degree
DOCTOR OF PHILOSOPHY

---

by
Danielle N. Feather
December 2016

Examining Committee Members:

Dr. Tanya Ferguson, PhD, Advisory Chair, Shriners Hospital Pediatric Research Center
Dr. Brad Rothberg, PhD, Co-Advisor, Department of Biochemistry
Dr. Dianne Soprano, PhD, Department of Biochemistry
Dr. Kathleen Giangiacomo, PhD, Department of Biochemistry
Dr. Benjamin Blass, PhD, External Member, Moulder Center for Drug Discovery Research

ABSTRACT

Cerebral Palsy (CP) is an umbrella term that describes abnormal motor movements that is caused by damage in the brain and, depending on the region(s) of the brain affected, can cause additional deficits. Roughly 30-50% of children with CP also have co-morbid cognitive impairments. The underlying insults that cause brain damage in CP are not fully understood. Research has shown that neonatal hypoxia-ischemia combined with intrauterine infection are the most common underlying causes of white matter damage (periventricular leukomalacia) and CP. Most research to date has focused on the role of oligodendrocytes due to the correlation of PVL (oligodendrocyte loss) and the development of CP. However, although oligodendrocyte loss is the prevalent brain damage noted in CP, this research has not lead to a cure; therefore, our focus has shifted toward a different cell type: astrocytes. Astrocytes maintain glutamate homeostasis through the sodium-dependent glutamate transporters, primarily GLT-1, protecting the neurons in the brain from excitotoxic injury.

Our hypothesis is that underlying cellular changes, beginning with loss of astrocytes and their glutamate uptake functions through GLT-1, sets the stage for the development of CP, including: periventricular leukomalacia, neuronal cell death, and motor and cognitive deficits. To test our hypothesis, we use a neonatal mouse model of CP that combines hypoxia, ischemia, and inflammation to induce PVL and neuronal death.

Using a battery of neonatal motor tests 48 hours after injury, mice with CP show significant motor deficits compared to shams. Additionally, adult mice with CP display motor deficits, indicating that this model has long lasting motor deficits and is an

appropriate model to study CP. Interestingly, adult mice also display cognitive deficits, the most common co-morbid condition associated with CP

Our preliminary data suggest a 6-8%, decrease in astrocytes in the ipsilateral hippocampus as early as six hours after injury and persists up to 24 hours. Similarly, there is a decrease in GLT-1 function 24 hours after injury. Interestingly, GLT-1 protein expression is not decreased in CP mice until 72 hours following injury, indicating that increased GLT-1 protein is not an early contributing factor in the observed functional changes. Neuronal cell damage is apparent 12 hours after injury and peaking at 18 hours; however, apoptosis begins 24 hours after injury, indicating that signs of neuron injury are delayed. To determine white matter injury, we examined two different white matter tracts: the corpus callosum and the pyramids in the brainstem. In both of these major white matter structures, examined in adulthood, volume is decreased.

Beta-lactam compounds are known to increase GLT-1 expression and function and are neuroprotective in injury models. Furthermore, they may offer a therapeutic treatment for CP. We show that MC-100093 (093), an experimental beta-lactam developed by our colleagues, and clavulanic acid (CA), a FDA-approved beta-lactam, can increase GLT-1 transporter activity and protein expression in our CP model, reduce early neuron damage and death, and improve the brainstem pyramid volume loss seen in the adult after injury. In addition to improved cellular outcomes, drug treatment improved behavioral deficits. Neonatal CP mice have improved motor abilities and adult CP mice have improved motor and cognitive skills. These results show that the loss of astrocytes and glutamate uptake through GLT-1 play a role in CP pathophysiology and that beta-lactams may offer a viable treatment option following CP insults.

In dedication to my parents and my husband,

for their love and support

as well as putting up with late nights, early mornings, and odd hours.

ACKNOWLEDGMENTS

I'd like to give an immense and special thank you to my mentor, advocate, and friend, Dr. Tanya Ferguson, for giving me an opportunity to mature as a scientist and a person; science wasn't always productive, but it was almost always fun. Amy He and Katherine Spence were integral members of the laboratory; without whom I would not have learned some of my greatest life lessons. Dr. Dale Haines deserves a special thank you. His patience and guidance on my ORP was invaluable and, with his dedication, I was able to elevate to PhD candidacy, thank you so much. Dr. Servio Ramirez and his lab continually supported this project and I thank them greatly. My gratitude also goes to Drs. Benjamin Blass, Wayne Childers, and Magid Abou-Bharbia for providing the therapeutics to make this project possible. They also provided insight into for the project and cheered the work along as the data progressed. My committee deserves a sincere and special thank you as well for dedicating time to attend my committee meetings, making me think beyond my data, offering guidance about my project and suggestions for next steps, and answering questions that went beyond my thesis project. I'd also like to thank Tracy Burton, Tuyet Sithiphavong, and Rosa Lordes Muniz for their administrative support throughout this whole process. Last, but not least, I'd like to extend my gratitude to Nikki McCormack, Tahiyana Khan, and Marzia Niazi, our undergraduate researchers, and Sophia Weng, our high school intern. I wasn't always the best at training, but you persevered. I hope you all got as much out of our work together as I did. Your dedication and excitement for science was both refreshing and contagious. I'm deeply grateful for the support from students, both graduate and undergraduate, faculty, and technicians that have helped support me in some way.

I'd also like to give a very big heartfelt thank you to my parents and my husband. Without whom, none of this would have been possible. Mom and dad, you have continually supported me though all of my ambitions, no matter how big, small, or silly. My Ph.D. is truly the culmination of all of your hard work as well. Rob, my husband, thank you so much for all that you do and all of the support you've provided over these last five years. I couldn't have done it without you. To my friends and family who cheered me on and asked questions, you all kept me going. Thank you all from the bottom of my heart!

TABLE OF CONTENTS

Page

LIST OF TABLES

Table Page

LIST OF FIGURES

LIST OF ABBREVIATIONS

°C: degrees Celsius

°: degree

µg: microgram

µg/mL: microgram per milliliter

µL: microliter

µm: micrometers

µM: micromolar

093: MC-100093

[^{3}H]-glutamate: tritiated glutamate

ABC: avidin-biotin complex

AMPA: α-amino-3-hydroxy-5-methyl-4-isoxazolepropionic acid

ANOVA: analysis of variance

AP4: activating enhancer binding protein 4

ATP: adenosine triphosphate

BCA: bicinchoninic acid

CA: clavulanic acid

Ca^{2+}: calcium ion

CA1: cornu amonis 1

CA3: cornu amonis 3

cAMP: cyclic adenosine monophosphate

CBF: cerebral blood flow

cm: centimeters

CNS: central nervous system

contra: contralateral

CP: cerebral palsy

CREB: cAMP response element-binging protein

DAB: 3,3’-diaminobenzidine

DAPI: 4’,6’-diamidino-2-phenylindole

DHHC: aspartic acid-histidine-histidine-cysteine

DHK: dihydrokainate

DNA: deoxyribonucleic acid

DPM: disintegrations per minute

DPX: distyrene, plasticizer, and xylene

dUTP: deoxyuridine triphosphate

E2F: E2 factor

EAAC1: excitatory amino acid carrier 1 in mice

EAAT: excitatory amino acid transporter

EAAT1: glutamate aspartate transporter in humans

EAAT2: glutamate transporter-1 in mice

EAAT3: excitatory amino acid carrier 1 in humans

EGR: early growth response

FDA: Food and Drug Administration

FJC: fluoro-jade C

g: gram

GCPII: glutamate carboxypeptidase II

GFAP: glial fibrillary acidic protein

GLAST: glutamate aspartate transporter in mice

GLT-1: glutamate transporter-1 in mice

Glt_{ph}: prokaryotic orthologue of glutamate transporter-1

GluR2: glutamate receptor subunit 2

HI: hypoxia-ischemia

HIE: hypoxic-ischemic encephalopathy

HIL: hypoxia-ischemia-lipopolysaccharide

HLS: hind limb suspension

HP: hairpin loop

hr: hour

IACUC: Institutional Animal Care and Use Committee

ipsi: ipsilateral

IκBα: nuclear factor of kappa light polypeptide gene enhancer in B-cells inhibitor, alpha

IUI: intrauterine infection

kDa: kilodaltons

Km: affinity

LPS: lipopolysaccharide

M: molar

mg/kg: milligram per kilogram

mL: milliliter

mM: millimolar

mmol: millimole

mol: mole

MRI: magnetic resonance imaging

mRNA: messenger RNA

n: number of animals

NAA: N-acetyl-aspartate

NAAG: N-acetyl-aspartyl-glutamate

NAALADase: N-acetylated alpha-linked acidic dipeptidase

Na,K-ATPase: sodium/potassium pump or sodium potassium ATPase

NF-κB: nuclear factor kappa-light-chain-enhancer of activated B cells

NIH: National Institutes of Health

NMDA: N-methyl-D-aspartate

N-myc: basic helix-loop-helix protein 37 or N-myc proto-oncogene

NOR: novel object recognition

NP-40: nonyl phenoxypolyethoxylethanol

PBS: phosphate buffered saline

pmol/mg*minute: picomole per milligram per minute

PKC: protein kinase C

PND: post-natal day

pre-OL: pre-myelinating oligodendrocyte

PVL: periventricular leukomalacia

ROS: reactive oxygen species

rpm: rotations per minute

S: sham

SDS: sodium dodecyl sulfate

SDS-PAGE: sodium dodecyl sulfate polyacrylamide gel electrophoresis

SEM: standard error of the mean

Sp1: specificity protein 1

TBOA: DL-*threo*-β-benzyloxyaspartate

TdT: terminal deoxynucleotidyl transferase

TUNEL: TdT dUTP nick end labeling

ULAR: University Laboratory Animal Resources

wk: week

CHAPTER 1

INTRODUCTION

History of Cerebral Palsy

Cerebral palsy (CP) was first described in the 1860s by Dr. William Little. Dr. Little correlated complicated births and deliveries as well as asphyxia with motor disorders including spasticity and rigidity (1). However, in 1893, Dr. Sigmund Freud believed that prenatal factors (not peri- or postnatal complications as hypothesized by Dr. Little) contributed to the development of CP. Dr. Freud hypothesized that a difficult birth is caused by a disruption to brain development in the womb (2). It would be over 100 years before Dr. Freud's hypothesis would be widely accepted in the medical field. In 1993, a US-population based study found that congenital CP was more prevalent than acquired CP in children (3). In addition, two separate population based studies found that the incidence of CP increased with decreasing gestational age (4,5), suggesting that CP most often occurs during gestational development. Therefore, it is now believed that the majority of CP cases occur in utero.

Cerebral Palsy Symptoms and Co-Morbid Conditions

Individuals with CP exhibit a wide variety of abnormal movements causing difficulty with fine and gross motor skills, such as hand preference and grasping, buttoning a shirt, or writing, and problems coordinating limb movement. In addition to motor disabilities, at least 40% of children with CP have some form of cognitive impairment that ranges from mild to severe (3,6,7). In fact, cognitive impairment is the most common co-

morbid deficit associated with CP. Many patients with CP also experience associated psychological disorders, which range from social interaction impairments to anxiety and depression (7–9).

Neuropathological Hallmarks of Cerebral Palsy

There are two major neuropathological hallmarks of CP: cerebral dysgenesis (CD) and periventricular leukomalacia (PVL). A systematic review of the literature notes that only 10% of CP patients have CD, as detected with magnetic resonance imaging (MRI) (10). However, white matter damage or PVL is the most common pathological finding in children with CP (10).

Clinically and epidemiologically, PVL is the most recognizable hallmark of CP (10). PVL typically occurs during the third trimester, when white matter is especially vulnerable to insults (11). One study found that PVL, detected by cerebral ultrasound, most commonly occurs in premature infants between 27-30 weeks of gestation (12). Three physiologic features of the immature brain make it vulnerable to insults causing white matter injury and PVL (13,14). First, the vascular supply to cerebral white matter is not well developed (15,16). This causes the cerebral blood flow (CBF) in white matter regions of the preterm infant to be around 5mL/100g/minute (17), which is far below the adult threshold of white matter viability of 15mL/100g/minute (18). Low CBF in the preterm brain is due to undeveloped anastomoses between the short and long vessels penetrating the periventricular white matter, which increase in the third trimester and post-term. Although the white matter in the preterm infant can survive low levels of blood flow, any perinatal insults leading to cerebral hypoperfusion, such as ischemia, causes white matter

distal from blood vessels to be highly vulnerable. Second, the immature infant has impaired cerebral blood flow regulation in response to changes in blood pressure (19,20). Part of this limited autoregulation is due to the absence of muscle in cerebral arterioles (21), which allows for arteriolar dilation and constriction. Thus, the normal range of arteriole pressure in preterm infants is narrow and decreases in systemic blood pressure are not well regulated. Third, the maturation state of immature oligodendrocytes appears to play a role in the development of PVL (22). In the third trimester, immature pre-myelinating oligodendrocytes (pre-OLs) are the predominant white matter cell type developing in the human brain while mature, myelinating oligodendrocyte numbers are still low (22). Pre-OLs are highly vulnerable to free radical attack as well receptor- and nonreceptor-mediated glutamate excitotoxicity (as reviewed in (13)), which is not seen in mature oligodendrocytes. Thus, the physiology of the white matter regions of the brain leave oligodendrocytes vulnerable to CP pathogenesis and PVL development; however, years of oligodendrocyte and white matter research has not reduced the incidence of CP.

Causes of Periventricular Leukomalacia and Cerebral Palsy

Hypoxia-ischemia

Hypoxia-ischemia (HI) can be caused by maternal or neonatal risk factors, including birth asphyxia, fetal or neonatal strokes, or maternal infection (23,24). However, early clinical studies (25–27) and a multi-variant analysis of the literature (28) show that birth asphyxia accounts for very few CP cases. On the other hand, it is thought that perinatal stroke, leading to HI in the developing brain, is a major cause of CP (29). A 2005 case-controlled study found that perinatal stroke (reported as a stroke that happens in utero or

up to 28 days after birth) occurs in 20 of every 100,000 births (30) and a retrospective study found that 58% of neonates with perinatal stroke were subsequently diagnosed with CP (31). By comparing the incidence of stroke in the perinatal and antenatal periods, Wu and colleagues determined that an HI event is 17 times more likely to occur during perinatal development than during childhood (32), meaning the immature, developing brain is far more vulnerable to HI than the mature brain.

After HI injury in animal models, glutamate is increased in the extracellular space (33) and persists in the damaged regions for a pro-longed period of time (34), possibly due to increased release of glutamate from presynaptic neurons or inhibited uptake of glutamate into astrocytes. High levels of extracellular glutamate can lead to overstimulation of glutamate receptors on neurons and immature oligodendrocytes, leading to excitotoxic cell death. To further implicate glutamate toxicity as a mechanism of cell loss in CP, mice were injected with ibotenate, a glutamatergic agonist, and a progressive loss of pre-oligodendrocytes and an increase in white matter lesion size was found (35). Ibotenate administration in neonatal rats induces cortical neuron loss, PVL, and increased ventricle dilation, all of which can be reduced with a glutamate receptor antagonist (36). Glutamate neurotoxicity was further implicated in the development of PVL by the administration of glutamate receptor antagonists to neonatal rats following HI insults (37–39). In these studies, the antagonists reduced gray and white matter damage. These results indicate that glutamate excitotoxicity may play a role in the development of HI induced PVL.

Infection and inflammation

Intrauterine infections (IUI) are one of the most prevalent insults during pregnancy and can lead to PVL in the infant (40). As early as 1955, Eastman and DeLeon reported a

seven-fold increase in the risk of CP when mothers presented with intrapartum fever (41). Intrauterine exposure to placental inflammation or to maternal infection were significantly correlated to the development of spastic CP (42) and maternal infection before or during pregnancy increased the risk of the infant developing CP (43). IUIs associated with congenital CP include chorioamnionitis, bacterial vaginosis, and urinary tract infections, as well as group B streptococcus, and Escherichia coli (23,44). Therefore, it is clear that infection and inflammation play a role in the development of CP.

Two human studies of neonates with PVL, showed that maternal infection lead to increased pro-inflammatory cytokine levels in umbilical cord blood or amniotic fluid (45,46). In addition, a postmortem case study of 22 human brains with PVL demonstrated increased immunohistochemical staining of pro-inflammatory cytokines in neurons of the hippocampus and cortex and, in one brain with astrogliosis, increased cytokines were noted in astrocytes (47). Furthermore, animal models support the human data. Pregnant rats, exposed to LPS, had pups with increased inflammatory cytokines in whole brain homogenates, increased apoptotic oligodendrocyte death, and decreased myelination (48). Lambs from LPS injected ewes showed similar patterns of damage (49,50). It appears that the mechanism by which infection causes PVL is through an increase in pro-inflammatory cytokines, which injure the developing brain.

A Role for Astrocytes Immediately Following Cerebral Palsy Insults

With research showing the role of glutamate excitotoxicity and cytokine-induced cell death of neurons and oligodendrocytes following neonatal HI and infection, identifying the status of astrocytes and their functions early after insults are important. Astrocytes are

responsible for many supportive functions in the central nervous system (CNS) (51). Among their roles, astrocytes provide ion balance, participate in synapse function, and maintain glutamate homeostasis, which are all very important for gray and white matter health. An early loss of astrocytes may cause the neonatal brain to lose the neurotrophic, ionic, and glutamatergic regulation normally provided by these cells after injury, leaving oligodendrocytes and neurons more susceptible to CP insults (Figure 1.1).

Soon after HI brain injury in the adult, astrocytes become reactive and undergo astrogliosis, or go through an increase in the number of cells and cell body size. However, in the neonate, HI first causes significant glial fibrillary acidic protein (GFAP)-positive astrocyte loss followed by delayed astrogliosis (52). In the rat, both GFAP and vimentin-positive astrocytes were lost after HI (52). In the neonatal brain of both humans and rats, apoptosis of at least 50% of GFAP and vimentin-positive astrocytes were noted early following HI insults (53). Studies of permanent and transient models of HI demonstrate decreased GFAP-reactive astrocytes early after injury, which precedes neuronal death (54,55). In addition, reversible neuron damage is noted within the first 16-22 hours after HI injury with irreversible damage increasing from 4-46 hours after injury (56). These studies suggest that astrocyte loss precedes neuron and oligodendrocyte damage and indicate that a critical period of astrocyte demise within the first 24-48 hours, which may cause neuron and oligodendrocyte vulnerability and death.

In our neonatal mouse model of CP where HI and inflammation are combined, astrogliosis peaks 96 hours after injury and mirrors PLV (57) and hippocampal neuronal damage (58); however, early astrocyte loss was not studied. Astrocytes in the neonatal brain may decrease early after CP insults and precede PVL injury, neuron loss, and

astrogliosis (Figure 1.1). The loss of astrocytes and their functions may cause an early critical window in which the extracellular environment becomes toxic to neurons and oligodendrocytes. In addition to astrocyte loss, this critical window may indicate a treatment time frame to address the loss of astrocytic functions to prevent neuron and oligodendrocyte loss.

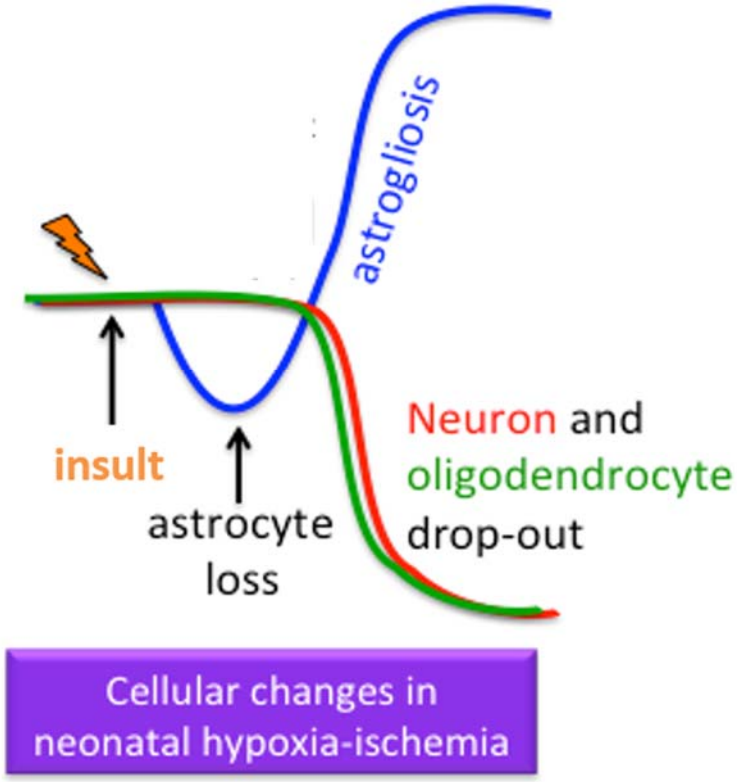

Figure 1.1. Astrocytes are lost early after neonatal insults. Astrocytes are the supportive cells in the brain. Among many roles, they provide energy support to nerve cells, maintain the extracellular ion balance, and provide glutamate removal from the synaptic cleft. When hypoxic-ischemic injury occurs in neonates, there is an early loss of astrocytes followed by delayed neuronal apoptosis and death of oligodendrocytes.

The Role of Glutamate

Glutamate is the most abundant excitatory neurotransmitter in the mammalian brain. Glutamate concentrations in the brain are approximately 5-15mmol per kg of wet weight, but most of the glutamate is intracellular (59). Extracellular concentrations of glutamate are kept around 3-4μM and, therefore, concentration gradients across the plasma membrane are several thousand-fold with the highest concentrations in nerve terminals (60). It is estimated that the concentration of glutamate at the synapse can increase to the millimolar range following synaptic release of glutamate (60). Excess glutamate release, as seen following HI or other neurological insults, can cause PVL (61), a neuropathological hallmark of CP. Excess glutamate can cause overstimulation of glutamate receptors, known as excitotoxicity, leading to increases in intracellular calcium, activation of proteases and caspases, and cell death, by apoptosis (62).

Glutamate receptors

During development, both α-amino-3-hydroxy-5-methyl-4-isoxazolepropionic acid (AMPA) and N-methyl-D-aspartate (NMDA) glutamate receptors are present on neurons and, to a lesser extent, oligodendrocytes. In the mature brain, AMPA receptors are calcium-impermeable because of a glutamate receptor subunit 2 (GluR2) that is highly expressed. However, in the immature brain, AMPA receptors are more calcium permeable due to lower GluR2 subunit expression (63). Also, calcium ion (Ca^{2+})-permeable NMDA receptor expression is at its highest in the developing brain of both rodents (post-natal day 7) (64) and humans (26 weeks to term) (65), during the time-period when CP is thought to occur in utero. Because glutamate stimulates both the AMPA and NMDA receptors, a glutamate-induced increase in intracellular Ca^{2+} occurs,

which, under pathological conditions, can contribute to cell death (61), primarily through caspase-activated cell death (66).

The glutamatergic synapse

The maintenance of extracellular glutamate concentrations is important for synaptic transmission and prevention of neurotoxicity. In addition, glutamate uptake is the only way to remove glutamate from the synapse or extracellular space to prevent exicitotoxicity. Under normal conditions, glutamate is released from the pre-synaptic neurons and stimulates the glutamate receptors located on the post-synaptic neuron and, to a lesser extent, pre-OLs. Extracellular glutamate is removed by glutamate transporters, mainly located on astrocytes (Figure 1.2a). Under HI conditions, excess glutamate is released from the pre-synaptic neuron and the high-affinity glutamate transporters, which are dependent on the sodium gradient, remove glutamate from the synapse by coupling the favorable transport of ions to the unfavorable transport of glutamate (Figure 1.2b). Thus, the glutamate transporters are coupled to the Na,K-ATPase, which requires adenosine triphosphate (ATP) to maintain the ion concentrations in and out of the cell. However, As the ATP-dependent pumps begin to fail due to the loss of glucose, the sodium gradient breaks down and the transporters stop working, leaving even more glutamate in the synaptic cleft. The excess glutamate causes overstimulation of the post-synaptic glutamate receptors on neurons and pre-OLs, leading to cell death.

Once in the astrocyte, glutamate is converted to glutamine via the glutamate-glutamine cycle by glutamine synthetase (60,67,68). Glutamine is not a neurotransmitter, therefore, it does not activate glutamate receptors and can be transported back to the pre-

synaptic neuron at high concentrations (69,70) for glutamate recycling (71). Glutamatergic neurons express glutamine transporters (72–74).

Glutamate transporters

To date, five sodium dependent glutamate transporters have been cloned in human and mouse: excitatory amino acid transporter (EAAT) 1-5. The glutamate aspartate transporter (GLAST in mice, EAAT1 in humans) and glutamate transporter 1 (GLT-1 in mice and EAAT2 in humans) are primarily found on glia cells and are the most abundant in the brain (75,76). Specifically, GLT-1 is the predominant astrocytic glutamate transporter in the mammalian forebrain, accounting for 90% of glutamate uptake (77). Since GLT-1 is the predominant glutamate transporter in the cerebrum and accounts for the majority of glutamate clearance, it will be the focus of our research. GLAST is more predominant in the cerebellum (60). Excitatory amino acid carrier 1 (EAAC1), or EAAT3 in humans, is expressed on neurons (75), primarily the post-synaptic neuron of a glutamatergic synapse, and oligodendrocytes (78). Rodent studies suggest that the glutamate clearance of EAAC1 is negligible compared to that of GLT-1 (79). EAAT4 is also a neuronal glutamate transporter, however, it is located on Purkinje cells in the cerebellum of mammals (80,81), and the concentration of EAAT4 in the forebrain is very low (80–82). EAAT5 is only found to be localized in the retina (83,84).

The exchange of glutamate from the extracellular space is catalyzed by co-transport of three sodium ions and one hydrogen ion and the anti-transport of one potassium ion (85). Therefore, glutamate uptake is driven by the ion gradient across the membrane, namely sodium and potassium (85–87). The removal of glutamate includes a positive inward current (85), or the net exchange is electrogenic (positive charge moving

in), and requires a net negative charge within the cell. Since glutamate transporters need an ionic gradient to operate, they are coupled to the sodium potassium pump, or the Na,K-ATPase (88).

The properties of the glutamate transporter subtypes vary. The reported affinities (Km) of GLAST, GLT-1, and EAAC1 are similar at, 7-20μM for GLAST, 12-18μM for GLT-1, and 8-30μM for EAAC1 (as reviewed in (60,89)). The reported Km for EAAT4 is the highest at 0.6-3.3 μM and EAAT5 is the lowest at 61-63 μM (as reviewed in (89)). Glutamate transport in GLAST, GLT-1, and EAAC1 takes approximately 60-80 milliseconds to complete a glutamate transport cycle (90–92); however, glutamate transport is much slower in EAAT4 and EAAT5 (89). It does appear that GLT-1 is more efficient in transport than GLAST as a glutamate molecule, bound to GLT-1, has a greater chance of being transported into the astrocyte than unbinding and remaining in the extracellular space (93). In terms of cellular concentration, GLAST is present on astrocytes at approximately 2300 molecules per μm^2 of plasma membrane and EAAC1 is present on neuronal dendrites at approximately 90 molecules per μm^2 of plasma membrane (89). GLT-1 is present on neuron terminals at 750 molecules per μm^2 of plasma membrane but on astrocytes at 7500 molecules per μm^2 of plasma membrane (89). Homozygote GLT1-knockout mice develop spontaneous epilepsy within the first three weeks of life and, by four weeks of age, approximately half of the mice die (77). Cell specific GLT-1 knockout mice show astrocytic GLT-1 knockout leading to epilepsy and a lethal phenotype, while neuronal-specific GLT1-knockout mice showed no phenotypic consequences (94). GLAST-deficient mice do not have as severe symptoms as GLT1-knockout mice and appear to develop normally after birth with decreased

glutamate uptake in regions where GLAST is highly expressed, such as the cerebellum (95). Mice lacking EAAC1 do not have epilepsy or neurodegeneration (96), consistent with the low expression levels of EAAC1. EAAT4 knockout mice appear normal with no lethal phenotype while EAAT5 is only expressed in the retina (89). These data indicate that astrocytic GLT-1 is responsible for neuroprotection against excitotoxicity and also show the importance of GLT-1 on astrocytes in synaptic glutamate clearance.

Astrocytes and GLT-1 as underlying causes of cerebral palsy

Following neonatal HI in both animal models of cerebral palsy as well as human post-mortem specimens, there is up to a 50% loss of astrocytes, and then delayed astrogliosis (52). Glutamate uptake would be interrupted with a loss of astrocytes since GLT-1 is mainly expressed by astrocytes and accounts for the majority of glutamate uptake. If astrocytes are lost first, decreased GLT-1 protein and transporter function would leave the developing cortex and oligodendrocytes vulnerable to excitotoxic damage and death by increased extracellular glutamate and overstimulation of AMPA and NMDA receptors. Knocking down GLT-1 protein expression causes a neurotoxic increase in glutamate concentrations (97). Last, GLT-1 knockout mice have spontaneous seizures and are at a higher risk to develop acute brain injury (77,94). Thus, following HI in neonates, early astrocyte loss, along with loss of glutamate homeostasis, ionic gradient balance, and neurotrophic support may be an underlying cause of CP and represent a potential therapeutic target.

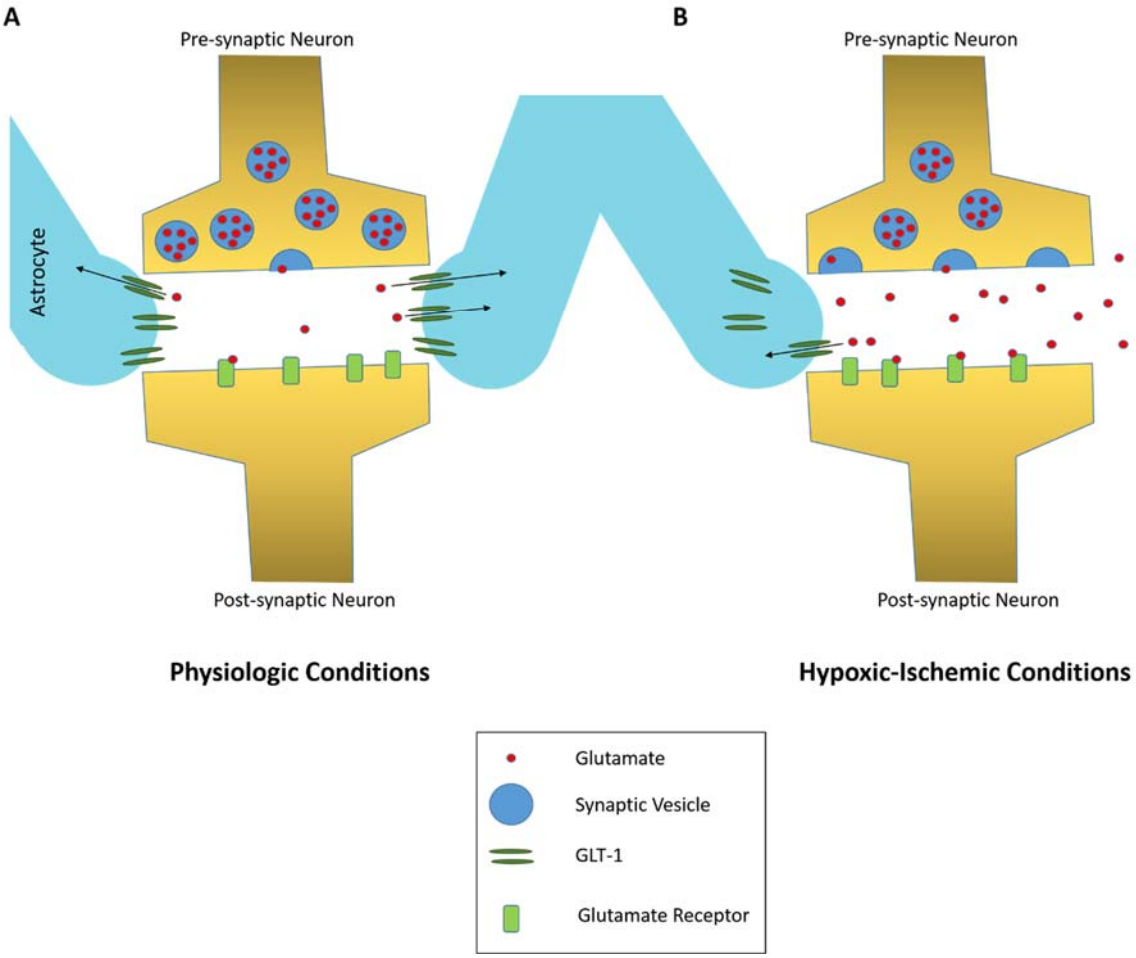

Figure 1.2. Schematic representation of a glutamatergic synapse under physiologic and hypoxic-ischemic conditions. A) Under physiologic conditions, glutamatergic synapses in the hippocampus and cortex are surrounded by astrocytes, which remove glutamate as it is released from the pre-synaptic neuron. Removal of glutamate by GLT-1 on astrocytes prevents the overstimulation of glutamate receptors on the post-synaptic neuron. B) Early after hypoxic-ischemic insults, astrocytes are lost and GLT-1 can be translocated from the remaining astrocyte cell membranes. The pre-synaptic neuron releases excess glutamate, which is not quickly removed from the synapse. Glutamate can then increase stimulation of glutamate receptors on the post-synaptic neuron. Glutamate can also escape the synapse and stimulate glutamate receptors on other neurons or on oligodendrocytes, causing excitotoxicity in surrounding regions as well.

GLT-1

GLT-1 was first cloned in 1992 from the rat brain (98). GLT-1 is highly expressed in the mammalian forebrain and plays an important role in glutamate homeostasis (as reviewed by (60)). The highest level of GLT-1 expression is noted in astrocytes, particularly in the hippocampus and the cortex (99,100). Furthermore, GLT-1 accounts for approximately 1% of the total protein in the brain (76), and contributes to around 90% of total glutamate uptake activity in the mouse forebrain ((77) and reviewed by (60,101)). In addition, GLT-1 is localized at synapses (60,102). The high concentration of GLT-1 on astrocytes in close proximity of synapses ensures that glutamate can be cleared quickly, prevent excess extracellular glutamate, and keep glutamate receptor stimulation at normal physiologic levels (Figure 1.2a).

GLT-1 structure

GLT-1 is located on human chromosome 11 between p12 and p13. It is approximately 168,859 base pairs long. GLT-1 is comprised of 11 exons with a long intron of 101,432 base pairs between exons 1 and 2 (Figure 1.3a). A 958 base pair region of the promoter is maximally activated in transcription (103,104). This promoter region contains nine putative transcription factor binding sites, including: one activating enhancer binding protein 4 (AP4), one specificity protein 1 (Sp1), one cyclic adenosine monophosphate (cAMP) response element-binging protein (CREB), one E2 factor (E2F), two early growth response (EGR), and three nuclear factor kappa-light-chain-enhancer of activated B cells (NF-κB) sites (104) (Figure 1.3b). Translation of GLT-1 mRNA results in a 574 amino acid protein with a molecular mass of approximately 62 kilodaltons (kDa).

Various isoforms of GLT-1 have been noted in the literature in mice, rats, and humans (98,105–111). Specifically, at least 3 different C- (75,108,112) and four distinct N-termini (105,110,111) are predicted using alternative exon splicing. C-terminal isoforms of GLT-1 are created by alternative exon splicing and immunohistochemistry has noted all three C-terminal isoforms in the CNS (75,108,112). At the N-terminal, differential exon use creates the various isoforms; however, CNS expression of the N-terminal isoforms has not been established (105,110,111). Thus, the combination of N- and C-termini can potentially predict that at least 12 isoforms exist; however, in mouse CNS, four major GLT-1 isoforms were found by mRNA analysis (113). GLT-1 subunits form oligomers (99,114–117), which predominantly include dimers and trimers (113,114,117). All four GLT-1 isoforms in the mouse brain can combine into homomeric and heteromeric complexes and these complexes are expressed at the surface of the astrocyte cell membranes (113). However, it does not appear that functional differences exist between the isoforms (113). GLT-1 isoform expression in astrocytes following neonatal HI injury has not been studied.

Full-length mammalian glutamate transporters have yet to be crystalized. In the 1990s, four groups tackled the topology of the mammalian glutamate transporters (118–121) and arrived at different conclusions for the overall structure. All groups agree that the first six transmembrane domains are α-helices, with a long loop between transmembrane domains three and four, and the N- and C-termini are intracellular. However, in 2004, the prokaryotic orthologue Glt_{ph} was crystalized (115) and provides an understanding of mammalian glutamate transporters. The crystal structure of Glt_{ph} predicted a trimer with each subunit having eight alpha-helical transmembrane domains

and two hairpin loops (Figure 1.4 and Figure 1.5 a, b) (115). The trimer is concave at the extracellular surface and convex at the cytoplasmic surface (Figure 1.5 c, d) and subunits interact via transmembrane domain 4 (115). The hairpins appear to be the functional units where glutamate binding between the tips of the two hairpin loops occurs and the mechanism of transport is through gating of both hairpin loops where hairpin 2 forms the extracellular gate and hairpin 1 forms the intracellular gate (115).

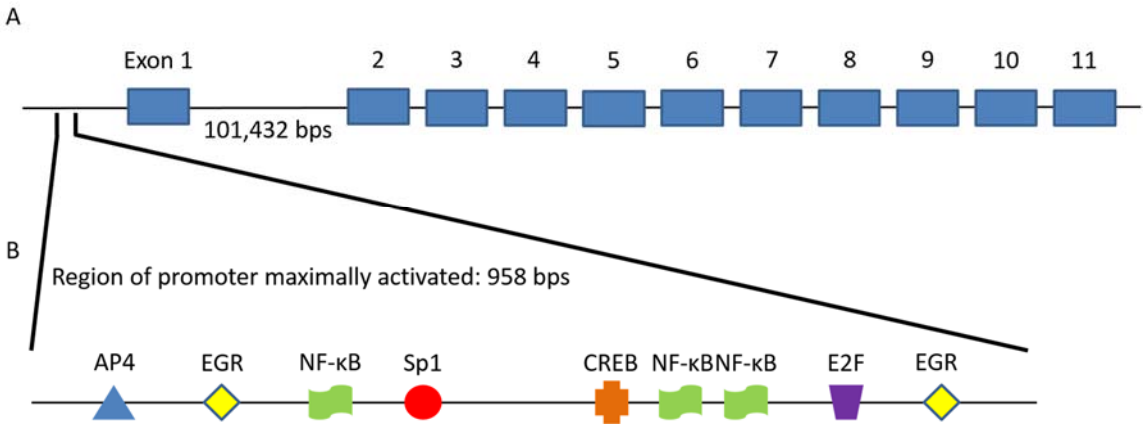

Figure 1.3. Schematic representation of the GLT-1 gene and the maximally active promoter region. A) Exons are indicated as blue boxes. 11 exons comprise the GLT-1 gene with a 101,432 base pair intron stretch between exons 1 and 2. B) A 958 base pair promoter region was found to be maximally active during GLT-1 transcription. Putative transcription factor binding regions are noted: activating enhancer binding protein 4 (AP4), early growth response protein (EGR), nuclear factor kappa-light-chain-enhancer of activated B cells (NF-κB), specificity protein 1 (SP1), cyclic adenosine monophosphate (cAMP) response element-binding protein (CREB), and E2 factor (E2F). The three NF-κB regions appear to be important as their sequences are conserved between human, rat, and mouse.

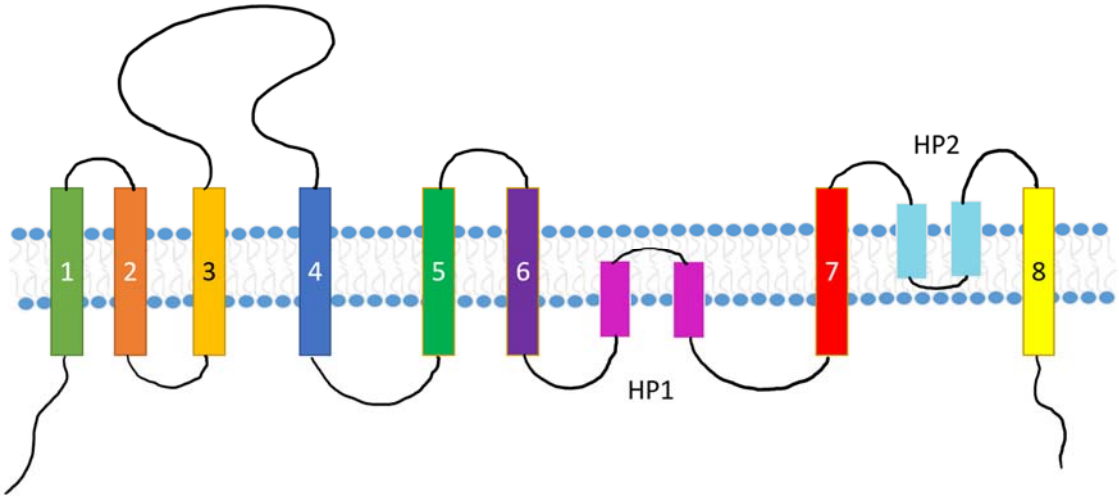

Figure 1.4. A schematic representation of mammalian GLT-1 transmembrane topology based on the crystal structure of GLT_{ph}. When crystalized, GLT_{ph} was shown to have 8 alpha helical transmembrane domains (numbered 1-8). A long protease sensitive and proline rich linker is noted between transmembrane domains 3 and 4 with two hairpin loops (HP1 and HP2) between transmembrane domains 6 and 7 and between transmembrane domains 7 and 8. The N- and C-termini are intracellular.

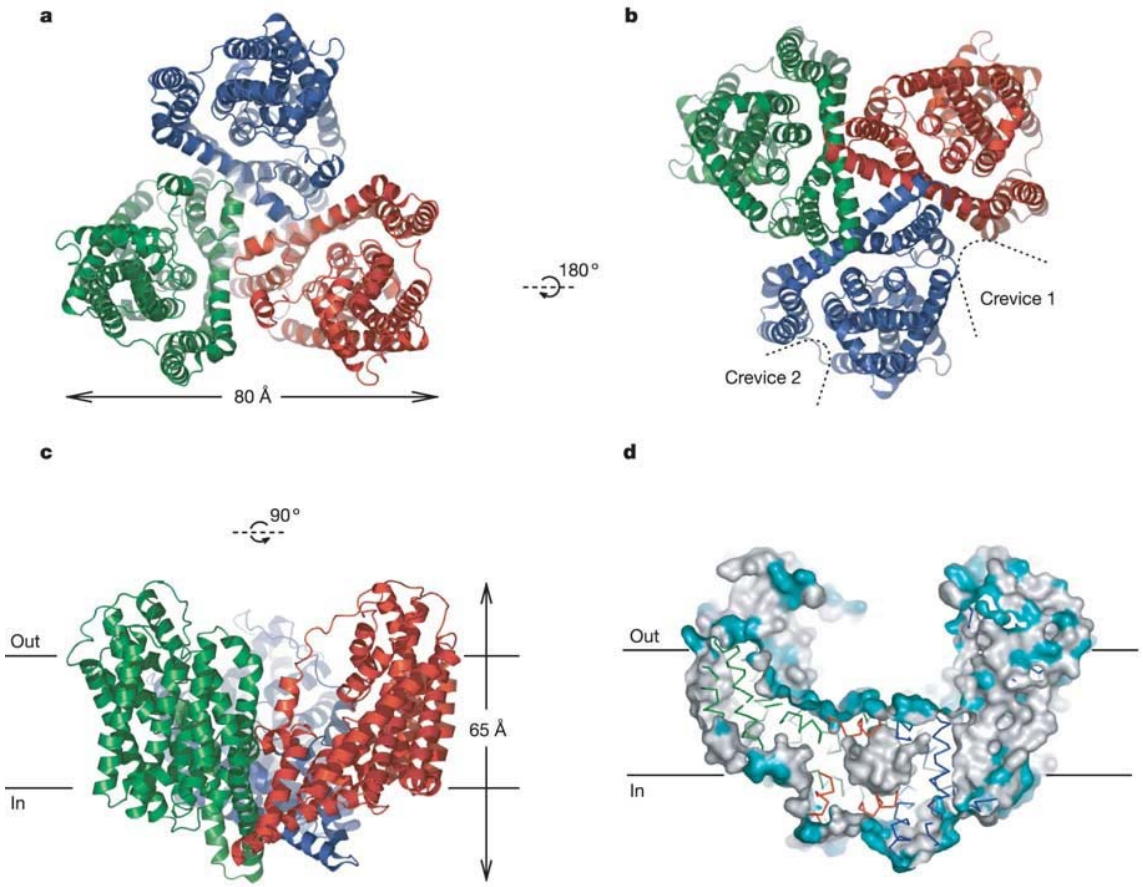

Figure 1.5. The structure of GLT_{ph} as found by Yernool et al. in 2004. The quaternary ribbon structure of GLT_{ph} as viewed from the extracellular (A) and intracellular (B) surfaces as well as a view of the quaternary structure within the cell membrane (C). Note that the GLT_{ph} subunits (blue, green, and red) form a trimer. B) Crevice 1 is formed by the interaction of transmembrane domain 4 interacting with the neighboring subunit white crevice 2 is formed from the tertiary structure of each subunit and is a lipid exposed space of each subunit of the protein. D) Representation of polar (cyan) and non-polar (white) residues through the center of the protein. The authors note that the white molecule in the center is unknown. The inside and outside of the cell and lipid bilayer are represented by solid lines (C, D). This figure is directly from the published paper by Yernol et al., 2004 (115).

Regulation of GLT-1 expression

Studies have shown that GLT-1 is transcriptionally regulated through NF-κB (122,123). NF-κB is ubiquitous in almost all mammalian cells and controls transcription of a wide variety of genes. NF-κB has also been shown to increase GLT-1 protein expression in astrocytes in a neuron-dependent manner (104), meaning the presence of neurons is necessary for astrocytic expression of GLT-1. The exact factor in neurons that modulates GLT-1 expression is currently unknown. In addition, CREB, in conjunction with NF-κB, has also been implicated in GLT-1 transcription (124,125). Basic helix-loop-helix protein 37 or N-myc proto-oncogene (N-myc) is also being explored as a negative regulator of GLT-1 gene transcription (123,126).

Post-translational modifications of GLT-1

Post-translational modification of GLT-1 occurs by many different mechanisms, including putative glycosylation, palmitoylation, and phosphorylation sites. GLT-1 in the mammalian brain is always glycosylated (113,116). However, glycosylation does not affect its transporting function or its localization at the cell surface as unglycosylated and glycosylated GLT-1 show similar uptake activity and localization at the surface of Xenopus oocytes (116). When subject to detergent, glycosylated GLT-1 was found to be more stable than unglycosylated GLT-1 (116), suggesting that glycosylation is needed for protein stabilization; however, the necessity of glycosylation is unknown.

Palmitoylation is a reversible lipid modification of proteins catalyzed by the DHHC (aspartic acid-histidine-histidine-cysteine) family of enzymes (127–131). Palmitoylation modulates protein and receptor content at the neuronal synapse and contributes to regulating synaptic plasticity (as reviewed by (132)). Specifically, a palmitoylation site at

cysteine 38 in GLT-1 has been found to be important for normal GLT-1 function in a mouse model of Huntington disease (133). While GLT-1 protein is still localized to the membrane without palmitoylation, glutamate uptake is drastically reduced (133,134). Palmitoylation has not been studied in neonatal HI brain injury; however, it may play a similar functional role as seen in Huntington disease.

Sumoylation may also occur on GLT-1. A fragment of the C-terminal of GLT-1 accumulates in the spinal cord of a mouse model of amyotrophic lateral sclerosis (ALS) and GLT-1 has been shown to be sumoylated (135). Recently, using immunoprecipitation and western blotting, sumoylation has been shown to occur on full length GLT-1 protein at lysine residues and affect its localization and function in primary rodent astrocytes, rat cerebral cortex, and human spinal cord homogenates (136). Sumoylation causes increased intracellular localization, meaning GLT-1 function and cell surface expression are reduced. In oxygen-glucose deprived organotypic rat hippocampal slices, a cell culture model of HI, increased overall sumoylation was noted as early as one hour after injury (137). In addition, increased sumoylation preceded hippocampal cell death, as noted by propidium iodide staining (137), suggesting that proteins important for neuron health may be downregulated by sumoylation. However, more work needs to be completed to determine sumoylation of GLT-1, as well as regulation of the sumoylating enzymes following HI injury in the neonatal brain.

Multiple phosphorylation sites are also noted on GLT-1 and phosphorylation of different sites may cause changes in GLT-1 localization. However, the role of phosphorylation in normal GLT-1 trafficking or in disease states, such as hypoxia-ischemia, is widely unknown. The activation of protein kinase C (PKC) in vitro causes

both the phosphorylation and ubiquitination of GLT-1, although these processes are independent of one another (138). PKC also causes internalization of GLT-1 from the astrocytic process cell membrane (139–141). In primary cultures of mixed neurons and astrocytes from embryonic rats, PKC activation decreased GLT-1 membrane localization without decreasing total protein expression (140,142). Furthermore, in a rat model of transient HI, PKC increased in membrane fractions and decreased in the cytoplasmic fractions in the ischemic penumbra and core as early as one hour after injury (143). These results indicate that PKC is translocated to the cell membrane during HI insults, and may act on GLT-1, causing a decrease in GLT-1 membrane expression. However, more work needs to be completed to link PKC and GLT-1 in HI injury in the neonatal brain.

Therapeutic Interventions to Treat Cerebral Palsy

Many human and animal studies show that excitotoxicity underlies PVL and neuron death in CP. Originally, drugs that block glutamate receptors were used to reduce excitotoxic cell death. Dixocilpine maleate (MK-801), which blocks the NMDA glutamate receptor, was shown to have neuroprotective benefits if given before or shortly after HI in neonatal rats (144,145); however, later experiments showed that blockage of glutamate receptors causes neuronal apoptosis in immature animals, without HI (146,147), indicating that inhibiting glutamate receptors can be detrimental to healthy neurons. Additionally, antagonizing glutamate receptors has not proven efficacious in humans. Therefore, other therapeutics may be more efficacious to treat excitotoxicity in CP injury.

There is evidence that the function of glutamate transporters, specifically GLT-1, is abnormal in neurological disorders such as epilepsy and stroke (as reviewed by (148)).

Decreased GLT-1 function would leave the neonatal brain vulnerable to glutamate-induced excitotoxicity. Therefore, targeting glutamate uptake has been proposed as a therapeutic strategy to reduce or eliminate brain damage soon after CP insults occur. In a study from the Rothstein lab, 1,040 compounds from the United States Food and Drug Administration's (FDA) approved compounds list were screened to find a drug compound that may modulate GLT-1 activity or function. Fifteen beta-lactams were found that increase GLT-1 protein levels (149). This study started a wave of research examining beta-lactam compounds for their neuroprotective effects.

Ceftriaxone

Ceftriaxone is a broad-spectrum β-lactam antibiotic that is used in neonates to treat infections such as sepsis, meningitis, and ophthalmia neonatorum (150). Ceftriaxone was of particular interest in early experiments as Rothstein's group showed a three-fold increase of GLT-1 protein levels in rats following 5-7 days of drug treatment and an increase in GLT-1 protein localized to the surface of astrocytes in cell co-cultures (149). Furthermore, ceftriaxone treatment caused an astrocyte-specific increase in GLT-1 promoter activity in GLT1-BAC-eGFP mice (green fluorescence protein (eGFAP) is expressed from activation of the GLT-1 promoter in a bacterial artificial chromosome (BAC)) and increased tritiated [^{3}H]-glutamate uptake activity in spinal cord slices. Since pathological decreases in GLT-1 transporters have been implicated in neuropathologies such as ischemia, Rothstein and colleagues pretreated cortical neuron/astrocyte co-cultures with ceftriaxone and showed decreased neuron death following oxygen-glucose deprivation, a method of mimicking ischemic insults in cell culture. Ceftriaxone administration in a mouse model of amyotrophic lateral sclerosis, which displays glutamate neurotoxicity and decreased

glutamate transporter expression, showed decreased neurodegeneration with increased GLT-1 expression (149). Furthermore, in a study of rat nucleus accumbens, ceftriaxone treatment reduced extracellular glutamate in cerebral spinal fluid, which was eliminated with the treatment of a GLT-1 specific inhibitor (151), indicating that ceftriaxone also increases GLT-1 function in addition to protein expression.

Preconditioning with ceftriaxone followed by HI insults in neonatal rats increased GLTl-1 mRNA and protein expression (152), reduced white matter injury and neuronal apoptosis, and improved behavioral outcomes (153). These data suggest that ceftriaxone pretreatment reduces the effects of HI injury.

Even with all of the positive outcomes of ceftriaxone, the drug has only shown effectiveness when administered prior to injury in neonatal HI models. Since CP occurs in utero and is not associated with a single specific event, it is almost impossible to predict which children will develop CP, severely limiting the therapeutic usefulness of this compound. Using ceftriaxone in neonates is of additional concern. The drug efficacy and safety data on ceftriaxone in the neonate are limited and fatal adverse events have been reported (150). Moreover, a literature review conducted by Steadman et al. confirmed that ceftriaxone may be unsafe for neonates less than 28 days of age (154). These data suggest that ceftriaxone is not a feasible compound to use in the treatment of CP.

Clavulanic acid

Another β-lactam drug that increases GLT-1 protein expression is clavulanic acid (CA) (155). Unlike ceftriaxone, CA does not have antibiotic properties, and therefore, can be administered without the concern of developing bacterial resistance. In addition, unlike ceftriaxone, it is orally bioavailable (156–158) and has a better blood-brain barrier

penetrability (159). Although experimental studies have not shown the effectiveness of CA when administered after HI insults, the pharmacokinetic properties of CA are better than ceftriaxone and, therefore, CA has the potential to be administered after insults have occurred. Interestingly, CA treatment in a model of excitotoxic insults delayed the onset of seizures, reduced seizure activity, and eliminated animal death (160). In addition, CA also abolished neuron cell death in the CA3 region of the hippocampus. Like ceftriaxone, CA also increases GLT-1 protein levels in the nucleus accumbens of mice (155), suggesting that CA has similar neuroprotective properties as ceftriaxone.

Statement of Goals

In summary, CP is a permanent, non-progressive movement disorder that is caused by damage to the developing fetal or infant brain. It occurs in approximately 2-4 of 1000 live births and is a prevalent disorder affecting approximately 800,000 individuals in the United States alone (161). With the improvements in survival rate of premature and low birth weight infants, as well as those with complications in utero or at birth, it is likely that we will see an increase in the prevalence of CP in developed countries. With more individuals identified with CP, with or without co-morbid conditions, the cost of care will increase (161,162). Therefore, the need to find the underlying causes of CP, as well as a cure, is imperative.

HI and inflammation are the most common insults contributing to the main pathological hallmarks of CP: PVL and neuron loss (29,40). When CP damage occurs in brain motor regions or their axonal projections, voluntary and postural movement can be compromised. If the injury extends beyond the motor regions to neighboring areas, sensory

and cognitive loss can also be seen. On a cellular level, HI and inflammation can lead to excess glutamate release and neuron and oligodendrocyte cell loss from excitotoxicity. Both developing oligodendrocytes, as well as neurons, contain glutamate receptors that are sensitive to excess extracellular glutamate. However, following HI, studies have shown that in the neonate, there is a loss of GFAP-immunoreactive astrocytes, as well as an increase in astrocyte apoptosis (52,53). This loss, along with the loss of the astrocyte glutamate transporter GLT-1, either due to astrocyte dysfunction/death or decreases in GLT-1 expression or function, will cause glutamate homeostasis at the synapse to fail, leading to neuron death and gray matter injury as well as oligodendrocyte death and PVL commonly seen in CP (54–56,163).

Therefore, we believe that the early loss of astrocytes contributes to the pathogenesis underlying CP injury. The overall hypothesis for this work is that *underlying cellular changes, beginning with the loss of astrocytes and their glutamate uptake functions, through GLT-1, set the stage for the development of CP, including: PVL, neuronal cell death, and motor and cognitive deficits*. In order to test our hypothesis, we used an established mouse model of CP that combines the three most common insults leading to PVL and CP, hypoxia, ischemia, and inflammation (163). We use post-natal day 6 mouse pups, as the brain development is similar to the third trimester in humans in terms of oligodendrocyte maturation and neuronal migration (164). Specifically, using this model system we tested our hypothesis with the following three aims:

Aim 1: Determine whether our CP mouse model has neonatal and adult motor and cognitive deficits following injury.

Animal models of CP replicate some of the brain injuries or motor deficits seen in humans (57,165); however, comprehensive behavioral testing in a model of CP throughout development (in both the neonate and adult) has not been performed.

Previous behavior testing by our colleague demonstrated both white and gray matter brain injury, as well as motor loss with spontaneous recovery two weeks following CP insults (57). However, these studies only examined one motor deficit (climbing), and did not use more sensitive motor testing to determine whether the deficit was due to weakness, coordination, or other motor/sensory problems. In addition, this study did not examine other types of behavior deficits, such as memory or sensory problems. As such, my first aim is to thoroughly characterize the behavioral deficits early after CP induction (post-natal day 8), as well as after the brain injury has stabilized in the adult (8 weeks old). We will use a battery of neonatal motor tests as well as adult motor and cognitive tests to determine behavioral deficits in our CP mice.

Aim 2: Determine whether astrocytes, as well as GLT-1 protein expression or function, are lost early following injury in a mouse model of CP.

Early astrocyte loss in the neonate is shown following HI insults (52,53); however, the status of astrocytes and glutamate uptake leading to CP injury is unknown. Astrocytes are critical for glutamate clearance from the mammalian forebrain through GLT-1 (65,162–164). The immediate loss of astrocytes and/or their functions following insults may leave the neonatal brain susceptible to excitotoxic injury. Therefore, my second aim is to

investigate the timeline of cell death, as well as GLT-1 expression and function early after CP insults.

In order to investigate this aim, we will use stereology to determine astrocyte and neuron counts, as well as hippocampal and white matter volume; fluoro-jade C and terminal deoxynucleotidyl transferase dUTP nick end labeling (TUNEL) staining to determine neuron damage and death, respectively; western blotting to determine GLT-1 expression; and glutamate uptake assays with specific inhibitors to determine GLT-1 function.

Aim 3: Determine whether CA and 093 administration will increase GLT-1 expression and/or function, leading to decreased neuron and white matter volume loss, and improve the motor and cognitive deficits in our CP model.

Even with decades of oligodendrocyte and neuron research following CP injury, we are no closer to a cure for CP. Beta-lactams have been previously shown to increase GLT-1 expression and function (149). Furthermore, beta-lactams have been shown to be neuroprotective in models of HI (149,152,153). Up-regulating GLT-1 on astrocytes may help re-establish glutamate homeostasis and prevent CP pathogenesis.

In this aim, we will use two beta-lactams, one FDA approved and one novel compound, and determine if these drugs can prevent brain damage in our mouse model of CP. To explore this aim, we will administer beta-lactams to mice immediately following CP insults. We then use our battery of neonatal and adult behavior tests to determine increased motor and cognitive function, stereology to count cells and determine white matter volume, western blots to determine increases in total GLT-1 protein expression, and glutamate uptake assays to specifically determine increased GLT-1 activity. In addition,

we will use fluoro-jade C and TUNEL staining to determine decreases in cell damage and death with beta-lactam treatment.

Overall, my research is important as astrocytes and their glutamate transporters, specifically GLT-1, may be the underlying cause of both the white matter injury leading to PVL, as well as the neuronal loss seen in CP. More importantly, there is currently no cure for CP. This research will explore the first potential treatment for CP by using beta-lactam drug administration immediately following injury for neuroprotection in our mouse model of CP.

CHAPTER 2

MATERIALS AND METHODS

Animals

All animal surgeries were performed in accordance with Temple University's University Laboratory Animal Resources (ULAR) department and Institutional Animal Care and Use Committee (IACUC) policies and procedures. C57BL/6 dams and sires were purchased from Charles River Laboratories and were housed in a temperature and humidity controlled environment with a 12-hour light/dark cycle (light on 7:00-19:00) with free access to food and water. Breeding pairs produced litter sizes between 5-10 pups.

Cerebral Palsy Induction Surgery

CP was induced in post-natal day (PND) 6 C57BL/6 pups of both sexes using a hypoxia chamber infused to 6% oxygen with nitrogen gas to simulate hypoxia, unilateral carotid occlusion to cause permanent unilateral ischemia, followed by a single intraperitoneal injection of lipopolysaccharide to induce systemic inflammation (HIL), as previously described by Shen et al. (163). PND 6 mouse pups are used as their neuron migration and oligodendrocyte maturation are similar to third trimester humans. We learned this CP surgery technique from Dr. Wenbin Deng and his lab, our collaborators at Shriners Hospitals for Children in Sacramento, California.

Briefly, pups were anesthetized on ice. Ischemia was induced by unilateral ligation of the right common carotid artery. Pups recovered for 1 hour, 30 minutes on a thermal 34 °C heating pad to monitor breathing and movement, then returned to the dam for an

additional 30 minutes. Next, pups were placed in a temperature regulated hypoxia chamber, set at 6% oxygen, for 35 minutes, at 34°C. LPS was injected intraperitoneally at 1mg/kg body weight then pups were returned to the dam. Sham animals were subjected to a sham surgery, consisting of isolation and visualization of the carotid artery without ligation, no hypoxia, followed by a sham injection of saline. Sham animals were away from the dam during recovery periods along with their experimental littermates.

Neonatal Motor Tests

On PND 8, 48 hours after CP induction, mouse pups are tested for neurobehavioral development (169). Pups were tested within a four-hour block before noon in order to eliminate time of day differences in behavior. Pups were removed from the dam for no more than 15-minutes at a time to prevent rapid loss of body heat and hunger/separation issues. In addition, pups were allowed to rest in between tests so that maximal efforts were elicited on each test. Pups were blinded to the experimenter during testing. All equipment was pre-scented and wiped with paper towels between each test.

The basis of the neonatal motor tests was adapted using Fox's battery of tests (170,171) and Wahlsten's adaption of Fox's tests (172), as well as Treat-NMD and other behavior publications, as indicated, and as described in the Feather-Ferguson Battery of Neonatal Motor Tests.

Ambulation

Crawling is a behavior developed early in the mouse pup, followed by a transition to walking between 5-10 days old (173). At PND 8, the ambulation test takes advantage of this transitional time course and differences in limb movement. The open field was

prepared by covering the surface with a Wypall (Kimberly-Clark) to provide traction for the pups.

Pups were place in an open field and ambulation was visualized for 3 minutes and scored. The following ambulation scale was used: 0 = no movement, 1 = crawling with asymmetric limb movement, 2 = slow crawling but symmetric limb movement, and 3 = fast crawling/walking.

Groups included sham, CP, CP+CA, and CP+093 with an n=7-10. An unpaired two-sample t-test was utilized to compare sham and CP mice using GraphPad Prism 6 software. To compare CP with CP mice receiving beta-lactam treatment, one-way ANOVA with Tukey's multiple comparisons was employed using GraphPad Prism 6 software.

Hind limb foot angle

There is a developmental change in the hind limb posture as the mouse matures from crawling to walking. When walking, the hind limbs are positioned under the body and the angle of the hind limbs is less than the angle seen in crawling. Even though the hind limb foot angle changes over time, mouse pups of the same age with different injury or diseases can be compared. This technique was developed by Feather and Ferguson and has been published (169). Again, the open field was prepared by covering the surface with a Wypall (Kimberly-Clark) to provide traction for the pups.

To determine the hind limb angle, a video camera was mounted above an open field area and the pup was recorded for two minutes. Video recordings were prepared in Microsoft PowerPoint and the angle of the hind limbs was determined by drawing a line through the center of the heel through the middle toe of each foot and recording the angle.

Three to five measurements were used per pup to calculate the average foot angle for each pup tested.

Groups included sham, CP, CP+CA, and CP+093 with an n=6-10. An unpaired two-sample t-test was utilized to compare sham and CP mice using GraphPad Prism 6 software. To compare CP with CP mice receiving beta-lactam treatment, one-way ANOVA with Tukey's multiple comparisons was employed using GraphPad Prism 6 software.

Hind limb suspension

The hind limb suspension test determines hind limb strength in neonates (174). This protocol was adapted from Treat-NMD (174).

A pup was placed face down into a 50mL conical tube with its hind legs hung over the rim facing the experimenter. Once released, the hind limb and tail posture of the pup was observed for one minute or until the pup fell into the tube and a hind limb suspension (HLS) score was given for the following criteria: score of 4 indicates normal hind limb separation with tail raised; score of 3 means weakness is apparent and hind limbs are closer together but they seldom touch each other; score of 2 indicates hind limbs are close to each other and often touching; score of 1 shows a weakness is apparent and the hind limbs are almost always in a clasped position with the tail raised; a score of 0 indicates constant clasping of the hind limbs with the tail lowered or failure to hold onto the tube for any period of time.

Groups included sham and CP pups with n=13. Statistical analysis was performed using an unpaired two-sample t-test to compare sham and CP mice with GraphPad Prism 6 software.

Four limb grip strength

This test examined the strength, rather than dexterity, of all four paws and was modified from the standard horizontal screen test in Fox's studies. In our study, the screen was rotated from a horizontal position, through a vertical position, to a horizontal inverted position to challenge the grasping of all four paws (adapted from Fox (170)).

A pup was placed on a piece of wire screen. After a five second habituation period, the screen was slowly inverted to 180 degrees (°). The angle of the screen when the pup fell off was measured with the protractor and recorded. The test was repeated three times and the average of the trials was recorded.

Groups included sham, CP, CP+CA, and CP+093 with an n=9-18. Statistical analysis was performed using an unpaired two-sample t-test to compare sham and CP mice with GraphPad Prism 6 software. To compare CP with CP mice receiving beta-lactam treatment, one-way ANOVA with Tukey's multiple comparisons was employed using GraphPad Prism 6 software.

Grasping reflex

In the grasping reflex test, each paw was tested individually in order to reveal front or hind limb issues, as well as side preference. This test does not distinguish grasping strength, only ability.

While holding the mouse by the scruff of its neck, each paw was stroked with the blunt end of a razor blade. Grasping was determined if the pup closed its paws over the end of the blade after stimulation. Results for each paw were recorded.

Groups included sham, CP, CP+CA, and CP+093 with an n=8-14. Statistical analysis was performed using an unpaired two-sample t-test to compare sham and CP mice

with GraphPad Prism 6 software. To compare CP with CP mice receiving beta-lactam treatment, one-way ANOVA with Tukey's multiple comparisons was employed using GraphPad Prism 6 software.

Hind limb right paw preference was determined with the following scoring system: grasping with only the right paw was given a score of 100%, grasping with only the left paw was given a score of -100%, and grasping with both paws was given a score of 0%. The average was then calculated If a pup didn't grasp with either paw, they were given no score and were not calculated into the average.

Groups included sham and CP mice with an n=12 for each group. Statistical analysis was performed using an unpaired two-sample t-test to compare sham and CP mice with GraphPad Prism 6 software.

Surface righting

The righting reflex demonstrates the ability for a mouse pup to be able to flip onto its feet from a supine position. This test examines coordination and trunk control (175).

Pups were placed on their backs on a bench pad and held for 3-5 seconds. Following the acclimation, the pup was released and a timer was immediately started. The time to return to prone position was recorded along with the direction of righting (left or right). The test was repeated three times.

Groups included sham (n=7) and CP (n=10) pups. Statistical analysis was performed using an unpaired two-sample t-test to compare sham and CP mice with GraphPad Prism 6 software.

Negative geotaxis

The negative geotaxis test assesses motor coordination in young mice.

The pup was placed on a 45° incline with its head facing down the hill. Following a brief (3-5 second) acclimation, the pup was released and a timer was started. The time and direction (clockwise or counter clockwise) to turn up the hill was recorded. The test was repeated for a total of three trials.

Groups included sham (n=7) and CP (n=10) pups. Statistical analysis was performed using an unpaired two-sample t-test to compare sham and CP mice with GraphPad Prism 6 software.

Cliff aversion

Cliff aversion tests labyrinth reflexes, as well as strength and coordination in neonatal mice (170,176). The box used was approximately 2.5 inches high and had a rough surface so the pups didn't slide. A padded surface was placed against the testing edge of the box to prevent injury in mice that fell.

Pups were placed on the top surface of the box with the digits and snout over the edge. The pup was released and a timer was started immediately. The time and direction of turn (clockwise or counter clockwise) was recorded. The test was stopped once both the snout and paws had been removed from the edge. Three trials were repeated for each mouse.

Groups included sham (n=9) and CP (n=12) pups. Statistical analysis was performed using an unpaired two-sample t-test to compare sham and CP mice with GraphPad Prism 6 software.

Adult Motor Tests

Motor tests were selected from Tests of Mouse Motor Behavior by Wahlsten, 2011 as well as the Stanford Behavioral and Functional Neuroscience (177,178). A battery of tests in eight week old adult mice, seven weeks after CP insults and treatment, is used to determine motor deficits. All equipment was pre-scented and wiped with paper towels between each test. Mice were blinded to the experimenter during testing by marking the tails of mice in each cage.

Gait analysis

The gait analysis determines the angle between the hind paws of mice. The technique used here was developed in our lab.

Mice were placed on a clear acrylic walkway and video recorded from underneath for 5 minutes. Video recordings were prepared in Microsoft PowerPoint and the angle of the hind limbs was determined by drawing a line from the center of the heel through the middle toe of each foot and recording the angle. Three angles were recorded per mouse and the average angle between the hind limbs was calculated. The acrylic walkway was cleaned between each mouse.

Groups included sham, CP, CP+CA, and CP+093 with an n=5-6 mice. Statistical analysis was performed using an unpaired two-sample t-test to compare sham and CP mice with GraphPad Prism 6 software. To compare CP with CP mice receiving beta-lactam treatment, one-way ANOVA with Tukey's multiple comparisons was employed using GraphPad Prism 6 software.

Cylinder rearing

The cylinder test for rearing assesses front paw and front limb impairment by observing weight support and limb strength during spontaneous vertical exploration of a cylinder. The cylinder was clear and was prepared by placing a precut piece of grade 1 filter paper (Whatman) at the bottom.

Mice were placed in the cylinder and observed from all sides using mirrors. The number of independent wall placements as well as paw use (right or left or both simultaneously) was observed and recorded for five minutes. Right paw preference was calculated as a percentage of total paw touches using the equation: (right − left)/(right + left + both) × 100. The cylinder was cleaned between each mouse.

Groups included sham, CP, CP+CA, and CP+093 with an n=9-26. Statistical analysis was performed using an unpaired two-sample t-test to compare sham and CP mice with GraphPad Prism 6 software. To compare CP with CP mice receiving beta-lactam treatment, one-way ANOVA with Tukey's multiple comparisons was employed using GraphPad Prism 6 software.

Rotarod

The rotarod is considered a test for motor coordination and balance. A single first pass is used to determine balance and coordination deficits in mice (179,180). Mice who did not participate in the test, by immediately falling off the rod, were given another trial. This type of behavior is rare and conspicuous (181). Mice with continued non-participation were excluded from the study.

The rotarod was set with an initial start speed of four rotations per minute (rpm) with an accelerating protocol up to 40rpm over five minutes (the speed of the rotarod

increased 1rpm every eight seconds). Once the mice were placed on the rotarod and facing forward, acceleration was started. Speed of the rod as well as latency to fall was recorded. The apparatus was wiped between each mouse.

Groups included sham, CP, CP+CA, and CP+093 with an n=7-12. Statistical analysis was performed using an unpaired two-sample t-test to compare sham and CP mice with GraphPad Prism 6 software. To compare CP with CP mice receiving beta-lactam treatment, one-way ANOVA with Tukey's multiple comparisons was employed using GraphPad Prism 6 software.

Adult Cognitive Tests

Cognitive deficits often manifest as co-morbid conditions along with the motor deficits seen in CP patients. Cognitive tests are used to determine learning and memory in mice. The specific tests here were selected from Tests of Mouse Motor Behavior by Wahlsten, 2011 as well as the Stanford Behavioral and Functional Neuroscience Laboratory based on their relevance for comparing cognitive abilities between mice (177,178). Tests were performed on eight week old adult mice. At least one week before testing, mice were handled every day. Prior to transporting the mice to the behavior room on the day of testing, the tails of the mice in each cage were marked to differentiate between the animals and to blind the researcher to injury and/or treatment. At least 1 hour prior to testing, the mice were brought to the quiet, dark behavior room and left in their home cage to acclimated to the behavior room. Thirty minutes before testing, mice were placed in the pre-scented object box and freely explored for five minutes to acclimate to the testing box.

Video recordings were obtained with a video camera attached to a Dell laptop running the AnyMaze (Stoelting, Illinois, USA) video tracking software.

Novel object recognition

Novel object recognition (NOR) is a cognitive test that assesses recognition memory. NOR exploits a mouse's spontaneous tendency to explore new items over familiar ones. A 12x12 inch open field box was used in this test. Bedding was added to the bottom of the box at a thickness of approximately 1cm to cover the floor. The box and bedding was pre-scented by naïve mice, not included in the study.

At the beginning of the test, two identical objects were placed in the corners of the box and mice were allowed to explore these object at will for five minutes. Following a two-hour delay in their home cage in the quiet behavior room, mice were placed back in the novel object box with one of the objects previously explored and one new object. The mice freely explored these objects for five minutes. Both the habituation and the experimental trials were recorded using a video tracking software (AnyMaze, Stoelting, Illinois, USA). Novel object exploration was determined as a percent by the formula ((Novel Object Exploration – Old Object Exploration)/(Novel Object Exploration + Old Object Exploration))*100%. An exploration of 50% indicates that the mouse does not prefer either object.

Groups included sham, CP, CP+CA, and CP+093 with an n=10-19. Statistical analysis was performed using an unpaired two-sample t-test to compare sham and CP mice with GraphPad Prism 6 software. To compare CP with CP mice receiving beta-lactam treatment, one-way ANOVA with Tukey's multiple comparisons was employed using GraphPad Prism 6 software.

Object location memory

The object location memory task evaluates spatial memory and discrimination, an aspect of cognition. A 12x12 inch open field box was used in this test. The walls of the exploration box were marked with visual cues of different shapes and colors. This allows the mice to distinguish relocation of an object. Bedding was added to the bottom of the box at a thickness of approximately 1cm to cover the floor. The box and bedding was pre-scented by naïve mice, not included in the study.

Two different objects were placed near two corners of the box. Mice freely explored the objects for five minutes then were placed back into their home cage in the quiet behavior room. After a two-hour delay, mice were place back into the box where one object was moved to another location. Both the habituation and the experimental trials were video recorded using a video tracking software (AnyMaze, Stoelting, Illinois, USA). The ability of mice to discriminate object location is determined by the formula (New Object Location – Old Object Location)/(New Object Location + Old Object Location). An exploration of 0 indicates that the mouse does not prefer either object.

Groups included sham (n=6) and CP (n=7) mice. Statistical analysis was performed using an unpaired two-sample t-test to compare sham and CP mice with GraphPad Prism 6 software.

Elevated plus maze

The elevated plus maze measures anxiety in mice. The maze consisted of two open arms and two enclosed arms with each pair of arms positioned opposite each other. The surface of the plus maze was painted gray and the walls of the closed arms were black. The apparatus was elevated 1.5 feet off of the floor and was lit evenly with two desk lamps.

Mice were video recorded from above for five minutes. The test was initiated by placing the mouse in the center of the maze, facing one of the open arms, and letting it move freely. The amount of time spent in each arm was recorded by the AnyMaze video tracking software system (Stoelting, Illinois, USA) attached to a video camera during five minutes of testing. The total distanced traveled, the time spent in each arm, the number of entries into each arm, and the percent of entries into the open arms were calculated by the AnyMaze software. The maze was carefully wiped down with water after each use.

Groups included sham (n=8) and CP (n=7) mice. Statistical analysis was performed using an unpaired two-sample t-test to compare sham and CP mice with GraphPad Prism 6 software.

Synaptosomal Uptake Assays of [^{3}H]-glutamate

Glutamate uptake assays are used to determine the amount of glutamate removed from the synapse over time. DHK and TBOA are used as competitive inhibitors of GLT-1.

CP mice were euthanized at 6, 12, 18, 24, 48 and 96 hours, 1 week and seven weeks following insults. Sham surgical animals were used as controls, as was the contralateral non-injured side of each surgical brain. Glutamate uptake assays were performed using a synaptosomal tissue preparation as previously described (182). Briefly, animals were euthanized and the brain was rapidly removed on ice, microdissected, and weighed. Tissue samples were placed into cold 0.32M sucrose, 20 times weight/volume, homogenized at 400rpm, and centrifuged at 2,500rpm for 10 minutes at 4°C. The supernatant was collected and centrifuged at 12,000rpm for 20 minutes at 4°C. The remaining pellet was washing in

2 times the initial volume of 0.32M sucrose and centrifuged at 12,500rpm for 20 minutes at 4°C. The resulting pellet was suspended in 2.5 times the initial volume in 0.32M sucrose and homogenized for use in the uptake assay.

The uptake assay contains pre-warmed test tubes (37°C) with 450µL sodium or choline buffer (140mM NaCl or choline chloride, 2.5mM KCl, 1.2mM $CaCl_2$, 1.2mM $MgCl_2$, 1.2mM K_2HPO_4, 10mM glucose, 5mM Tris base, and 10mM HEPES), 50µL of hot cocktail (sodium or choline buffer with a mixture of 9.9µM glutamate and 0.1µM [^{3}H]-glutamate (PerkinElmer)), and the addition of 50µL of inhibitor (3mM DHK or 20µM TBOA (Tocris)). 50µL of the synaptosomes were added to the tubes in duplicate every 15 seconds. The assay is stopped after three minutes by adding 2ml of ice-cold choline buffer and placing samples on ice. Samples were collected onto glass filter paper using a cell harvester, washed three times with cold choline buffer, and read by a liquid scintillation counter. Controls included tubes with hot cocktail and choline buffer as well as glutamate transporter inhibitors, DHK and TBOA, in sodium buffer with hot cocktail. A BCA protein analysis kit (Pierce) was used to determine protein concentration of duplicate samples.

GLT-1 specific glutamate uptake activity, expressed as pmol/mg*minute, was determined by subtracting the average uptake after DHK inhibition from the average of total uptake to determine relative GLT-1 activity in disintegrations per minute (DPM). Relative GLT-1 activity is divided by (milligrams of protein x specific activity of the [^{3}H]-glutamate in curies/mol x DPM/curie of the scintillation counter x the length of the assay).

Groups included sham, CP, CP+CA, and CP+093 with an n=3-5. Statistical analysis was performed using an unpaired two-sample t-test to compare sham and CP mice with GraphPad Prism 6 software. To compare CP with CP mice receiving beta-lactam treatment

at the same time point, one-way ANOVA with Tukey's multiple comparisons was employed using GraphPad Prism 6 software.

SDS-PAGE and Western Blot Analysis

To measure GLT-1 protein expression in sham, CP, and CP drug treated brains over time, protein samples were gathered from the contralateral and ipsilateral cortex and hippocampus.

Sham and CP mice were euthanized at 6, 12, 18, 24, 48 and 96 hours, 1 week and seven weeks following injury. Whole brains with the cerebellums and brainstems removed were hemisected, the hippocampus removed and stored on ice, then the remaining brain structures were removed until only the cortex remained. Each sample was then weighed and lysed in 100uL NP40 lysis buffer (Novex) with 500µM phenylmethylsulfonyl, 1mM dithiothreitol, and 1µg/mL protease inhibitor cocktail. Protein analysis was determined in duplicate using a BCA protein analysis kit (Pierce). 20µg of protein was mixed with 5µL of four times concentrated Laemmli buffer and lysis buffer up to 20µL. 20µL The mixed samples were subject to SDS-PAGE on 4-10% SDS polyacrylamide gels (Bio-Rad) and transferred to Immuno-Blot nitrocellulose membrane. Membranes were stained with Ponceau S solution (Sigma) to visualize protein then blocked with Odyssey blocking buffer (Licor), and incubated with antibodies specific to GLT-1 (Millipore) and actin (Sigma) at 4°C overnight. Blots were washed three times with phosphate buffer saline at room temperature for a total of 30 minutes then incubated with near-infrared secondary antibodies (goat anti-rabbit, goat anti-mouse; Licor) and analyzed on an Odyssey Imaging System (Licor). Densitometric measurements were obtained using ImageJ (NIH) and

normalized to actin (Sigma), as a loading control. Controls included protein samples from sham contralateral and ipsilateral cortex and hippocampus for each time point.

Groups included sham, CP, CP+CA, and CP+093 with an n=3-5. Statistical analysis was performed using an unpaired two-sample t-test to compare sham and CP mice with GraphPad Prism 6 software. To compare CP with CP mice receiving beta-lactam treatment in each time point, one-way ANOVA with Tukey's multiple comparisons was employed using GraphPad Prism 6 software.

Immunohistochemistry

Tissue processing

Sham and CP C57BL/6 mice were euthanized at 6, 12, 18, 24, 48 and 96 hours, one week, and seven weeks following injury. Sham surgical animals were used as control in addition to the contralateral non-injured side. Animals were transcardially perfused with cold phosphate-buffered saline (PBS) followed by 4% paraformaldehyde, post-fixed overnight in 4% paraformaldehyde, and cryoprotected in buffered 30% sucrose for at least 48 hours at 4°C. Sections were frozen in OCT embedding compound (Tissue Tek) and cut on a cryostat at 12µm or at 60µm.

Staining for apoptosis

DNA fragmentation was detected using an in situ cell death detection terminal dUTP nick-end labeling (TUNEL) apoptosis detection kit (Roche Applied Sciences, Germany), following the manufacturer's instruction. Briefly, sections were cut at 12µm, every 20th section through the entire brain. Tissue sections were mounted onto gelatin subbed slides. Slides were washed twice with phosphate buffered saline (PBS). 50µL of

TUNEL reaction mixture was applied to each slide and covered with parafilm. Samples were placed in a dark slide box and incubated for one hour at 37°C. Cell nuclei were visualized using 4',6'-diamidino-2-phenylindole (DAPI). Slides were rinsed three times with PBS and mounted with ProLong Gold antifade medium (ThermoFisher Scientific).

Positive controls were made by incubating sections with DNAse I enzyme in 1mg/mL buffered bovine serum albumin (BSA) for 10 minutes at room temperature. Negative controls were obtained by incubating slides with the labeling solution only, without terminal deoxynucleotidyl transferase (TdT) enzyme, for one hour at 37°C.

Staining for neurodegeneration

Fluoro-Jade C (FJC) staining is used to visualize degenerating neurons regardless of insult, damage, or cell death mechanism. Of the neurodegenerative dyes, FJC has the highest signal to noise as well as the highest resolution (183).

To identify any damaged or degenerating neurons, a FJC ready-to-dilute staining kit (Biosensis, USA) was used according to manufacturer's instructions. Briefly, tissue sections were cut at 12µm and every 20th section was mounted onto gelatin subbed slides. Slides were incubated for five minutes in sodium hydroxide then rinsed in 70% ethanol followed by distilled water. Slides were incubated in potassium permanganate for 10 minutes followed by two rinses of distilled water. Finally, slides were incubated in a solution of FJC, DAPI, and distilled water for 10 minutes followed by three rinses of distilled water. Slides were dried on a slide warmer at 56°C and cleared by an immersion in xylene. Coverslips were applied with DPX mounting media. Neurons were determined based on location and morphology.

GFAP-immunoreactivity staining

Tissue sections were cut at 60µm and floated in PBS. First, endogenous peroxidases were inactivated with 0.3% hydrogen peroxide for 30 minutes. Sections were washed with PBS then incubated for 20 minutes in 5% fish gelatin block followed by incubation in GFAP primary antibody (Abcam) diluted 1:100 in 5% fish gelatin overnight at 4°C. Sections were washed 3x10 minutes with PBS then incubated for 30 minutes in biotinylated secondary antibody (Vectastain Elite ABC kit, Vector Laboratories) followed by a second 3x10 minutes rinse in PBS and incubation for 30 minutes in avidin-biotin complex (ABC) reagent (Vectastain Elite ABC kit, Vector Laboratories). Sections were washed with PBS and incubated in 3,3'-diaminobenzidine (DAB) substrate (MP Biomedicals) for approximately one minute until desired stain intensity developed. Sections were rinsed with PBS, float mounted onto gelatin subbed slides, counterstained with cresyl violet, and coverslipped with Permount (Sigma).

Cresyl violet staining

Cresyl violet was used for staining nissl substance, ribosomes and rough endoplasmic reticulum, predominantly in neurons.

The protocol is from neurosciencecourses.com (184). Briefly, 0.2g cresyl violet acetate (Sigma) was dissolved in 150mL deionized water and buffered to pH 3.5 with acetic acid and sodium acetate. Tissue was cut at 60µm and mounted on subbed slides and dried. Sections were rehydrated in deionized water for five minutes then submerged in pre-warmed cresyl violet solution for eight minutes at 60°C. Slides were washed for 5 minutes in deionized water followed by three minutes in 70% alcohol. Slides were switched to 90% alcohol with 0.1% sodium acetate for one minute followed by a quick immersion in 100%

ethanol and cleared in fresh citrus clearing solvent (Thermo Scientific) and coverslipped with Permount (Sigma).

Klüver-Barrera staining

Luxol-fast blue is a copper phthalocyanine dye that stains lipoproteins in the myelin sheath.

Briefly, tissue was cut at 60µm and mounted on subbed slides and dried. Slides were rehydrated in distilled water and incubated in Luxol Fast Blue (Sigma) stain for one hour at 60°C then rinsed in distilled water. Slides were quickly immersed in 0.05% lithium carbonate then in two changes of 70% alcohol to clearly distinguish white and gray matter. Slides were rinsed in distilled water then stained with cresyl violet and coverslipped as outlined above.

Stereology for Volume and Hippocampal Cell Numbers

To accurately count astrocytes and neurons in the hippocampus, 60µm serial sections were collected throughout the entire hippocampus according to standard stereological practice (185), as well as course material from the Neurostereology Workshop, Marine Biology Laboratory, Woods Hole, Massachusetts attended by Danielle Feather on March 15-20, 2014, taught by Dr. Mark J. West. Dr. West also reviewed the stereological methodology to be used in this study. Sections were stained as follows: cresyl violet for volume measurements of the hippocampus and neuron counts in eight week old adult mice; GFAP and DAB staining for astrocyte counts in neonatal mice; Klüver-Barrera staining of myelin to determine volume of white matter regions. The ipsilateral and contralateral hippocampus, corpus callosum, and brainstem pyramid were treated as

separate regions. We used the Cavalieri's unbiased estimate of volume to determine white matter volume in the brainstem pyramids and corpus callosum and the optical fractionator technique to determine total cell numbers throughout the hippocampus. Stereological analysis was performed on a dedicated stereology rig, which included StereoInvestigator (Microbrightfield Bioscience, Williston, VT), attached to a Leica DM6000 microscope with scanning stage motor and a focus measure encoder, SOLA SE light source, Hamamatsu ORCA-Flash 4.0 sCMOS camera and separate QImaging CCD camera, all run by a Dell Precision T5600 workstation.

Cavalieri's estimator of volume was performed under 10x magnification. A grid of specified size (Table 2.1) was used to determine volume. Volume was calculated using the equation:

$$\hat{V} = A_p m' \bar{t} \left(\sum_{i=1}^{n} P_i \right)$$

where A_p: area associated with a point, g: grid size, m': section evaluation interval, t: mean section cut thickness, p_i: points counted on grid. All measurements were determined based on pilot studies for precise estimates versus number of points in the grid.

Table 2.1. Sampling parameters used to determine brainstem pyramid and corpus callosum volume using StereoInvestigator.

	Pyramids	Corpus Callosum
Grid Size (µm)	50	50
Associated Area (µm²)	2500	2500
Section Cut Thickness (µm)	20	60
Section Evaluation Interval	10	6
Associated Volume (µm³)	500000	900000

Optical fractionator counts were performed under 40x magnification by placing n dissectors over the region of interest and counting the total number of cells within the dissector. The parameters for the dissector are as listed (Table 2.2). Total number of cells were calculated using the equation:

$$N = \sum Q^{-} \cdot \frac{t}{h} \cdot \frac{1}{asf} \cdot \frac{1}{ssf}$$

where Q-: Particles counted, t: Section mounted thickness, h: Counting frame height, asf: Area sampling fraction, and ssf: Section sampling fraction. The guard zone was chosen based on previous studies (186) and cells were analyzed when the top of the cell body first came into focus. The other parameters were determined based on a pilot study of cell number as well as discussions with Dr. Mark J. West.

Groups included sham, CP, CP+CA, and CP+093 with an n=3-6. Statistical analysis was performed using an unpaired two-sample t-test to compare sham and CP mice with GraphPad Prism 6 software. To compare CP with CP mice receiving beta-lactam treatment in each time point, one-way ANOVA with Tukey's multiple comparisons was employed using GraphPad Prism 6 software.

Table 2.2. Sampling parameters used to count astrocytes versus neurons using the optical fractionator in StereoInvestigator.

	Astrocytes	Neurons
Counting Frame Area (XY) (μm²)	625	2500
Dissector Height (Z) (μm)	12	35
Dissector Volume (XYZ) (μm³)	7500	87500
Guard Zone Distance (μm)	5	5
Counting Frame Width (X) (μm)	25	50
Counting Frame Height (Y) (μm)	25	50
Sampling Grid (X) (μm)	300	500
Sampling Grid (Y) (μm)	300	500
Sampling Grid Area (XY) (μm²)	90000	250000
Section Thickness (μm)	60	60
Section Evaluation Interval	6	6

Beta-lactam Treatment

Beta-lactams are given to mice to increase GLT-1 expression and function and to determine their efficacy as a treatment for CP. Clavulanic acid (Sigma) or 093 (Moulder Center for Drug Discovery, Temple University), were administered as an intraperitoneal injection at 10mg/kg immediately following LPS injection as well as every 24 hours for four days after surgery (five injections total; Figure 2.1). The concentration as well as the repeated injection schedule is based off of previous studies of clavulanic acid in mice and neonates as well as previous studies using ceftriaxone (149,155,157,187,188).

Behavioral analysis was conducted on CP mice with drug treatment at PND 8 (neonatal motor tests) and at eight weeks old (adult motor and cognitive tests). CP mice with drug treatment were euthanized at 6, 12, 18, 24, 48 and 96 hours, 1 week and seven weeks following injury and appropriate experiments were completed.

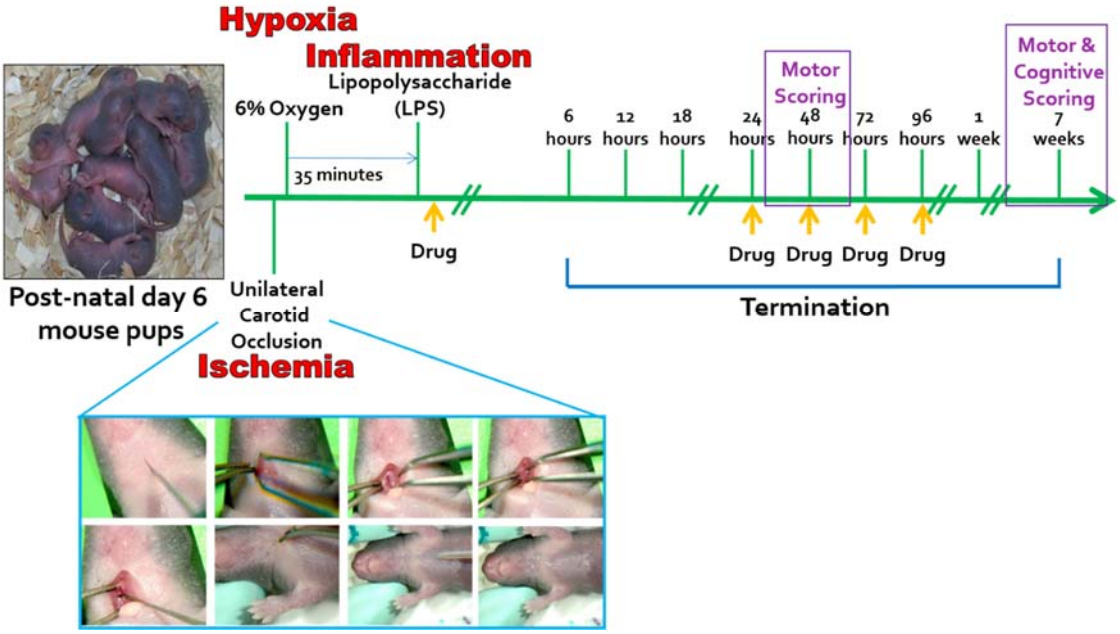

Figure 2.1. Timeline of CP insults, treatment, and termination. Hypoxia, ischemia, and inflammation are induced in PND 6 mouse pups. Behavioral tests are performed 48 hours after insults (PND 8) in the neonate and seven weeks after insults (eight weeks old) in adult mice. Beta-lactam drug treatment is performed immediately after CP is induced and a single injection is given every 24 hours over the next four days (five injections total from PND 6-10). Termination for further experiments was from six hours to seven weeks after insults.

Statistical Analysis

As experimental gender differences were not noted, male and female mice were analyzed as a cohort. Pups from at least two different breeding pairs were used. GraphPad Prism 5 was used to graph and analyze results. Data are expressed as mean ± standard error of the mean (SEM) except where noted. Parametric tests are analyzed by a t-test or multiple t-test. Data comparing CP to CP with beta-lactam drug treatment were analyzed using one-way ANOVA with Tukey's multiple comparisons to determine significance. Data comparing values over time use a two-way ANOVA to determine overall significance with a post-hoc one-way ANOVA with Tukey's multiple comparisons to determine significance within each time point. Data are considered to be statistically significant when $p<0.05$.

CHAPTER 3

BEHAVIORAL DEFICITS IN A MOUSE MODEL OF CP

The most classic definition of CP was suggested by Dr. Bax and an international working group, which stated that CP is "a disorder of movement and posture due to a defect or lesion in the immature brain" (189). Gait abnormalities are one of the main symptoms noted in CP patients. In addition, individuals with CP also have weakened trunk muscles and deficient postural control (190–192) and hand preference can also be a sign of CP (193,194). Muscle weakness often underlies motor problems as adolescents with CP have been shown to be up to 50% weaker than their non-CP counterparts (195). Furthermore, co-morbid conditions, the most common being cognitive deficits, and associated psychological problems are often reported in CP patients (8,9).

Motor deficits have been found in rodents following combined neonatal HI and LPS insults. Two to three weeks after insults, Girard and colleagues found that rats subject to combined fetal exposure of LPS and neonatal HI had less spontaneous locomotor activity and increased anxiety-like behavior in an open-field test (165). Furthermore, well after combined LPS and HI in the neonate, adult rats also demonstrated balance and coordination deficits on a rotarod test. In our neonatal mouse model of CP, combining HI and LPS injections at post-natal day 6, our collaborators found that mice with CP had neurological deficits when assessed for spontaneous activity, symmetrical limb movement, and climbing. However, they also showed spontaneous recovery in these tests 15 days after injury. Cognitive deficits were not assessed in our CP model. Therefore, by using neonatal and adult specific behavior tests, we determined whether CP mice had long-lasting motor and cognitive deficits that could be recorded.

Aim

Aim: Determine whether our CP mouse model causes neonatal and adult motor and cognitive deficits following injury.

Neonatal Motor Results

Transition from crawling to walking is delayed in CP

Ambulation was assessed in pups by scoring gait symmetry and limb-paw movement during a straight walk. At 48 hours after surgery (PND 8), CP mice had less symmetric limb movement and a "crawling" gait as compared to their sham counterparts (Figure 3.1a). By one week after injury (PND 13), both CP and sham mice have transitioned to walking, which occurs between 5-10 days of age.

Hind limb foot angle is increased in neonatal CP mice

Hind limb foot-angle was measured to determine gait stability. Eight-day-old sham mouse pups walk with their hind paws lateral to their body but facing forward, compared to CP mice, who have splayed hind paws when walking in a straight line (Figure 3.1b). The angle between the hind-limbs of sham mice is approximately 55°, whereas CP mice display a hind limb angle of almost 80°.

CP mice have weaker hind limbs

Hind limb strength was assessed in CP mice at 48 hours following injury (PND 8) using the hind limb suspension test. When suspended from the side of a conical tube, the hind limbs in CP mice were closer together than those in sham mice and the limbs of CP mice occasionally touched, indicating hind limb weakness (Figure 3.1c). Sham mice

consistently displayed a strong posture where their hind limbs were spread wider than their body width and their tails were straight up.

Paw strength is decreased in neonatal CP mice

Four limb grip tests strength, rather than dexterity or linear force, in the digits and paws. CP pups (PND 8, 48 hours after injury) were not able maintain their grip while the surface was inverted and fell of the mesh at 69°, which was significantly less then sham mice (96°) (Figure 3.1d).

Grasping reflex is diminished in CP mice

The grasping reflex test is used to demonstrate fine motor skills in young mice. At 48 hours after injury (PND 8), CP mice demonstrate a decrease in grasping reflex. They grasp with fewer paws than sham mice (Figure 3.1e). In addition to grasping with fewer paws, there was a significant right paw preference in the hind limbs (Figure 3.1f), indicating fine motor deficits contralateral to injury. One week after injury (PND 13), HIL mice still grasp with fewer paws, indicating that they continue to have deficits in grasping (Figure 3.1g).

Surface righting does not show distinguishable differences

Postural assessment in CP patients show less trunk control while performing tasks such as sitting, standing and walking. Hence, surface righting was used to assess trunk control in CP mice (48 hours after injury, PND 8). Compared to sham pups, CP mice do not show significant deficits when righting (data not shown). CP mice can quickly right themselves and do not show a preference to turn toward one side or the other.

No variations are detected in negative geotaxis testing

CP patients often have spasticity, which interferes with coordinated movements. In young pups, negative geotaxis tests motor coordination and balance while turning up an incline. CP mice (PND 8) do not show coordination deficits when challenged with negative geotaxis, nor do they demonstrate balance issues on the incline, as compared to sham mice (data not shown). Additionally, CP mice did not show a preference to turn toward one side versus another when re-orienting.

Deficits are not present in the cliff aversion test

The cliff aversion test also determines coordinated movement of all four limbs. However, rather than turning up an incline, mice must balance with part of their body weight unsupported, then turn away from the edge of cliff. CP mice (PND 8) did not show delayed movement away from the cliff, preference to turn toward one side or another, or a decreased ability to support themselves on the side of the cliff before turning (data not shown).

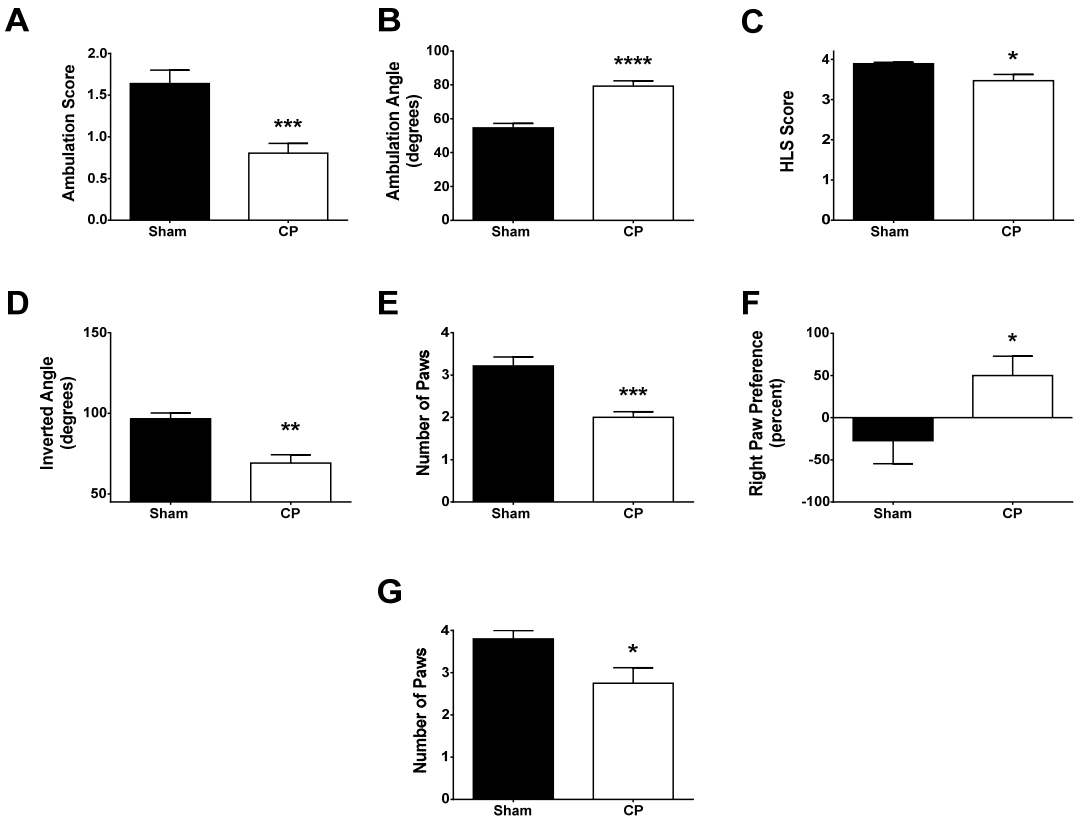

Figure 3.1. Neonatal CP mice show motor deficits 48 hours after insults are induced. Motor tests were performed in PND 6 pups, 48 hours after injury, to determine deficits in gait (ambulation: A, $p<0.0005$; hind limb angle: B, $p<0.0001$), hind limb (C, $p<0.05$) and paw (D, $p<0.005$) strength, as well as deficits in grasping (E, $p<0.0005$) and paw preference (F, $p<0.05$). One week after injury (PND 13), grasping deficits were still noted in CP mice (G, $p<0.05$). In A-G, sham is represented by black bars and CP is represented by white bars. A two-sample t-test was performed comparing sham and CP animals and $p<0.05$ (*) was considered significant. Data are shown as a bar graph and expressed as mean ± SEM, n = 6-18.

Adult Motor Results

CP mice show gait abnormalities into adulthood

Since gait abnormalities were found in neonatal CP mice, hind limb angle was also assessed in adult mice with CP. Hind-limb angle in adult mice decreased compared to neonatal pups. However, similar to neonatal mice with CP, adult CP mice ambulate with a greater angle between their hind limbs, 60°, when compared to shams, who have an angle of 43° between their hind limbs (Figure 3.2a).

Left paw weakness is noted in adult CP mice

The cylinder rearing test indicates paw preference as well as limb weakness. In the rearing test, CP mice display significant right paw preference (Figure 3.2b). This indicates left side weakness, which correlates with right sided ischemic injury. Sham mice display a slight propensity for left side preference; however, these data are not statistically significant and C57BL/6 mice, the strain used in our study, are generally ambidextrous (196).

Adult CP mice have balance and coordination deficits

The rotarod test was used to determine balance and coordination deficits. Using a protocol in which speed is increased over time, the speed at which the mice fell off was recorded and deficits in CP mice were determined. Compared to sham mice, adult mice with CP performed worse on the rotarod and sham mice run at speeds greater than 50% of CP mice (Figure 3.2c).

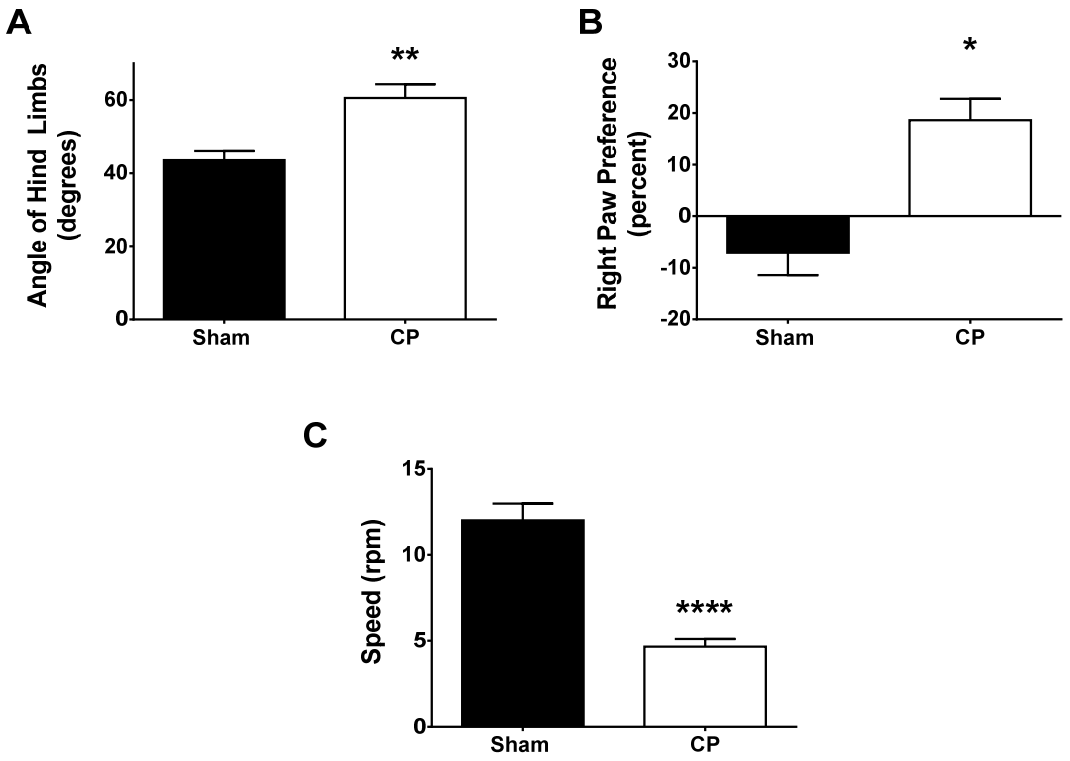

Figure 3.2. Seven weeks after injury, adult CP mice have motor deficits. Motor tests were performed on eight week old mice, seven weeks after injury, to determine motor deficits. Increased hind limb angle (A, $p<0.005$), increased right paw preference (B, $p<0.05$), and balance and coordination deficits (C, $p<0.0001$) were noted in adult CP mice. In A-C, sham is represented by black bars and CP is represented by white bars. A two-sample t-test was performed comparing sham and CP animals and $p<0.05$ (*) was considered significant. Data are shown as a bar graph and expressed as mean ± SEM, n = 5-26.

Adult Cognitive Results

Adult CP mice show short-term recognition memory deficits

As cognitive deficits are the most common co-morbid condition associated with human CP, cognition was assessed in our mouse model. Novel object recognition was used to determine short-term recognition memory. When compared to shams, adult CP mice show deficits in recognizing a novel object (Figure 3.3a). Object recognition in CP mice is reduced by about 30% compared to sham animals. However, CP mice do not spend less time exploring the objects (total exploration time) or ambulating around the field (total time and distance moved) (data not shown), showing that differences are not due to anxiety or immobility.

Short-term spatial discrimination deficits are noted in CP mice

The object-location memory task is used to determine short-term spatial discrimination, another aspect of cognition. CP mice do not discriminate between the new and old location of an object (Figure 3.3b). In fact, discrimination is reduced by approximately 40%. Again, total exploration time and ambulation time and distance are not affected in CP mice (data not shown).

CP mice display normal anxiety behaviors

The elevated plus maze is used to test anxiety related behaviors in mice. Both sham and CP mice spend significantly less time in the open arms compared to the closed arms (data not shown); however, there is no difference in length of time spent in open arms between sham and CP mice. Additionally, no difference was seen in the number of entries into the closed or open arms or the amount of time spent in the arm regions between sham and CP mice (data not shown).

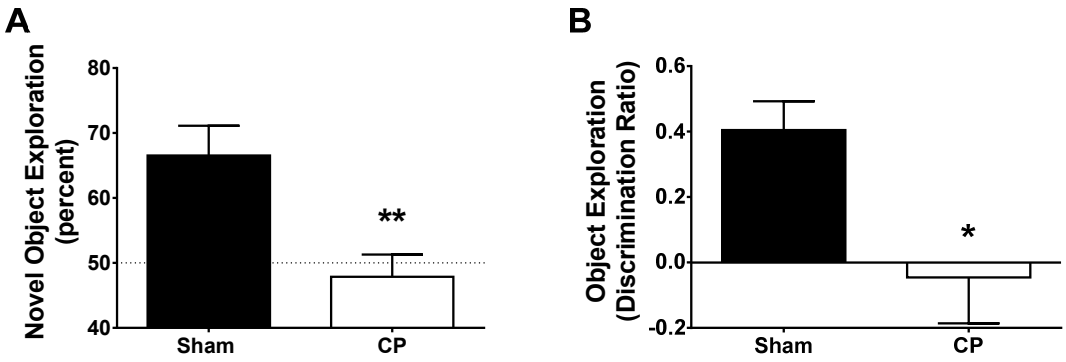

Figure 3.3. Adult CP mice have cognitive deficits. Seven weeks after CP insults were induced (mice were eight weeks old), cognitive tests were performed. CP mice demonstrated significant cognitive deficits in the novel object recognition test (A, $p<0.005$) and object location memory (B, $p<0.05$). In A, the dotted line represents 50% exploration, indicating that mice do not explore the novel object more than the old object. In A and B, sham is represented by black bars and CP is represented by white bars. A two-sample t-test was performed comparing sham and CP animals and $p<0.05$ (*) was considered significant. Data are shown as a bar graph and expressed as mean ± SEM, n = 6-19.

Discussion

The aim of this study was to determine whether our mouse CP model causes motor and cognitive deficits. Using a battery of neonatal motor tests, which we published in the Journal of Visualized Experiments earlier this year (169), as well as standard adult motor and cognitive tests, we determined that mice receiving the combination of HIL have motor deficits early in life that persist into adulthood. In addition, we showed that adult CP mice also have cognitive deficits.

CP mice display mobility and gait abnormalities 48 hours after injury and at eight weeks old, as evidenced by overall ambulation as well as the hind limb angle (Figure 3.1a, b and Figure 3.2a). Gait abnormalities are one of the key features of CP (197) and any animal model should display similar motor deficits. Impairments in neonatal strength and grasping reflexes were also apparent (Figure 3.1c-g), another early sign of CP (7). In the adult, CP mice have limb weakness and paw preference (Figure 3.2b). These results are analogous to the human condition as hand preference and reduced strength are seen in CP patients (193–195). In addition to motor deficits, adult CP mice also have cognitive deficits, as evidenced by decreased ability to learn or remember an object's novelty or location (Figure 3.3a, b, respectively). These results are supported by Huang and colleagues, who demonstrated that perinatal HI in the rat caused long-term cognitive deficits in the adult (198). Similarly, CP patients have difficulties in short-term memory (199,200).

Three neonatal tests, negative geotaxis, cliff aversion, and surface righting reflex, did not show significant changes between sham and CP mice. Negative geotaxis and cliff aversion tests determine coordinated movement in response to vestibular input. Any results

in these tests would have been interesting as difficulties in motor and balance, such as those seen in CP patients and mice, can suggest vestibular problems (201), possibly indicating cerebellum or brainstem injury. However, occlusion of the common carotid artery and hypoxia for 35 minutes causes selective white matter injury in the cerebrum without significant cortical gray matter damage (58); therefore, our mice do not show vestibular deficits. CP patients presenting with vestibular problems may have had an ischemic insult affecting blood flow to the cerebellum or brainstem, which can disrupt sensory pathways and lead to vestibular problems. The surface righting test determines trunk control when turning over to a prone position. CP patients have been shown to have impaired trunk control and muscle weakness while sitting and walking (192,202,203). However, since mice are quadrupeds, they do not use their trunk muscles for upright sitting and walking; therefore, muscular organization is not as defined in the mouse as it is in the human (204). Because of this, CP mice do not show impaired trunk control.

The elevated plus maze did not show differences between sham and CP mice, indicating that CP mice do not have increased anxiety compared to sham animals. This finding is in contrast to findings by Girard, showing that the combination of HI and LPS in the neonate increased anxiety-like behavior in an open field (165). Girard showed that rats, subjected to HIL, travel less distance, are immobile for longer periods of time, and do not explore the center of the open field box. They also show that, in contrast, control rats travel greater distances and explore more of the box; however, Girard did not address anxiety-like behavior, or thigmotaxis, in control rats. Girard also noted that CP rats perform worse on the rotarod test, which indicate ambulatory deficits. However, rather than increased anxiety, exploration of CP rats in the open field could decrease because of ambulatory

issues, and this was not addressed in Girard's research. Furthermore, research conducted on human CP patients note anxiety issues that are centered around social interaction (205,206). Therefore, future studies should be conducted on CP mice to determine increased anxiety during social interaction.

The results presented here provide evidence of short- and long-term behavioral deficits in CP mice and suggest a continuum of motor and cognitive deficits from the neonate to the adult. These findings are similar to those seen in humans with CP. Collectively, these data are the first evidence that a mouse model recapitulates many of the behavioral deficits seen in CP patients. Furthermore, researchers can now use this model to determine the efficacy of treatment on both cellular and behavioral changes in CP.

CHAPTER 4

GFAP-POSITIVE ASTROCYTE LOSS, INCLUDING THE LOSS OF GLT-1, OCCURS VERY EARLY AFTER CEREBRAL PALSY INSULTS

The role of astrocytes in the CNS is ever-changing. Once thought to be the glut of the brain and of no purpose other than as holding material for the might neuron, the astrocyte is now recognized for a variety of essential functions. One major function is its response after injury. Contrary to cell culture data (207), astrocytes in the neonate are susceptible to HI insults. In the neonatal human, approximately 80% of GFAP-positive astrocytes were apoptotic early after HI insults (53). In rat models of permanent (54) and transient (55,208) ischemic insults, significant astrocyte cell loss occurred within the first 48 hours of injury. In neonatal rat models of HI, apoptotic GFAP-positive astrocytes increased over the first 72 hours following insults (53) with apoptotic astrocytes in the white matter (as a percent of total apoptotic cells) accounting for 31% at four hours, 51% at 12 hours, and 57% at 72 hours of cells lost (52). These studies suggest that astrocyte loss occurs following HI insults. The loss of astrocytes may cause a decrease in glutamate uptake and an increase in glutamate concentrations, which could become toxic very quickly.

To support this idea, GLT-1 protein knockdown in rats caused a 58% loss in GLT-1 protein with a 56% loss in glutamate transport and a 32-fold increase in extracellular glutamate, with neuron degeneration also found (97). GLT-1 knockout mice show increased extracellular glutamate, selective neuronal degeneration in the hippocampus, and increased injury following neurotrauma (77). When GLT-1 was knocked down in an adult

rat model of HI, a significant increase in infarct volume and exacerbated neuronal damage was noted in the cortex and striatum (209). Furthermore, in animal models of HI, decreased GLT-1 expression and activity has been noted within 24 hours following insults (210,211) and precedes neuronal death (211). The decrease of GLT-1 protein and increase in extracellular glutamate and neuron death, suggests that neurons died via excitotoxic mechanisms.

Therefore, it seems that a decrease in glutamate clearance by GLT-1 could accompany astrocyte loss and increase excitotoxic damage of neurons and oligodendrocytes early after neonatal CP insults. The contribution of astrocytes and glutamate clearance to excitotoxic cell death in CP brain injury will be examined.

Aims

Aim 1: To determine whether astrocytes are lost following injury in a mouse model of CP.

Aim 2: To determine whether GLT-1 protein expression or function changes following CP induction.

Results

GFAP-positive astrocyte loss is apparent very early after insults

Recent studies show that astrocytes may play an early role in HI brain damage (52,212). In our model, even as early as 6 hours following injury, there is an approximately 36% decrease in GFAP-immunoreactive astrocytes in the ipsilateral hippocampus of CP mice when compared to the contralateral hippocampus (Figure 4.1a). In the ipsilateral

versus contralateral hippocampus, at 12, 18, and 24 hours after injury, GFAP-immunoreactive astrocytes are significantly decreased by 23%, 27%, and 38%, respectively. By 48 hours following injury, GFAP-positive astrocyte numbers on the ipsilateral side have returned to contralateral and sham levels. The combination of hypoxia and lipopolysaccharide, contralateral to ischemic injury, does not cause GFAP-immunoreactive astrocyte cell loss compared to sham animals.

Neuron damage occurs very early after injury but death is delayed

The total number of neurons was determined in the hippocampi of adult mice at eight weeks old. Counts were determined in the ipsilateral sham hippocampus as well as the contralateral and ipsilateral CP hippocampi. Total neurons in the ipsilateral hippocampi of CP mice were approximately 40% less than that of sham or the contralateral CP hippocampi (Figure 4.1b). The combination of hypoxia and inflammation in the contralateral hippocampus did not cause neuron loss compared to sham mice. Interestingly, with the loss of neurons and astrocytes after CP insults, the ipsilateral hippocampus did not decrease in size (Figure 4.1c). The hippocampus does appear to increase in size normally over development.

FJC staining is used to detect damaged and degenerating neurons. Analysis of FJC staining from six hours to one week after injury revealed hippocampal neuron damage beginning at 12 hours, peaking at 18-24 hours, and minimal damage around 48 hours post-injury (Figure 4.2). Substantial damage is mostly noted in the cornu amonis 1 (CA1) and CA3 regions. Neuron damage in the motor cortex is not present.

DNA strand breaks, indicating apoptosis, were detected using the TUNEL assay. TUNEL positive cells were noted at 24 hours with a peak in cell death 48 hours following

CP injury (Figure 4.3). Apoptosis was most prevalent in CA1 (data not shown) and CA3 regions of interest. The other time points tested did not have TUNEL-positive cells. TUNEL-positive cells were determined to be neurons based on morphology and location.

White matter volume is decreased after injury

In patients with CP, diffusion tensor imaging shows decreased density, and, hence, decreased volume, in white matter regions of the brain (213). Therefore, using stereology and Cavalieri's estimator of volume, we determine total volume in two important white matter regions of the mouse brain shown to decrease in adult CP patients: the corpus callosum and the pyramidal tracts in the brainstem. Seven weeks after injury, both white matter regions showed decreased volume in the ipsilateral brain hemisphere (Figure 4.4). Total volume in the corpus callosum ipsilateral to injury was approximately 13.5% smaller compared to the contralateral side (Figure 4.4a). The white matter volume in the brain stem pyramids decreased by approximately 16.5% in the ipsilateral pyramidal tract compared to the contralateral pyramidal tract (Figure 4.4b). Both the contralateral corpus callosum and pyramidal tract were not significantly different from sham animals.

GLT-1 protein levels are decreased 72 hours after injury

Changes in GLT-1 protein expression leading to neurological injury has been implicated in many neurological disorders (as reviewed by (214)), including ischemia. Therefore, we evaluated GLT-1 protein expression in the ipsilateral hippocampus and cortex as well as the contralateral hippocampus and cortex. Of these four regions, the ipsilateral hippocampus is the only region of interest that showed decreased GLT-1 protein amounts. GLT-1 protein is not decreased within the first 48 hours after injury (Figure 4.5a); however, a 15% decrease of GLT-1 protein is noted 72 hours following injury, with a 53%

decrease at 96 hours, 51% decrease at 1 week, and a 33% decrease 7 weeks after CP insults compared to the sham ipsilateral hippocampus. GLT-1 protein levels were normalized to actin and compared to sham at the same time point and in the ipsilateral regions of the brain (Figure 4.5b). GLT-1 protein expression in the ipsilateral hippocampus was also decreased compared to the contralateral hippocampus.

GLT-1 function decreases after injury

Changes in GLT-1 protein amounts are delayed after injury; however, it is thought that GLT-1 plays a significant role in excitotoxic brain damage following insults (214). Therefore, we used crude synaptosomal preparations from the contralateral and ipsilateral hippocampi and cortices to determine GLT-1 functions following injury. With glutamate transporter specific inhibitors, we were able to isolate GLT-1 function in synaptosomes. Of the four regions monitored, the ipsilateral hippocampus is the only region that showed significant changes in GLT-1 function. Following a small but insignificant increase in GLT-1 12 hours after injury, a 40% decrease was noted in GLT-1 function 24 hours after injury (Figure 4.5c). Moreover, when using TBOA to block all glutamate transporters, no detectable differences in glutamate transport were noted in the hippocampus over the 12 to 24-hour time course of GLT-1 dysregulation, indicating that GLAST and EAAC1 function in the hippocampus are unchanged following injury (Figure 4.5d).

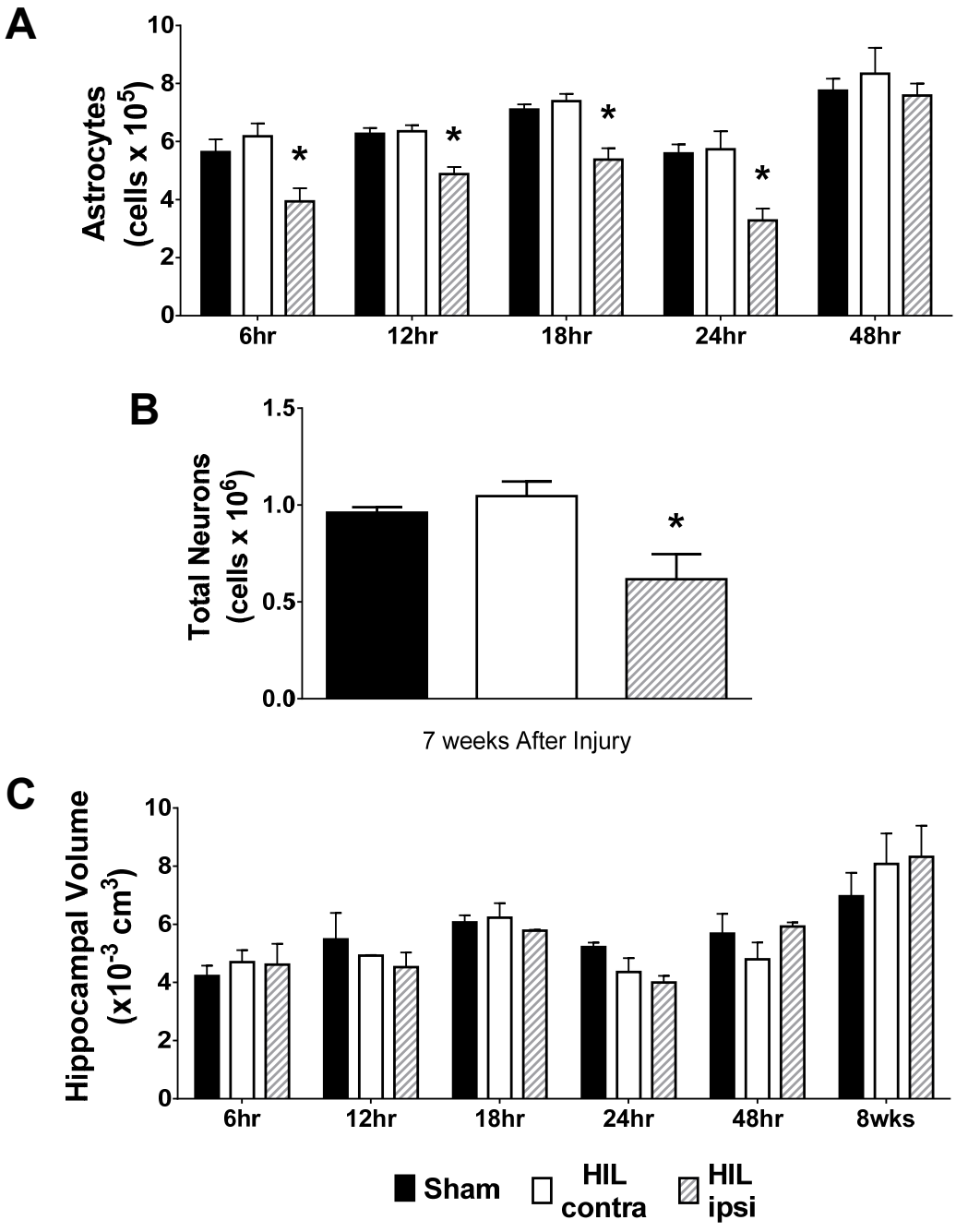
A
Astrocytes (cells x 10^5)
10
8
6
4
2
0
*
*
*
*
6hr
12hr
18hr
24hr
48hr
B
Total Neurons (cells x 10^6)
1.5
1.0
0.5
0.0
*
7 weeks After Injury
C
Hippocampal Volume (x10^-3 cm^3)
10
8
6
4
2
0
6hr
12hr
18hr
24hr
48hr
8wks
Sham
HIL contra
HIL ipsi

Figure 4.1. The total number of GFAP-positive astrocytes are decreased early after injury and neuron loss is apparent once injury is established. (A) Astrocyte counts were obtained using stereological methods. GFAP-immunoreactive astrocytes were counted in the ipsilateral sham hippocampus (black bars) as well as the contralateral (white bars) and ipsilateral (gray striped bars) CP hippocampus from 6-48 hours after injury. The total number of astrocytes in the ipsilateral hippocampus were significantly decreased 6-24 hours after injury ($p<0.05$). Overall significance was determined using a two-way ANOVA with Tukey's multiple comparisons where $p<0.05$ within each time point. (B) Seven weeks after injury, sections were taken throughout the entire hippocampus and stained with cresyl violet. Neurons were determined based on location and morphology. The total number of neurons in the ipsilateral sham (black bar), CP contralateral (white bar), and CP ipsilateral (gray striped bar) hippocampus were determined using stereological technique. The total number of neurons was decreased in the ipsilateral hippocampus ($p<0.05$). Significance was determined using one-way ANOVA with Tukey's multiple comparisons. (C) Hippocampal volume was measured using Cavalieri's estimator of volume. Although cell numbers decrease at all time points counted, hippocampal volume does not change. Overall significance was determined using two-way ANOVA. Data are expressed as mean ± SEM, n=3-6.

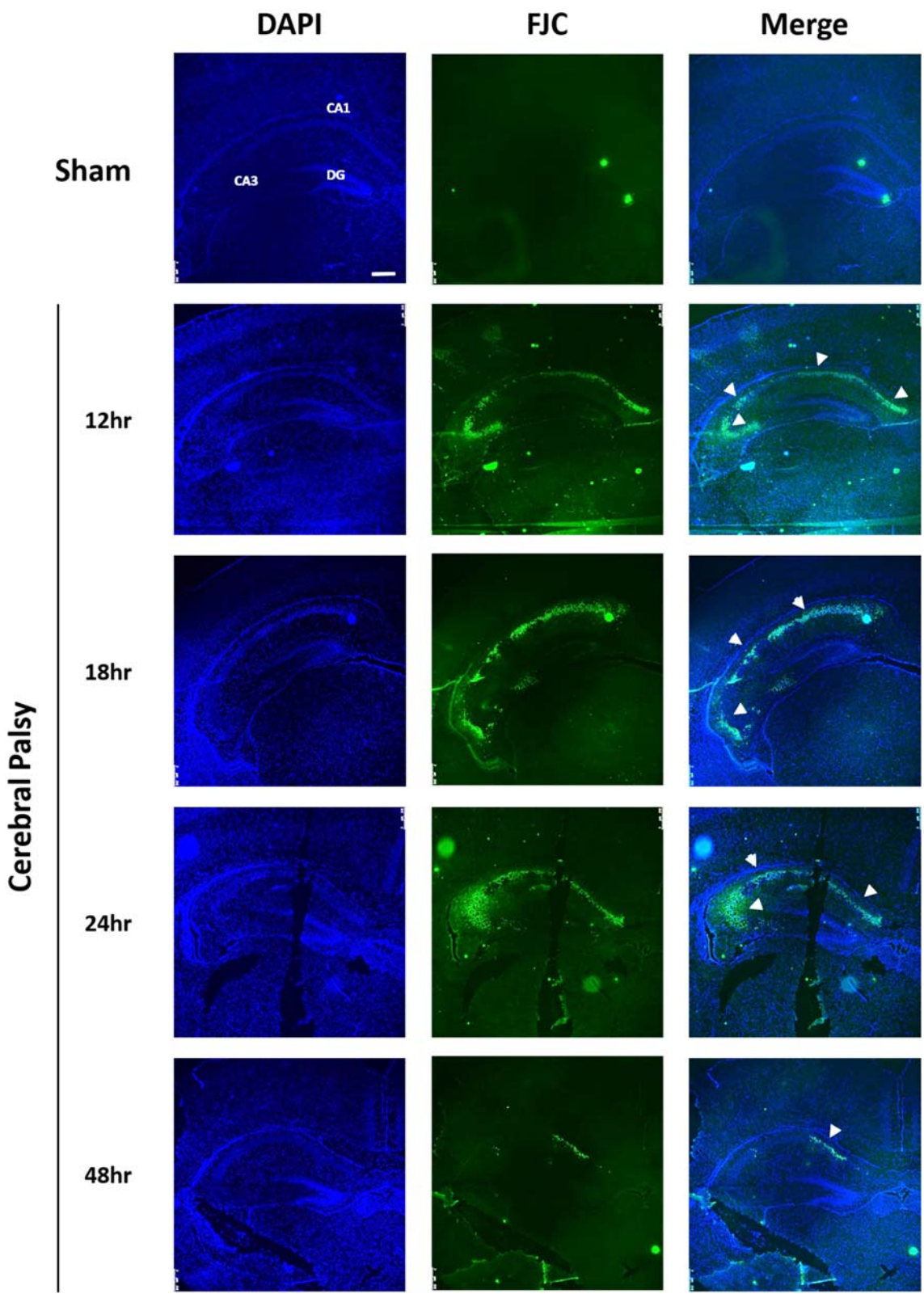
DAPI
FJC
Merge
Sham
CA1
CA3
DG
Cerebral Palsy
12hr
18hr
24hr
48hr

Figure 4.2. Neuron damage is noted in the ipsilateral hippocampus of CP mice. Fluoro-jade C staining of hippocampal sections was used to detect neuron damage. The third column shows nuclear staining (DAPI, blue) and apoptotic neurons (green) with regions of greatest damage highlighted (white arrow heads). Representative sections are shown. Sham mice were stained at 18 hours. CP mice were stained at all time points but damage was only noted from 12-48 hours, as shown. Scale bar, 200μm, applies to all panels. Sham DAPI staining is labeled with the anatomical regions in each image, DG = dentate gyrus, CA = cornu amonis. n = 3-5

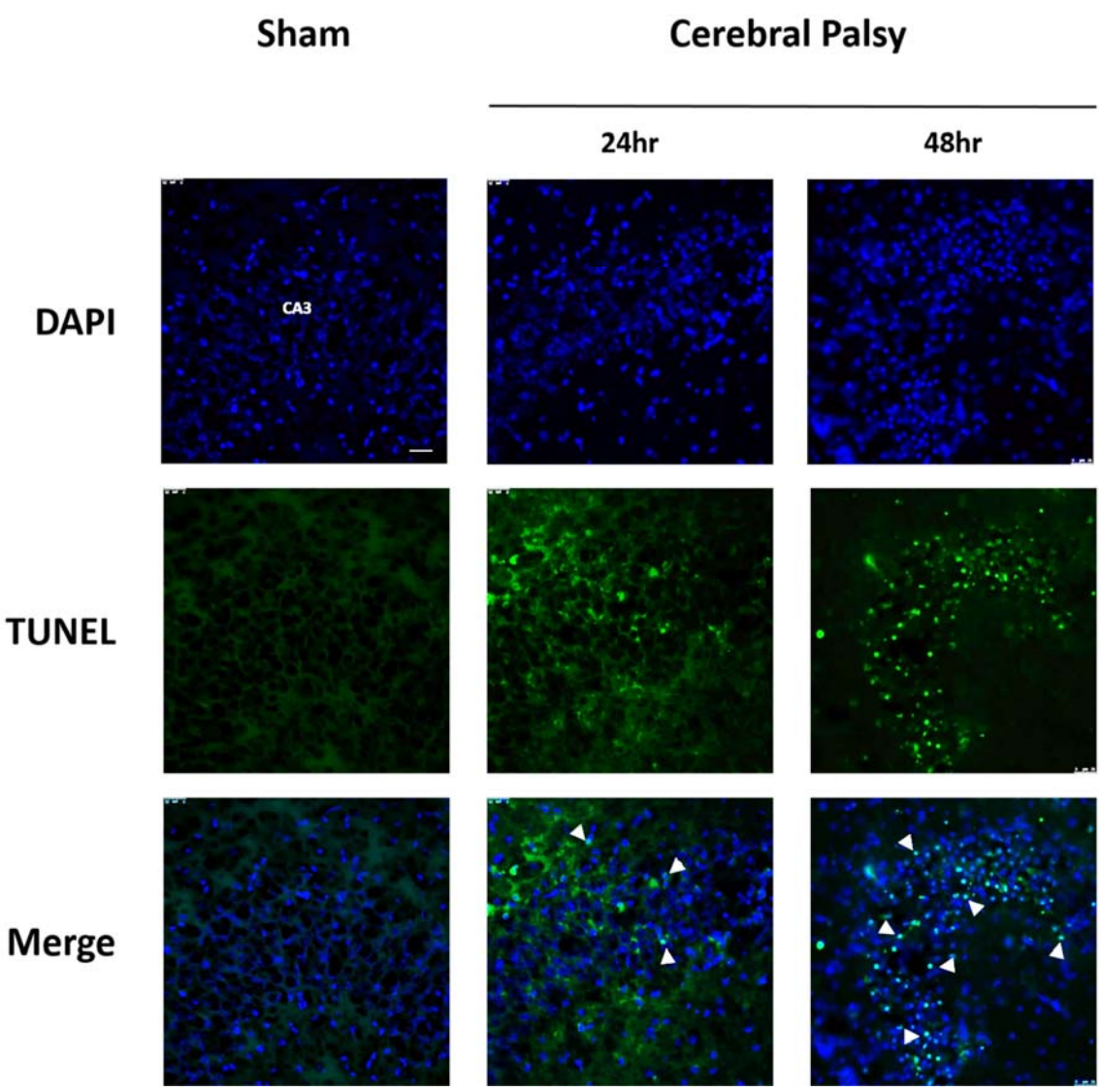

Figure 4.3. Apoptotic neurons are noted in the ipsilateral hippocampus in CP mice. Apoptotic cells were detected using a TUNEL assay. A few apoptotic neurons first appear 24 hours after injury. The number of TUNEL positive apoptotic neurons increases at 48 hours but only minor apoptosis is noted in neurons of CP mice after 48 hours. Sham mice do not show TUNEL staining at any time point. The third row of panels shows nuclear staining (DAPI, blue) and apoptotic neurons (green) with regions of greatest damage highlighted (white arrow heads). Representative sections are shown. Sham mice were stained at 48 hours. CP mice were stained at all time points but damage was only noted at 24 and 48 hours, as shown. Scale bar, 25μm, applies to all panels. All images show ipsilateral CA3 hippocampal staining, noted in the sham image. n = 3-5

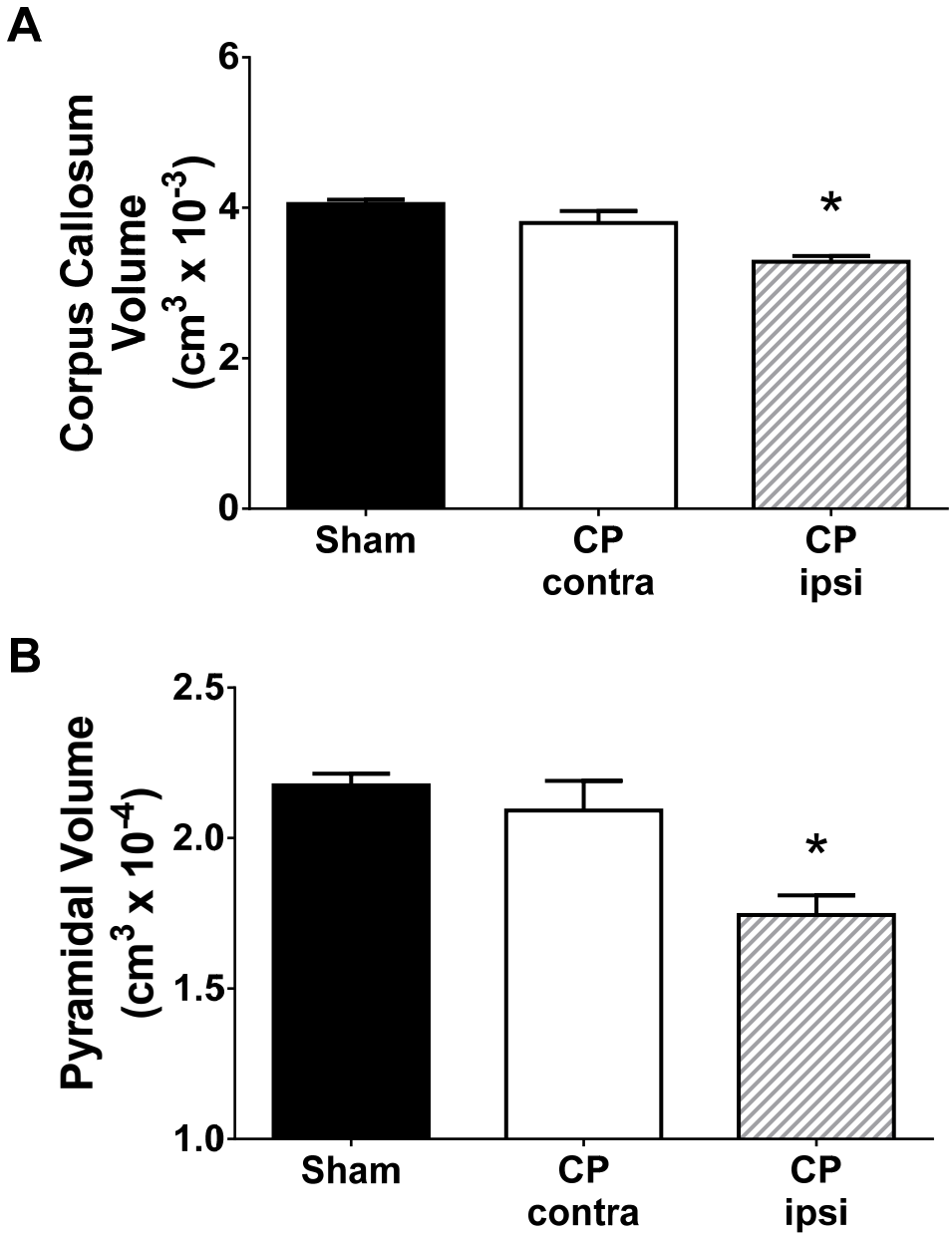

Figure 4.4. White matter volume is decreased seven weeks after CP injury. Seven weeks after injury (mice were eight weeks old), sections were taken throughout the entire corpus callosum (A) or brainstem pyramids (B) and sections were stained. Volume was determined using stereological methods and Cavalieri's estimator of volume. Volume of the white matter regions in the ipsilateral sham (black bar), CP contralateral (contra, white bar), and CP ipsilateral (ipsi, gray striped bar) were determined. The total volume of each white matter regions was decreased in the ipsilateral hemisphere of CP brains compared to sham ($p<0.05$) Significance was determined using one-way ANOVA with Tukey's multiple comparisons. Data are expressed as mean ± SEM, n=3-6.

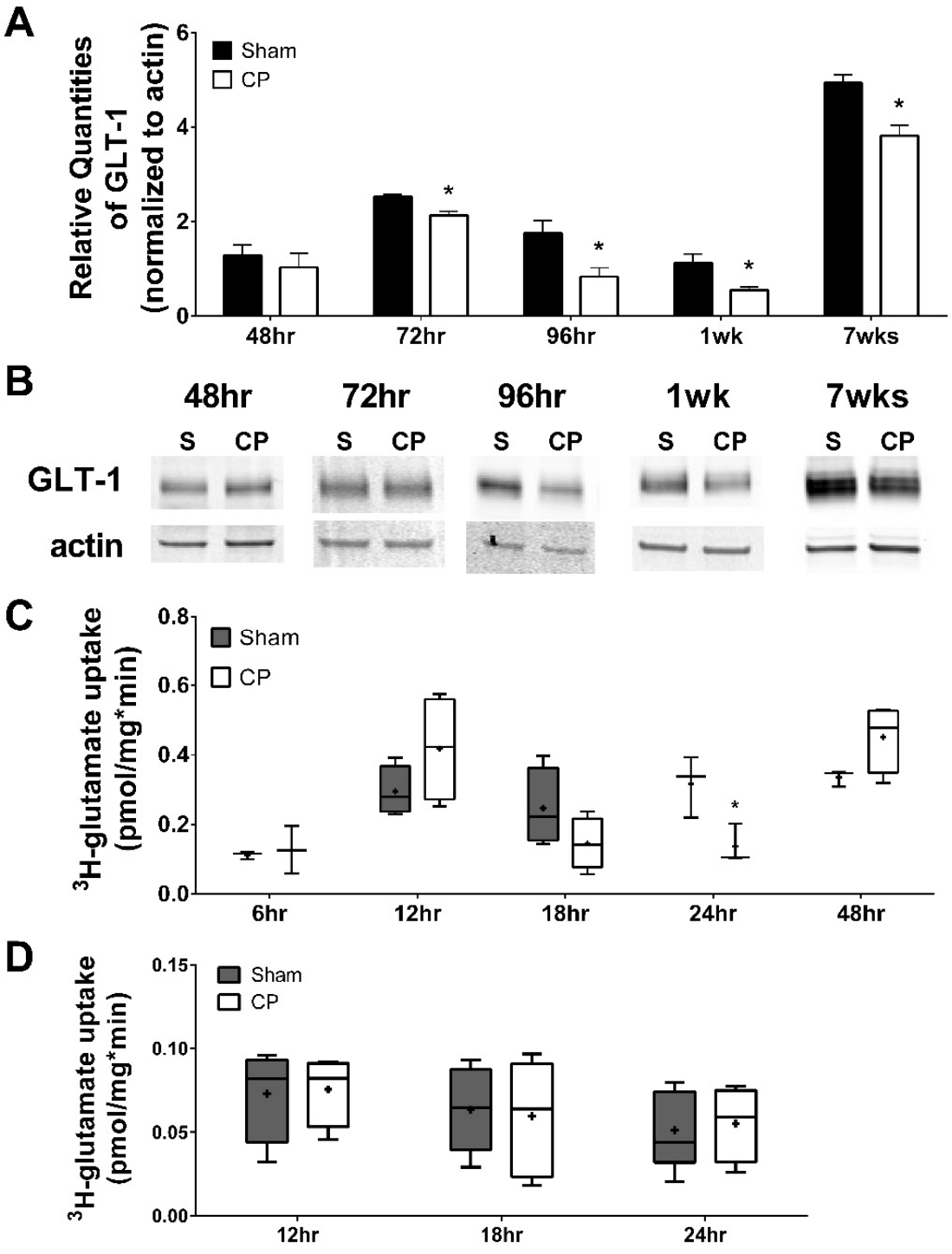
A
Relative Quantities of GLT-1 (normalized to actin)
Sham
CP
0
2
4
6
*
48hr
72hr
96hr
1wk
7wks
B
48hr
72hr
96hr
1wk
7wks
S
CP
GLT-1
actin
C
^{3}H-glutamate uptake (pmol/mg*min)
Sham
CP
0.0
0.2
0.4
0.6
0.8
6hr
12hr
18hr
24hr
48hr
D
^{3}H-glutamate uptake (pmol/mg*min)
Sham
CP
0.00
0.05
0.10
0.15
12hr
18hr
24hr

Figure 4.5. GLT-1 protein expression and function is decreased in the ipsilateral hippocampus following CP injury. A) Densitometric analysis from western blots of GLT-1 and actin in ipsilateral sham and CP hippocampus. GLT-1 was normalized to actin (loading control) and the ratios were plotted on a bar graph. GLT-1 protein expression was decreased in CP (white mice) compared to sham (black bars) mice, 72 hours after CP insults. Significance was determined using two-way ANOVA with post-hoc Tukey's multiple comparisons with $p<0.05$. Data are expressed as mean ± SEM, n = 3-5. B) Representative western blots showing GLT-1 and actin loading. Sham mice = S, Cerebral palsy mice = CP. GLT-1 was detected at 62kDa and actin was detected at 42 kDa. Synaptosomes were prepared from sham (gray bars) and CP (white bars) ipsilateral hippocampus and GLT-1 (C) mediated and GLAST/EAAC1 (D) mediated glutamate uptake was determined over an early time course following CP injury. GLT-1 function was decreased 24 hours after injury, which was restored by 48 hours. GLT-1 function is determined by DHK inhibition. GLAST/EAAC1 function was not changed over the early time course. GLAST/EAAC1 function is determined by TBOA inhibition. In C and D, data are expressed as a box and whisker plot with upper and lower bars at the minimum and maximum values, the line at the median, and the + at the mean n = 3-5. Overall significance was determined using a two-way ANOVA with post-hoc Tukey's multiple comparisons with $p<0.05$.

Discussion

Our results show that GFAP-positive astrocyte loss precedes neuron and oligodendrocyte death in CP injury. A decrease in glutamate clearance through GLT-1 is also shown early, and suggests that glutamate-sensitive neurons and oligodendrocytes are left vulnerable to excitotoxicity early after CP insults. Gray and white matter damage can cause neonatal motor deficits that persist into adulthood and may include cognitive disability. GFAP-positive astrocyte loss and GLT-1 dysfunction early after injury may be an underlying cause for the behavioral deficits noted in our CP mice (Chapter 3).

Current studies have not established the role of GLT-1 in a triple-hit (hypoxia-ischemia-inflammation) injury model of CP. Our results show that GFAP-immunoreactive astrocytes in the ipsilateral hippocampus are lost within 6 hours after CP insults and are not restored to sham levels until 48 hours after injury (Figure 4.1a). In addition to this early loss in GFAP-positive astrocytes, we also found significantly decreased GLT-1-dependent glutamate uptake at 24 hours (Figure 4.5b). Glutamate uptake by GLT-1 was not restored until 48 hours after injury, the same time that GFAP-reactive astrocytes were restored.

Neuron damage was noted 12 hours after injury (Figure 4.2), when GLT-1 first appears dysregulated, and neuronal apoptosis begins 24 hours after injury (Figure 4.3). Moreover, data from the Deng lab reported that white matter injury is most robust 96 hours following CP insults (163). These results provide evidence that astrocyte loss and dysfunctional GLT-1 precedes neuron and oligodendrocyte death.

One of the significant findings in this study was the loss of GFAP-positive astrocytes prior to neuron damage and gray and white matter death. Astrocyte loss early after neonatal insults have been implicated in human ischemic insults (52,53). Astrocytes

can be lost or injured due to oxygen and glucose depletion from HI (215). However, in our model, GFAP-positive astrocytes were lost early following injury but apoptotic astrocytes were not noted. In agreement with these findings, a model of transient ischemia in an adult rats did not cause astrocyte apoptosis, but did downregulate GFAP-immunoreactivity in astrocytes (216). Downregulation of GFAP in astrocytes could indicate astrocyte dysfunction early after injury, which may cause loss of potassium homeostasis, tropic support, and extracellular glutamate clearance.

GLT-1 was found to be dysfunctional in the ipsilateral hippocampus very early after insults. Although we show abnormalities in GLT-1 glutamate uptake activity, we found no changes in protein levels. Glutamate uptake into synaptosomes can be either through neurons, which contain very low levels of GLT-1, or through astrocytes, which contain the majority of GLT-1 protein (217). Weller and colleagues showed that the specific upregulation of GLT-1 in astrocytes increased DHK sensitive glutamate uptake in synaptosomes (218). However, recently, Petr and his group isolated synaptosomal preparations from transgenic mice with neuron- or astrocyte-specific GLT-1 knockouts and found that uptake mediated by neuronal GLT-1 was over-represented in synaptosome preparations (94). However, in Petr's studies, up to 40% of synaptosomal glutamate uptake was still due to GLT-1 expressed in astrocytes ((94) and reviewed by (219)). Using radioactive aspartate, an amino acid that can also be taken up by glutamate transporters, it has been shown that unlike aspartate uptake in hippocampal slices from the adult rodent brain (220), neurons in the immature, developing rodent brain (up to post-natal day 10) do not accumulate aspartate (221), suggesting that immature neurons do not express GLT-1. Furthermore, we did not detect changes in glutamate uptake from GLAST, which is

expressed at low levels in the immature hippocampus (80), and EAAC1, which is expressed primarily in neurons (60), with TBOA inhibition, indicating that changes in GLT-1 are probably due to astrocytes. Decreased glutamate uptake due to neuronal damage would include a decrease in EAAC1-mediated glutamate uptake, which is not seen. Therefore, the amount of glutamate uptake is attributed to astrocytic GLT-1.

Our data indicate that, with the decreased number of GFAP reactive astrocytes, comes a decrease in GLT-1 activity. Supporting decreased GLT-1 function, transient global HI in adult rats caused a significant reduction of the inward current evoked by astrocytic GLT-1 within the first 24 hours after insults (222). However, mechanisms exploring reduced GLT-1 function following HI are unknown.

Since GLT-1 transporter activity was less but protein levels were not changed, this could indicate post-translational modifications of GLT-1, causing transporter function to decrease, and leading to increased extracellular glutamate and excitotoxicity. Palmitoylation, a process in which a fatty acid is selectively attached to a cysteine, is important for changing the hydrophobicity of proteins, possibly for insertion into the cell membrane. In addition, palmitoylation may be involved in protein-protein interactions and in trafficking proteins within the cell. GLT-1 has putative palmitoylation sites and was found to be important for astrocytic GLT-1 function in a mouse model of Huntington's disease, a neurodegenerative disease that may involve an excitotoxic mechanism of cell death (133,134). Although not studied in hypoxia-ischemia, mutating GLT-1 at cysteine-38, the preferred palmitoylation site in the HD model, and expressing the mutation in cell culture, a 40% reduction in glutamate uptake activity was noted (133). Interestingly, 24 hours after insults in our model, there was an approximately 40% decrease in GLT-1

mediated glutamate uptake in CP mice. Thus, decreased palmitoylation of GLT-1 may be responsible for decreasing glutamate transporter activity following HIL in our model.

Sumoylation has been shown to cause GLT-1 internalization from the plasma membrane (136). In cell cultures, sumoylation of GLT-1 decreased glutamate uptake by changing GLT-1 localization and lowering the levels of GLT-1 protein at the cell surface but not lowering the protein expression of GLT-1 (136). In rat organotypic slice cultures following oxygen-glucose deprivation to mimic HI injury, total sumo-conjugated protein was increased (137). Therefore, increased sumoylation of GLT-1 could also reduce GLT-1 function without changing the amount of total GLT-1 protein expression.

It is also possible that protein kinase C (PKC) pathways are activated following CP insults causing internalization of GLT-1, thus, reducing GLT-1 function without changing total protein expression. Following transient HI, PKC increased in membrane fractions from the ischemic core (143), showing that PKC localization is changed after insults. Activation of PKC causes internalization of GLT-1 from the astrocyte cell surface (138,140,142). Therefore, the internalization of astrocytic GLT-1 by PKC may occur very early following CP insults, which would also decrease GLT-1 activity without changing total protein levels. Furthermore, post-translational modifications of proteins can occur quickly to change their activity or location.

In our studies, GLT -1 protein expression was decreased 72 hours after injury and continued to be lower for as long as seven weeks after injury. Multiple studies have shown decreased GLT-1 mRNA after HI insults (222–224). Following HI insults in the rat, GLT-1 mRNA was decreased in the CA1 region of the hippocampus 55-71% one day after insults and 68-75% four days after insults (224). If PKC or sumoylation mechanisms are

causing the internalization of GLT-1 after HI insults in our CP mouse model, it is possible that internalized GLT-1 protein remains stable very early after insults while GLT-1 mRNA is degraded. A paper by Zelenia and Robinson, published in 2000, showed that GLT-1 protein is stable for approximately 24 hours and was hyper-stabilized during periods of GLT-1 mRNA degradation in cell cultures (225). Hyperstabilization of internalized GLT-1 protein during early GLT-1 mRNA degradation could cause decreased GLT-1 function without changes in GLT-1 protein expression early after injury, followed by a delayed decreased in protein expression.

Interestingly, we found that neuron damage occurred 12 hours after injury in the ipsilateral hippocampus, neuron death in the ipsilateral hippocampus occurred maximally 48 hours after injury, and neuron loss was apparent seven weeks after injury. However, the loss of GFAP-reactive astrocytes began as early as 6 hours following injury and decreased GLT-1 function was noted 24 hours following injury. These data indicate that the loss of astrocytes and their functions precede neuron loss in our mouse model of CP.

It is clear from decades of studies that oligodendrocytes and neurons are extremely sensitive during development and an insult, such as HIL, may lead to cerebral palsy. However, illuminating the role of astrocytes very early after CP insults may change the way in which CP is studied and treated. In addition, future studies may determine disruptions in potassium homeostasis as well as decreased trophic support and increased harmful cytokines following CP insults, as astrocytes also contribute to these functions in the brain.

CHAPTER 5

BETA-LACTAM DRUG TREATMENT IS NEUROPROTECTIVE IN OUR MODEL OF CEREBRAL PALSY

Ceftriaxone has been shown to be neuroprotective and improve motor and cognitive outcomes following HI injury in the adult and neonatal rat (152,153,226,227). Studies have correlated the neuroprotective potential of ceftriaxone to an increase in GLT-1 function and protein expression (152,160,228). It appears that the increase in GLT-1 protein expression is through NF-κB-mediated transcriptional regulation. To elucidate if ceftriaxone increases GLT-1 protein expression through NF-κB, Lee and colleagues used primary human fetal astrocytes cultured with ceftriaxone and NF-κB inhibitors and found that the inhibition of NF-κB caused a decrease in GLT-1 promoter activity and protein expression (228). Furthermore, ceftriaxone caused the cytoplasmic degradation of IκBα (nuclear factor of kappa light polypeptide gene enhancer in B-cells inhibitor, alpha) and the translocation of p65, a subunit of NF-κB, into the nucleus, as well as an increase in luciferase activity driven by an NF-κB promoter region. These results suggest that ceftriaxone mediates GLT-1 protein expression through transcriptional regulation by NF-κB. Ceftriaxone treatment leading to NF-κB activation and translocation was also confirmed in a rat model of hemorrhage (229). Thus, ceftriaxone regulates GLT-1 protein expression and function through NF-κB and is neuroprotective in HI and excitotoxic brain insult models.

Although ceftriaxone seems like the perfect neuroprotective compound, it must be given in very high concentrations to reduce neurodegeneration in the brain due to its poor

blood brain barrier penetrability. Ceftriaxone also has antibiotic properties, making its clinical usefulness limited. When the ability of Ceftriaxone to increase GLT-1 expression was first reported (149), other compounds besides ceftriaxone were discovered, but they did not have as great an effect on GLT-1. One of the key features of all the compounds was that all of them had a beta-lactam ring. If the ring is the part of the structure that is able to modulate GLT-1 expression, then other compounds with a ring may work as well.

Clavulanic acid (CA) is similar to ceftriaxone in that it has a beta-lactam ring. However, CA also has a much better brain penetrability and can be given at lower doses than ceftriaxone. In addition, CA does not have antibiotic properties that would cause antibiotic resistance. Although CA has not been administered in a model of HI, it has been shown to reduce neuron death in mouse and rat models of neurological disease (160). Furthermore, CA administration showed a 2.5-fold increase in GLT-1 protein expression over control mice (155).

In addition to CA, we tested another beta-lactam compound, MC-100093 (093), designed by the Moulder Center for Drug Discovery Research at Temple University. Preliminary results obtained by the Moulder Center show that 093 does not have antibiotic properties.093 has also been used in a rat drug addiction study and shown to be both safe and efficacious. Following chronic cocaine administration, GLT-1 protein expression is decreased in the nucleus accumbens; however, 093 administration increases GLT-1 protein expression to sham levels.

We will test the neuroprotective properties of CA and 093 in our mouse model of CP. Since these compounds are beta-lactams, similar to ceftriaxone but with better blood brain barrier penetration, the hypothesis is that CA and 093 treatment after neonatal CP

insults will increase GLT-1 function and protein expression, reduce excitotoxicity following HI, and will confer neuroprotection.

Aims

Aim 1: Determine whether CA and 093 administration in our mouse CP model will increase GLT-1 expression and/or function.

Aim 2: Determine whether CA and 093 can decrease neuron and white matter volume loss in our CP model.

Aim 3: Determine whether CA and 093 can improve the motor and cognitive deficits in our CP model.

Results

GLT-1 function and protein expression are increased in CP mice with beta-lactam treatment

Many studies have shown that administration of beta-lactam compounds increases GLT-1 function and protein levels (149,155). In our early studies, we determined that GLT-1 function was decreased very early after CP insults with a recovery of function by 48 hours (Chapter 4). Additionally, we showed that GLT-1 protein was significantly decreased 72 hours to seven weeks after CP insults (Chapter 4).

With beta-lactam treatment, GLT-1 function did not show the small increase 12 hours after injury compared to injured, untreated animals and was normalized closer to sham levels by 18 and 24 hours after CP insults (Figure 5.1a). 093 treatment showed a significant increase in GLT-1 activity in CP mice at 18 and 24 hours after insults. CA

treatment showed a trend in improved GLT-1 activity 18 hours after injury and significantly increased GLT-1 function at 24 hours compared to CP mice without treatment. All other time points tested (72 hours to seven weeks after insults) did not show significant differences in GLT-1 function with treatment.

Glutamate aspartate transporter (GLAST; primarily in astrocytes of the cerebellum) and excitatory amino acid carrier 1 (EAAC1; primarily in neurons) activity, which was determined by TBOA inhibition, showed a trend in glutamate uptake in CP mice with beta-lactam treatment 18 and 24 hours after insults, with no significant changes noted at other time points (Figure 5.1b).

Beta-lactam administration increased GLT-1 protein levels from 48 hours to one week after insults (Figure 5.1c, d). With 093 treatment, GLT-1 protein was increased from 48 hours to 1 week, while CA administration produced a mild increase in GLT-1 protein levels at 48 to 96 hours after insults but was only significant 1 week following CP insults (Figure 5.1c). This may indicate that, like ceftriaxone, CA requires longer treatment to increase GLT-1 protein expression. All other time points tested (six hours to 24 hours) were not significantly different from GLT-1 protein levels in sham and CP.

Total number of GFAP-positive astrocytes in the hippocampus do not change with drug treatment

We have shown that GFAP-positive astrocyte numbers decrease 6-24 hours after injury in the ipsilateral hippocampus. The number of GFAP-positive astrocytes does not improve with beta-lactam drug treatment (data not shown).

CA treatment preserves neurons while 093 treatment delays neuron damage and reduces neuron death in the hippocampus early after injury

Previous studies have shown that CA reduced neuron loss in rodent models of neurological diseases (160). In our studies, beta-lactam treatment results in less or delayed neuron damage in the ipsilateral hippocampus early after injury (Figure 5.2). CA treatment shows an overall reduction in neuron damage while 093 treatment delays neuron damage. Additionally, beta-lactam treatment reduces neuronal apoptosis within the first few days following CP insults (Figure 5.3). Interestingly, specific to 093 treatment, apoptotic cell also death appears to be delayed compared to untreated CP mice.

When examining hippocampal volume, the volume was not significantly different between all groups (Sham, CP, and CP+drug) (Figure 5.4a). In beta-lactam treated animals, ipsilateral hippocampal volume shows a downward trend compared to mice without beta-lactam treatment. However, in the ipsilateral hippocampi treated with beta-lactams, there was a trend toward increased total neuron numbers (Figure 5.4b).

Beta-lactam treatment preserves white matter loss

Previously we showed that white matter volume decreased in two major regions following CP injury (Chapter 4). After beta-lactam treatment, the pyramidal tracts of CP mice show slight but significant improvement in volume on the ipsilateral side compared to CP mice without treatment (Figure 5.5a). No difference was noted in the shams or contralateral sides (Figure 5.5b).

Neonatal motor deficits are improved with beta-lactam administration

Neonatal CP mice were shown to have motor deficits 48 hours after injury (Chapter 3). Mid-way through the beta-lactam treatment protocol, 48 hours following insults,

neonatal mice were tested for motor deficits and compared to age-matched CP mice without treatment as well as sham mice. Beta-lactam treatment improved neonatal motor deficits, specifically ambulation score, ambulation angle, four limb grip strength, and grasping (Figure 5.6). CP mice with beta-lactam treatment had an improved ambulation score, indicating that their walking posture was more normal (Figure 5.6a). In addition, their hind limb ambulation angle decreased from 79° to 58° and 44° with CA and 093 treatments, respectively (Figure 5.6b). When testing four limb grip strength, the angle at which pups fell off improved from 69° to 93° with CA treatment and 96° with 093 treatment, demonstrating an improvement in paw strength (Figure 5.6c). Lastly, with beta-lactam treatment, grasping reflexes in CP mice developed similarly to shams and mice were able to grasp with more paws (Figure 5.6d). These tests, taken together, show that beta-lactam treatment helps preserve both gross and fine motor skills in our CP model.

Beta-lactam treatment in sham animals did not demonstrate any difference in motor testing from sham animals who were not treated (data not shown).

Adult behavior is improved with beta-lactam treatment

Adult CP mice were shown to have both motor and cognitive deficits following neonatal CP insults (Chapter 3). As a reminder, beta-lactam treatment was administered from PND 6-10, at which point the animals were allowed to live freely with its littermates until they reach 8 weeks old (adult).

Adult CP mice given beta-lactam compounds had improvements in both motor and cognitive abilities when compared to adult CP mice without treatment (Figure 5.7). Beta-lactam treatment reduced hind limb angle in CP mice from 60° to 48.5° (either treatment), close to sham levels (43.5°) (Figure 5.7a). Paw preference was abolished from an 18%

right paw preference to around 0% when comparing non-treated adult CP mice to treated mice, respectively (Figure 5.7b).

Rotarod testing revealed that adult CP mice treated with beta-lactam treatments were able to reach speeds of approximately double that of untreated CP mice (Figure 5.7c), indicating that early beta-lactam treatment improve balance and coordination in adult CP mice. These results show that beta-lactam treatment improves long-term motor deficits. In determining cognitive improvements with the novel object recognition test, beta-lactam treatment caused a 14% improvement in object recognition in CP mice (Figure 5.7d). No change was noted in motor or cognitive performance in sham mice with or without treatment (data not shown).

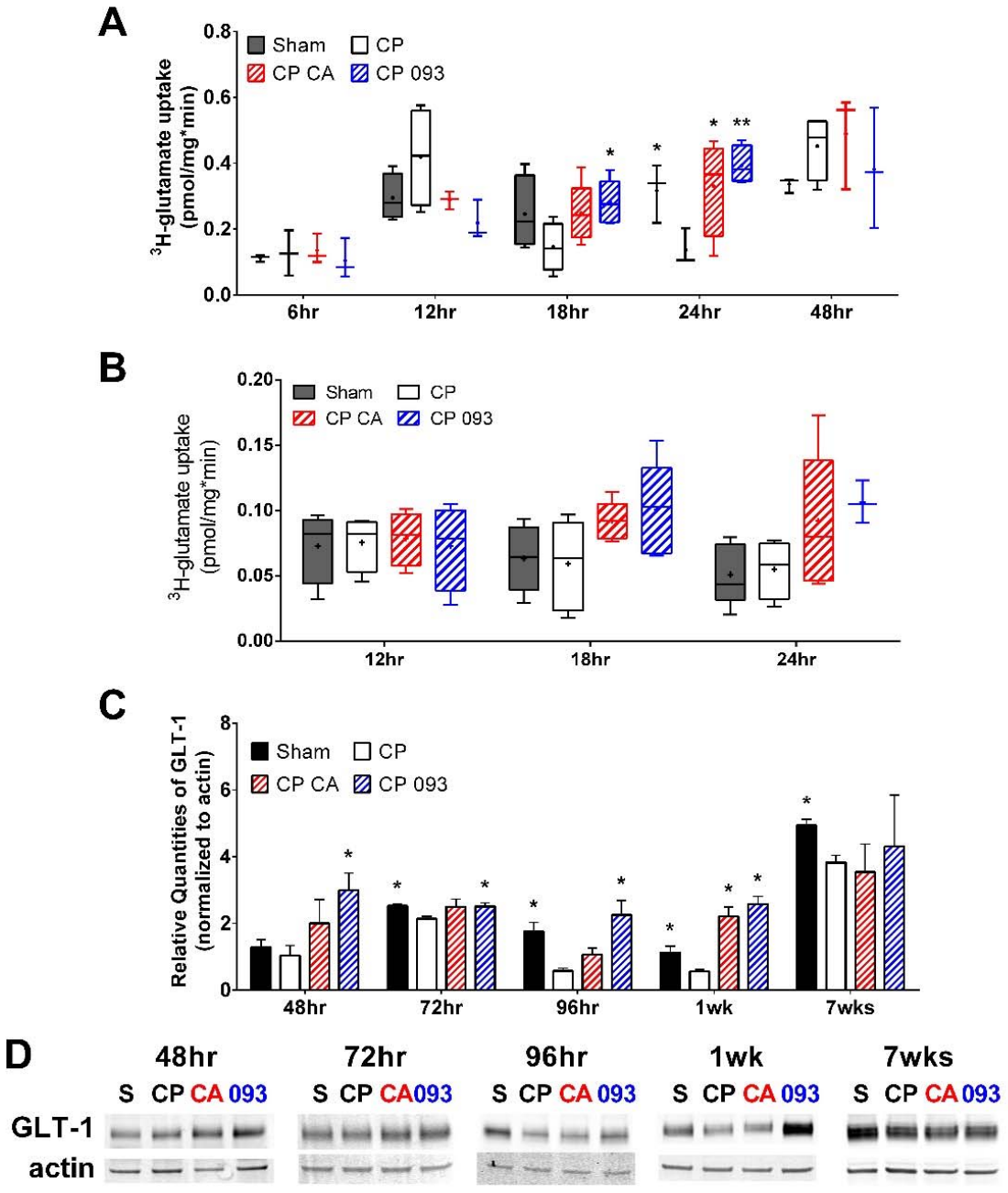
A
Sham
CP
CP CA
CP 093
^{3}H-glutamate uptake (pmol/mg*min)
0.8
0.6
0.4
0.2
0.0
6hr
12hr
18hr
24hr
48hr
B
Sham
CP
CP CA
CP 093
^{3}H-glutamate uptake (pmol/mg*min)
0.20
0.15
0.10
0.05
0.00
12hr
18hr
24hr
C
Sham
CP
CP CA
CP 093
Relative Quantities of GLT-1 (normalized to actin)
8
6
4
2
0
48hr
72hr
96hr
1wk
7wks
D
48hr
72hr
96hr
1wk
7wks
S CP CA 093
GLT-1
actin

Figure 5.1. Beta-lactam administration increased GLT-1 function and protein expression. A) Increased GLT-1 activity is noted from 18 to 24 hours in CP mice with beta-lactam treatment. Although not significant, CA treatment in CP mice shows a trend toward increasing GLT-1 function in CP mice 18 hours after injury with a significant increase at 24 hours. 093 treatment in CP mice displays a significant increase in GLT-1 function at 18 and 24 hours following injury. GLT-1 activity in CP treated mice was compared to CP mice with sham as a reference. B) GLAST/EAAC1 mediated glutamate uptake was determined over an early time course following CP injury and beta-lactam treatment. In A and B, specific activity was determined with glutamate transporter inhibitions (DHK and TBOA). Synaptosomes were prepared from sham (gray bars), CP (white bars), CP with CA treatment (red striped bars), and CP with 093 treatment (blue bars) ipsilateral hippocampus and GLT-1. A, B) Data are expressed as a box and whisker plot with upper and lower bars at the minimum and maximum values, the line at the median, and the + at the mean n = 3-5. Overall significance was determined using a two-way ANOVA with post-hoc Tukey's multiple comparisons with $p<0.05$ to determine significance within time points. C) Densitometric analysis from western blots of GLT-1 protein expression normalized to actin in ipsilateral sham (black bars), CP (white bars), CP+CA (red striped bars), and CP+093 (blue striped bars) hippocampus. Beta-lactam treatment increased GLT-1 protein expression. Overall significance was determined using two-way ANOVA and Tukey's multiple comparisons with $p<0.05$ to determine significance within each time point. Data are expressed as mean ± SEM n = 3-5. D) Representative western blots from 48 hours to seven weeks showing GLT-1 and actin loading. Sham mice = S, Cerebral palsy mice = CP. GLT-1 was detected at 62kDa and actin was detected at 42 kDa. Sham mice = S, Cerebral Palsy mice = CP, CP + CA = CA, CP + 093 = 093. GLT-1 was detected at 62kDa and actin was detected at 42 kDa.

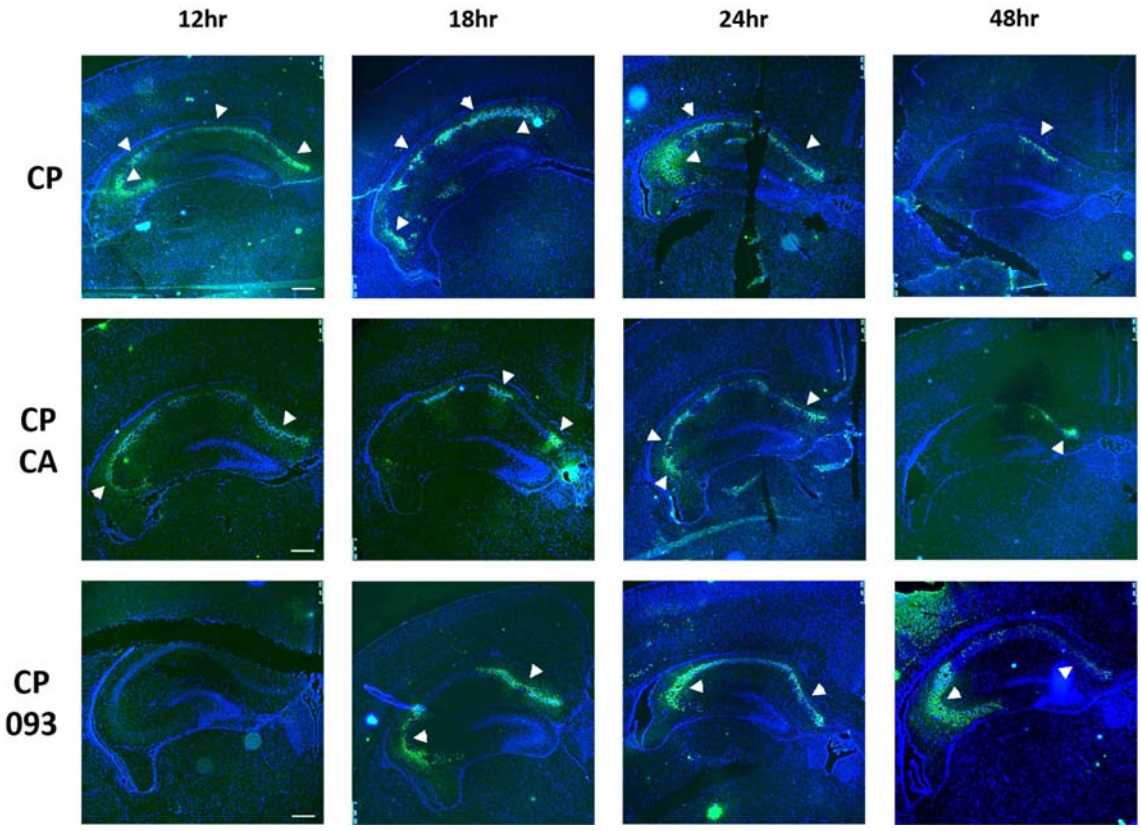

Figure 5.2. Neuron damage is decreased with CA treatment and delayed with 093 treatment. Fluoro-jade C staining of hippocampal sections was used to detect neuron damage. Representative sections are shown with nuclear staining (DAPI, blue) and apoptotic neurons (green) with regions of greatest damage highlighted (white arrow heads). In CP mice (top), injured neurons first appear at 12 hours, peak around 24 hours, and subside at 48 hours after injury. With CA treatment (middle), neuron damage is reduced from 12-48 hours after injury. 093 treatment (bottom), shows delayed apoptotic neuron staining at 18 hours and persisting until 48 hours. Scale bar, 200µm, applies to all panels. n = 3-5.

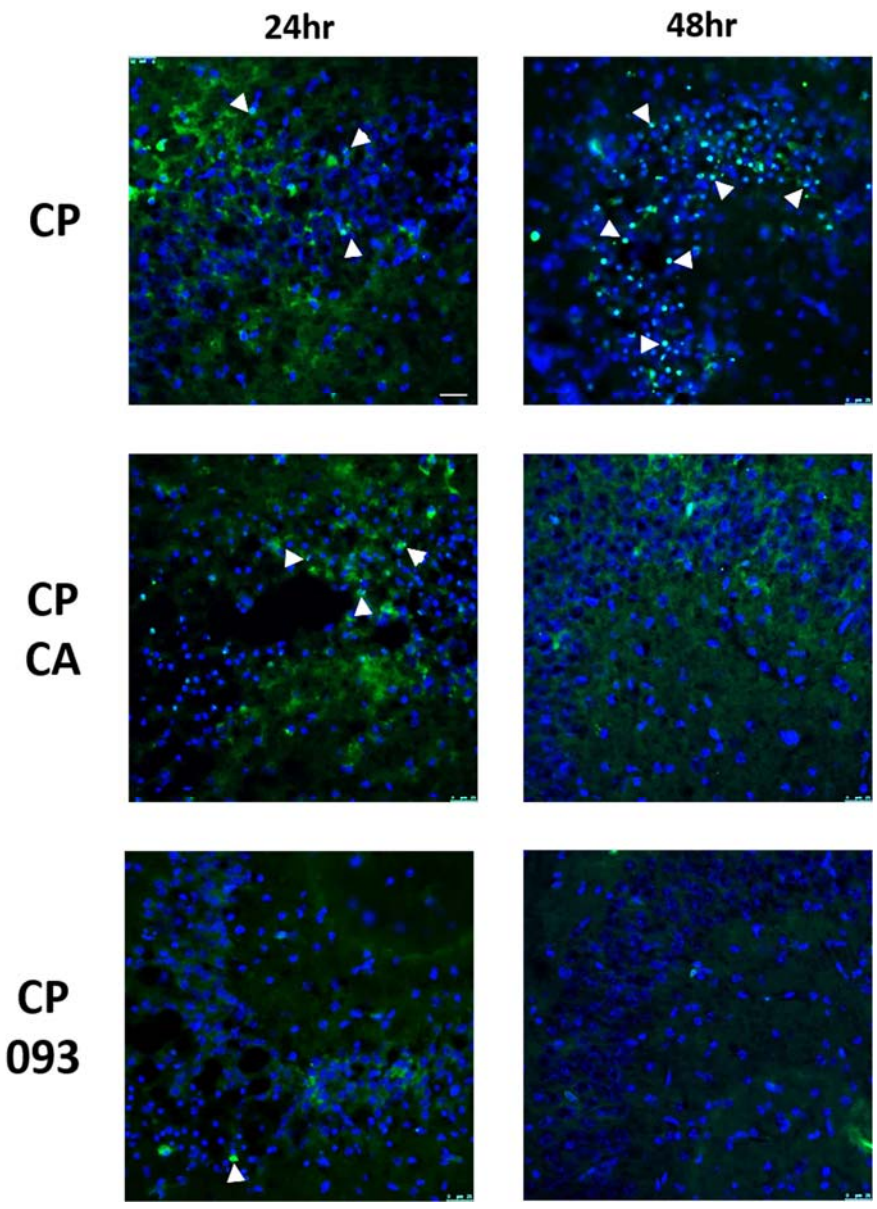

Figure 5.3. Beta-lactam treatment reduces apoptotic neurons in the ipsilateral hippocampus of CP mice. Apoptotic cells were detected using a TUNEL assay. A few apoptotic neurons first appear in CP mice 24 hours after injury and increase at 48 hours. Twenty-four hours after injury, decreased apoptosis is noted in CP mice with beta-lactam treatment (CA = middle, 093 = bottom) with no apoptosis noted at 48 hours. White arrow heads indicate apoptotic cells with DAPI (blue) and TUNEL (green) overlay. Representative sections are shown. Sham mice were stained at 48 hours. CP mice were stained at all time points but damage was only noted at 24 and 48 hours, as shown. Scale bar, 25µm, applies to all panels. All images show ipsilateral CA3 hippocampal staining. n = 3-5

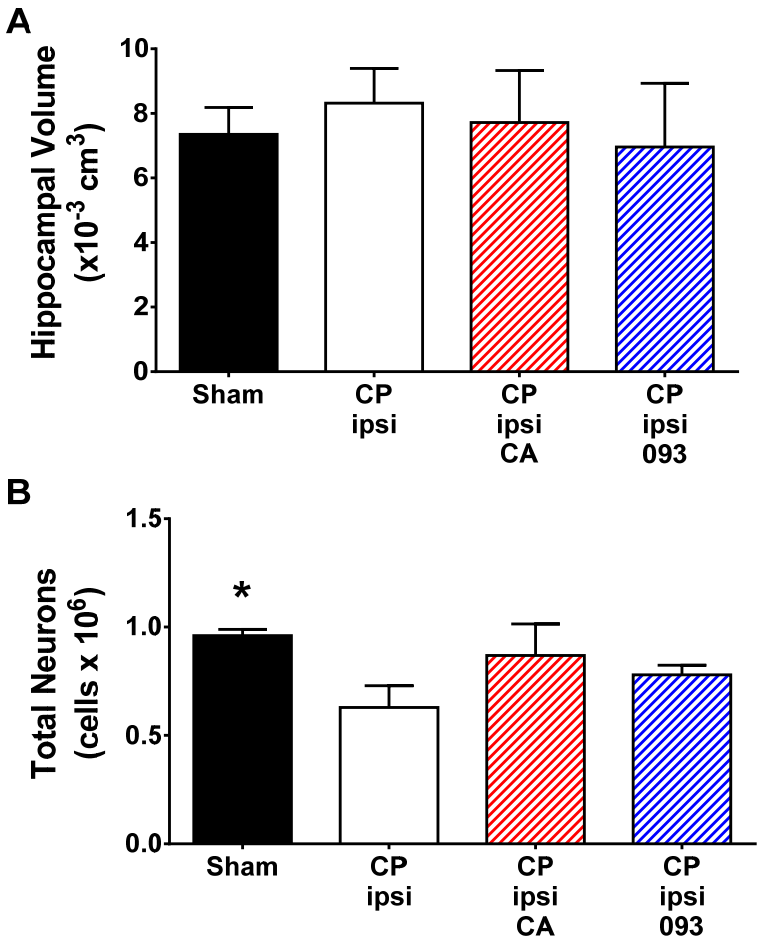

Figure 5.4. Hippocampal volume was not changed and neuronal cell numbers only slightly increased with beta-lactam treatment. Seven weeks after injury, sections were taken throughout the entire ipsilateral (ipsi) hippocampus and stained with cresyl violet. (A) The volume of the hippocampus was measured using Cavalieri's estimator of volume. The volume of the ipsilateral hippocampus with drug treatment (CP+CA = red striped bar, CP+093 = blue striped bar) does not change significantly from sham (black bar) or the ipsilateral (white bar) hippocampus in CP brains. (B) Neurons were counted throughout the entire hippocampus using systematic random sampling and the optical fractionator method. Ipsilateral hippocampi of both drug treatments (CP+CA = red striped bars, CP+093 + blue striped bars) show a trend toward increased neuron cell number but are not significant compared to neuron cell counts in the ipsilateral hippocampus of CP mice (white bar). Sham ipsilateral hippocampus is represented by the black bar. In both A and B, one-way ANOVA with Tukey's multiple comparisons post-hoc analysis was performed and $p<0.05$ (*) was considered significant. Data are expressed as mean ± SEM, n=3-6.

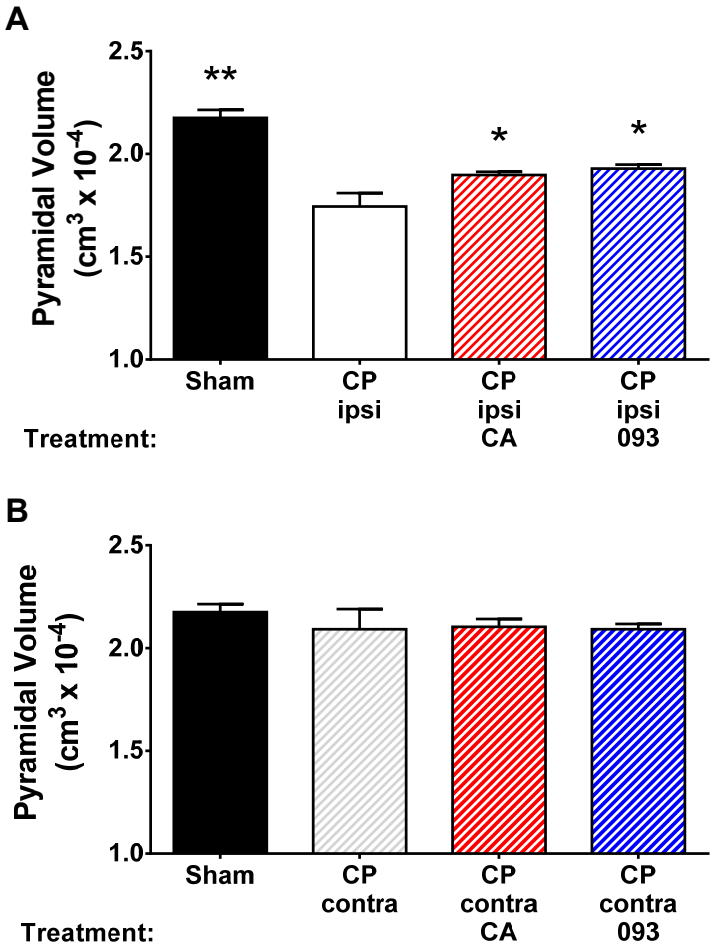

Figure 5.5. White matter volume in the ipsilateral brainstem pyramid is improved in CP mice treated with beta-lactam drugs. White matter staining was performed seven weeks after injury by Klüver-Barrera staining and stereology using Cavalieri's estimator of volume. A) Treatment of CP mice with beta-lactam compounds (CP+CA = red striped bar, CP+093 = blue striped bar) increased the volume of the ipsilateral (ipsi) pyramid compared to CP mice without treatment (white bar). Sham mice (black bar) was used as a control. B) The contralateral (contra) pyramid volumes are not significant between sham (black bar) and CP (white gray stripes) mice with or without administration of beta-lactams (CA = red with white stripes, 093 = blue with white stripes). In A and B, data are expressed as mean ± SEM, n=3-6. Statistical analysis was performed using a one-way ANOVA followed by Tukey's multiple comparison post-hoc analysis where $p<0.05$ (*).

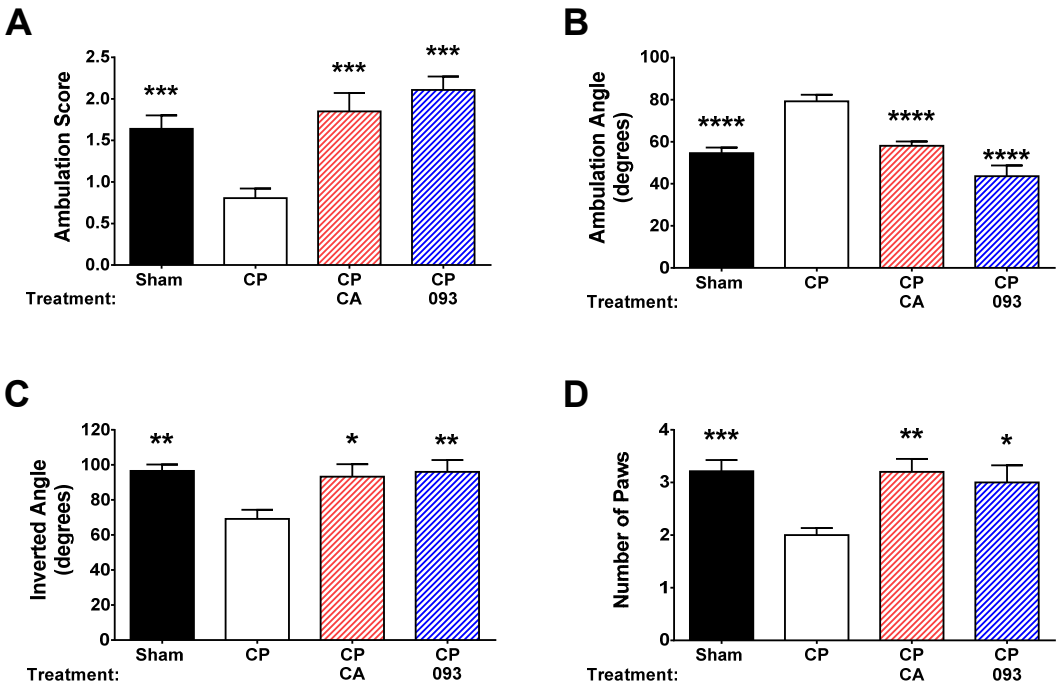

Figure 5.6. Neonatal motor deficits in CP mice are improved with beta-lactam treatment. Motor tests were performed in PND 6 CP pups, 48 hours after injury, with and without beta-lactam treatment to determine improvements in motor deficits. CA (red striped bar) and 093 (blue striped bar) improved gait analysis (ambulation: A, $p<0.0005$; hind limb ambulation angle: B, $p<0.0001$), four paw suspension (C, $p<0.05$), and grasping (D, $p<0.05$). In A-D, sham is represented by black bars, CP is represented by white bars, CP+CA is red striped bars, and CP+093 is blue striped bars. One-way ANOVA with Tukey's multiple comparisons post-hoc analysis was performed and $p<0.05$ (*) was considered significant. Other statistics include $p<0.005$ (**), $p<0.0005$ (***), and $p<0.0001$ (****). Data are expressed as mean ± SEM, n = 6-18.

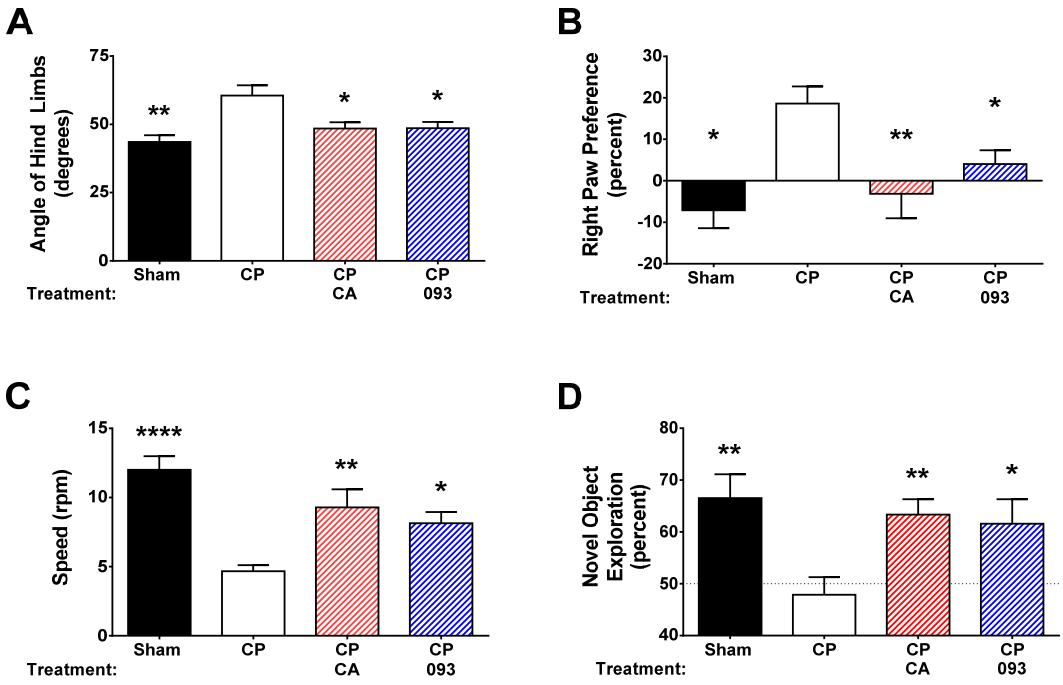

Figure 5.7. Behavioral deficits in adult CP mice are improved with beta-lactam drug treatment. Motor tests were performed on eight week old CP mice, seven weeks after injury, to determine improvements in motor deficits following beta-lactam treatment. Increased hind limb ambulation angle (A, $p<0.05$), right paw preference (B, $p<0.05$), and rotarod speed (C, $p<0.05$). (D) CP mice with beta-lactam treatment demonstrate improved cognition in the novel object recognition test ($p<0.05$). The dotted line represents 50% exploration, indicating that mice do not explore the novel object more than the old object. In A-D, sham is represented by black bars, CP is represented by white bars, CP+CA is red striped bars, and CP+093 is blue striped bars. One-way ANOVA with Tukey's multiple comparisons post-hoc analysis was performed and $p<0.05$ (*) was considered significant. Other statistics include $p<0.005$ (**), $p<0.0005$ (***), and $p<0.0001$ (****). Data are expressed as mean ± SEM, n = 5-26.

Discussion

Our results show that beta-lactams maintain GLT-1 function near sham levels early after injury, with significant improvements in GLT-1 activity noted at 24 hours with 093 treatment. GLT-1 protein levels are increased with beta-lactams later after injury, between 48 hours and 1 week. Furthermore, early neuron damage (Figure 5.2) as well as apoptotic neuron death (Figure 5.3) was decreased with beta-lactam drug treatment. An increasing trend in TBOA-sensitive glutamate uptake was also noted with beta-lactam treatment 18 and 24 hours after injury, with 093 treatment significantly increasing TBOA-sensitive GLAST and EAAC1 glutamate uptake 24 hours following insults. We also noted a trend in increased hippocampal neuron number seven weeks after injury and beta-lactam administration (Figure 5.4). In addition to reduced neuron damage and death, white matter was increased in CP mice treated with beta-lactams as evidenced by increases in brain stem pyramid volume (Figure 5.5).

Not only are cellular changes improved following CP insults with beta-lactams, neonatal and adult behavioral deficits were improved with beta-lactam treatment (Figure 5.6 and 5.7). Overall, these results show that beta-lactam treatment immediately following insults improve GLT-1 dysfunction and are neuroprotective in CP.

An important finding in these studies is that GLT-1 function and expression is increased with beta-lactam treatment. Early after injury, beta-lactam treatment caused a normalization of GLT-1 function with a trend in increased GLT-1 activity 18 and 24 hours after insult, but no changes in protein expression were detected. In an HI model in hippocampal slice cultures, administration of ceftriaxone decreased glutamate receptor stimulation in individual neurons and delayed hippocampal field potentials without an

increase in GLT-1 protein expression, indicating an increase in glutamate transporter function with beta-lactam treatment (227). Furthermore, in primary astrocyte cultures, ceftriaxone treatment increased glutamate uptake without increasing GLT-1 protein levels (226), supporting the ability of beta-lactams to increase GLT-1 function without protein expression.

It is possible that, in addition to improved GLT-1 activity, beta-lactams are decreasing injury early after insults through other mechanisms. Transition metals such as copper and iron can convert superoxide into aggressive reactive oxygen species and increase following ischemia (as reviewed by (230)). CA, however, is potentially neuroprotective by reducing ROS (231). Iron chelators can be neuroprotective against neonatal HI (232), and beta-lactams have been shown to be metal chelators (233), possibly reducing the damage done by transition metals and reactive oxygen species following CP insults. Transition metals can be detected in the blood serum of CP mice using ion chromatography and could be tested with and without beta-lactam administration.

Another potential beta-lactam mechanism of action early after insults is through the N-acetylated alpha-linked acidic dipeptidase (NAALADase), also called glutamate carboxypeptidase II (GCPII). GCPII is a neuropeptidase responsible for the extracellular hydrolysis of the neuropeptide N-acetyl-aspartyl-glutamate (NAAG) into N-acetyl-aspartate (NAA) and glutamate (234). The generation of extracellular glutamate through NAAG hydrolysis could lead to increased excitotoxicity under insults such as hypoxia-ischemia and inflammation. GCPII is observed in the human brain (235) and is expressed in the hippocampus (236), predominantly by astrocytes (237). The active site of GCPII is very similar to that of beta-lactamase, therefore, beta-lactams could potentially inhibit

GCPII cleavage of NAAG into NAA and glutamate. Consistent with this theory, studies have shown that the inhibition or deletion of GCPII is neuroprotective against excitatory insult in models of ischemia (238,239). Interestingly, beta-lactams are able to inhibit GCPII, reduce glutamate, and were protective against inflammation in a rat model of paw edema (240). The contribution of GCPII to injury in CP mice can be determined by inducing CP in GCPII deletion mice and determining the outcomes of injury with and without administration of beta-lactam compounds.

In our studies, increased GLT-1 protein expression without function was noted later after injury. Increased protein expression following beta-lactam administration may occur by activation of the NF-κB pathway, consistent with other findings (104,122,123). Future experiments could elucidate the contribution of NF-κB to GLT-1 protein levels by manipulation of the NF-κB pathways (241). However, GLT-1 protein levels do not appear to be important early after injury as levels are not increased until at least 48 hours and, at this time, GLT-1 activity is not significantly increased, indicating that the increased protein in our model is not active. GLT-1 protein localization could be determined through cellular fractionation of whole brain into cytoplasm and membrane samples followed by western blotting.

Beta-lactam treatment also decreased neuron damage and apoptosis early after injury; however, treatment showed a trend in improving long term neuronal survival but did not significantly improve total neuron numbers. These data suggest tertiary injury may occur causing the loss of mature neurons at a later time point, which is not blocked by the early time course of beta-lactam treatment. Tertiary injury in HI insults can include increased accumulation of transition metals (242), increased exposure to glucocorticoids

(243), and the generation of oxidative stress (244). In addition, as reviewed by Thorton, tertiary cell loss can also occur due to prolonged inflammatory responses, increased susceptibility to glutamate signaling, as well as impaired oligodendrocyte maturation and myelination (245). These mechanisms could cause neuron death that is delayed by weeks.

Another important finding in these studies is that beta-lactams improve behavioral deficits in CP mice. Minor but significant improvements in white matter and only a trend in increasing ipsilateral hippocampal neuron number suggests that functional reorganization and neuronal plasticity may occur following injury or during juvenile development. Functional reorganization without a significant increase in white matter volume may include synaptic rearrangement and reorganization (246,247) and axonal growth and new synapse formation (248) (as reviewed by (249)). Our data, showing a trend but not significant improvements in total hippocampal neuron numbers but improvements in adult motor and cognitive deficits, indicate that synaptic plasticity is likely occurring in the CP mice. It is possible that beta-lactam administration reduces extracellular glutamate through increased GLT-1 activity, allowing for less gray and white matter damage and an environment that facilitates synapse strengthening and reorganization.

The data presented here are the first pre-clinical evidence that beta-lactams may be efficacious immediately following HI and inflammatory insults leading to CP. Currently, there are no cures for CP and beta-lactam compounds may present a viable option.

CHAPTER 6

CONCLUSION

For decades, the focus of CP injury has been on oligodendrocytes because of PVL, the neuropathological hallmark in human CP patients. Here, we focus on astrocytes as an underlying cause to white matter injury. By using a novel CP mouse model that combined hypoxia, ischemia, and inflammation to better replicate the neuropathological findings of CP, we were able to establish an overall time course of cell death, implicate astrocyte and GLT-1 loss as a possible underlying mechanism for gray and white matter damage, and show changes in gross and fine motor behavior in both neonates and adults.

By establishing the time course of cell death, we predicted that there would be a treatment window within the first 48 hours after insults. By using beta-lactam compounds to increase GLT-1 function during the proposed treatment window, we were able to reduced neuron damage and apoptosis early after injury, increased white matter volume in the adult, and improve behavioral deficits in the neonate and the adult. This is the first time, to our knowledge, that astrocytes and GLT-1 have been implicated in CP pathophysiology and that a treatment window immediately after insults has been proposed. In conclusion, we have shown that underlying cellular changes, beginning with loss of astrocytes, sets the stage for the development of CP, including: PVL, neuronal cell death, and motor and cognitive deficits.

CHAPTER 7

FUTURE DIRECTIONS

Determining the Ideal Course of Beta-lactam Treatment

In the studies here, the dosing protocol of beta-lactam compounds were based off of previous studies of clavulanic acid as well as ceftriaxone (149,155,188) as well as the recommended doses from the Moulder Center for Drug Discovery Research, who provided the 093 compound. However, this treatment course may not offer the best neuroprotective outcomes. Therefore, other treatment protocols should be considered.

CA has a low half-life, approximately one hour, compared to ceftriaxone, which has a half-life of around 6-9 hours. Single daily dosing protocols, such as those for ceftriaxone, may not be appropriate for CA with a short half-life, suggesting that the neuroprotective potential of CA may increase with multiple daily dosing. When Augmentin, amoxicillin mixed with CA, is administered to neonates with infections, the recommended dose is 30mg amoxicillin/7.5mg CA per kg/day, divided every 12 hours. Calculating the concentration of CA indicates that neonates receive approximately 3.75mg/kg/dose. Clinical trials suggest that pediatric patients (2 months to 12 years of age) can receive doses of Augmentin containing 10mg/kg/day of CA divided every eight house. Although not tested in animals, these studies suggest that our dose of beta-lactam compounds may be appropriate, but spreading the dose over multiple daily injections may be beneficial.

In addition, the current administration protocol is five intraperitoneal injections of beta-lactam compounds over the first 96 hours following injury. Since our studies showed

that CA appears to exert its neuroprotective effects within the first 48 hours, a shorter course of beta-lactam administration, over the first 48 hours, should be tested. Last, it would be imperative to determine if beta-lactam administration could be delayed after insults and still exert the same neuroprotection. Administering beta-lactam compounds hours or days after injury would help narrow down the treatment window following insults.

Transcriptional or Post-Translational Changes of GLT-1 Following CP Injury

Our studies, and those of ceftriaxone, indicate that post-translational modifications early after insults may increase glutamate clearance in addition to increasing GLT-1 protein expression. However, mechanisms of GLT-1 function and expression following neonatal CP insults as well as CA and 093 treatment are unknown.

Post-translational modifications, such as palmitoylation or sumoylation, may play a role in GLT-1 function early after injury. Palmitated GLT-1 can be detected using acyl-biotin exchange (250). Sumoylation of GLT-1 in our model of CP could be determined by immunoprecipitation of SUMO proteins from whole brain extracts followed by western blotting for GLT-1 (135).

Transcriptional regulation of GLT-1 can also be explored in our model. GLT-1 mRNA can be detected by real-time quantitative polymerase chain reaction (RT-PCR) (222). Transcription of GLT-1 through the NF-κB pathway can be determined by inhibiting the NF-κB pathway at various proteins (241). The use of GLT1-BAC-eGFP reporter mice could also help to elucidate transcription of GLT-1 by NF-κB.

Biomarkers to Detect CP Brain Injury

In order to progress toward a cure for CP, we need to find better and earlier identification methods of neonatal HI and other risk factors. One of the major problems with early CP diagnosis is that imaging techniques are not sensitive enough to detect early or diffuse signs of brain injury (251). In CP, detection is complicated further by the fact that the majority of cases occur in utero, with no indication that fetal injury has occurred. Therefore, it may be weeks, months, or even years after the initial insult before the first confirmatory imaging studies are performed, delaying treatment or rendering certain therapeutic interventions useless. Biomarkers can be used to detect brain injury and predict outcomes (252) and may be used to assess the efficacy of therapeutic interventions. Since our studies show an early decrease in GFAP positive astrocytes, followed by later neuron and oligodendrocyte loss, multiple biomarkers may be used to determine the presence of CP injury as well as the progression of cell loss. In a 2006 study, maternal biomarkers were used to detect in utero intraventricular hemorrhage (253), demonstrating that maternal blood sampling may be used to monitor the health status of the fetus. However, no studies have examined whether biomarkers can be used to detect in utero PVL (254) or CP.

Current common biomarkers of brain injury include GFAP and serum protein 100-beta (s100β) for astrocytes, neuron-specific nuclear protein neuronal nuclei (NeuN) and ubiquitin protein hydrolase-1 (UCH-L1) to detect neurons, and myelin basic protein (MBP) for oligodendrocyte detection (as reviewed by (254)). An enzyme-linked immunosorbent assay (ELISA) can be used to measure the concentration of antibodies in blood serum. ELISAs can be constructed with the ELISA development kits. Blood serum can then be added and the markers will be captured and detected and concentrations can be determined.

Testing Beta-lactam Neuroprotection in Humans

Currently, there is no cure for CP or HI insults before or during birth. In our mouse model of CP, the FDA-approved compound CA and a novel compound with similar structure (093) displayed neuroprotection early after neonatal HIL insults. Furthermore, these compounds improved neonatal and adult motor and cognitive deficits in this model without harmful behavioral outcomes in sham mice. To determine if our results could translate to humans, preliminary studies in neonates could be conducted.

Studies may include the administration of beta-lactam compounds to infants with complicated births and deliveries or clinical hypoxic-ischemic encephalopathy (HIE). These insults occur during labor and, therefore, drug administration could occur at time of insult, similar to our mouse model of CP. Currently in the Philadelphia, PA area, neonates from difficult labors are being transferred to St. Christopher's Hospital in Philadelphia where they are administered drugs and undergo hyperthermia in an attempt to reduce brain injury. A small pilot study could be conducted on these infants where beta-lactams are administered within the first six hours of insults. Based on the administration of Augmentin/clavulanic acid and tolerance in pediatric patients, dosing of beta-lactams would begin at 10mg/kg/day administered in half doses every 12 hours (5mg/kg/day administered twice a day) (157).

Additionally, beta-lactams could be administered to women that present with CP risk factors during the third trimester of their pregnancy. Clavulanic acid is already FDA approved for use in pregnant women and infants. Studies would first have to be performed to determine how well beta-lactam compounds cross the placenta as well as the amount of beta-lactam that penetrates the fetal brain when administered to mothers. However, because

clavulanic acid does not have antibiotic properties and because sham animals with beta-lactam administration do not have adverse cellular or behavioral outcomes, it may be a viable option for administration in pregnant women with CP risk factors.

REFERENCES CITED

1. Little W. On the influence of abnormal parturition, difficult labours, premature birth, and asphyxia neonatorum, on the mental and physical condition of the child, especially in relation to deformities. Lancet. 1853;3:293.

2. Freud S. Les diplegies cerebrales infantiles. Paris: Paris: G. Masson; 1893. 178-183 p.

3. Murphy C, Yeargin-Allsopp, Decoufle P, Drews C. Prevelance of cerebral palsy among ten-year-old children in metropolitan Atlanta, 1985 through 1987. J Pediatr. 1993;123(5):S13–9.

4. Blair E, Watson L. Epidemiology of cerebral palsy. Paediatr Child Health (Oxford). 2006;11:117–25.

5. Himmelmann K, Hagberg G, Beckung E, Olow B, Wendt LV. The changing panorama of cerebral palsy in Sweden. VII. Prevalence and origin in the birth year period 1987-90. Acta Paediatr. 2005;94:287–94.

6. United Cerebral Palsy [Internet]. 2015 [cited 2016 May 26]. Available from: ucp.org

7. Cerebral Palsy [Internet]. Cerebral Palsy Alliance. 2016 [cited 2016 May 2]. Available from: https://www.cerebralpalsy.org.au/

8. Sigurdardottir S, Indredavik MS, Eiriksdottir A, Einarsdottir K, Gudmundsson HS, Vik T. Behavioural and emotional symptoms of preschool children with cerebral palsy: A population-based study. Dev Med Child Neurol. 2010;52(11):1056–61.

9. Parkes J, White-Koning M, Dickinson HO, Thyen U, Arnaud C, Beckung E, et al. Psychological problems in children with cerebral palsy: A cross-sectional European study. J Child Psychol Psychiatry Allied Discip. 2008;49(4):405–13.

10. Korzeniewski SJ, Birbeck G, DeLano MC, Potchen MJ, Paneth N. A systematic review of neuroimaging for cerebral palsy. J Child Neurol. 2008;23(2):216–27.

11. Cerebral Palsy : Hope Through Research [Internet]. NINDS. [cited 2016 Jun 29]. Available from: http://www.ninds.nih.gov/disorders/cerebral_palsy/detail_cerebral_palsy.htm

12. Zupan V, Gonzalez P, Lacaze-Masmonteil T, Boithias C, D'Allest AM, Dehan M, et al. Periventricular leukomalacia: risk factors revisited. Dev Med Child Neurol [Internet]. 1996;38(12):1061–7. Available from: http://www.ncbi.nlm.nih.gov/pubmed/8973291

13. Volpe JJ. Neurobiology of periventricular leukomalacia in the premature infant. Pediatr Res. 2001;50(5):553–62.

14. Khwaja O, Volpe JJ. Pathogenesis of cerebral white matter injury of prematurity. Arch Dis Child Fetal Neonatal Ed [Internet]. 2008;93(2):F153–61. Available from: http://www.pubmedcentral.nih.gov/articlerender.fcgi?artid=2569152&tool=pmcentrez&rendertype=abstract

15. Takashima S, Tanaka K. Development of cerebrovascular architecture and its relationship to periventricular leukomalacia. Arch Neurol. 1978;35(1):11–6.

16. Ballabh P, Braun A, Nedergaard M. Anatomic analysis of blood vessels in germinal matrix, cerebral cortex, and white matter in developing infants. Pediatr Res. 2004;56(1):117–24.

17. Altman DI, Powers WJ, Perlman JM, Herscovitch P, Volpe SL, Volpe JJ. Cerebral blood flow requirement for brain viability in newborn infants is lower than in adults. Ann Neurol. 1988;24:218–26.

18. Powers WJ, Grubb RL, Darriet D, Raichle ME. Cerebral blood flow and cerebral metabolic rate of oxygen requirements for cerebral function and viability in humans. J Cereb Blood Flow Metab [Internet]. 1985;5(4):600–8. Available from: http://jcb.sagepub.com/content/5/4/600.abstract

19. Pryds O, Greisen G, Lou H, Frils-Hansen B. Heterogeneity of cerebral vasoreactivity in preterm infants supported by mechanical ventilation. J Pediatr. 1989;115(4):638–45.

20. Børch K, Greisen G. Blood Flow Distribution in the Normal Human Preterm Brain. Pediatr Res. 1998;43(1):28–33.

21. Kuban KC, Gilles FH. Human telencephalic angiogenesis. Ann Neurol. 1985;17:539–48.

22. Back S a, Luo NL, Borenstein NS, Levine JM, Volpe JJ, Kinney HC. Late oligodendrocyte progenitors coincide with the developmental window of vulnerability for human perinatal white matter injury. J Neurosci. 2001;21(4):1302–12.

23. Nelson KBMD, Grether JKP. Causes of cerebral palsy. Curr Opin Pediatr. 1999. p. 487–91.

24. Nelson K. Thrombophilias, perinatal stroke, and cerebral palsy. Clin Obs Gynecol [Internet]. 2006;49(4):875–84. Available from: http://www.ncbi.nlm.nih.gov/pubmed/17082682

25. Nelson KB, Ellenberg JH. Antecedents of Cerebral Palsy: Multivariate Analysis of Risk. N Engl J Med. 1986;315:81–6.

26. Blair E, Stanley FJ. Intrapartum asphyxia: A rare cause of cerebral palsy. J Pediatr. 1988;112(4):515–9.

27. Dixon G, Badawi N, Kurinczuk J, Keogh J, Silburn S, Zubrick S, et al. Early Developmental Outcomes Aftern Newborn Encephalopathy. Pediatrics. 2002;109(1):26–33.

28. Ellenberg JH, Nelson KB. The association of cerebral palsy with birth asphyxia: a definitional quagmire. Dev Med Child Neurol. 2013;55:210–6.

29. Tan S. Fault and blame, insults to the perinatal brain may be remote from time of birth. Clin Perinatol. 2014;41(1):105–17.

30. Lee J, Croen L a, Backstrand KH, Yoshida CK, Henning LH, Lindan C, et al. Maternal and Infant Characteristics Associated with Perinatal Arterial Stroke in the Infant. JAMA. 2005;293(6):723–9.

31. Lee J, Croen L a, Lindan C, Nash KB, Yoshida CK, Ferriero DM, et al. Predictors of outcome in perinatal arterial stroke: a population-based study. Ann Neurol [Internet]. 2005;58(2):303–8. Available from: http://www.ncbi.nlm.nih.gov/pubmed/16010659

32. Wu YW, Lynch JK, Nelson KB. Perinatal arterial stroke: Understanding mechanisms and outcomes. Semin Neurol. 2005;25(4):424–34.

33. Andiné P, Sandberg M, Bågenholm R, Lehmann a, Hagberg H. Intra- and extracellular changes of amino acids in the cerebral cortex of the neonatal rat during hypoxic-ischemia. Brain Res Dev Brain Res [Internet]. 1991;64(1-2):115–20. Available from: http://www.ncbi.nlm.nih.gov/pubmed/1786636

34. Puka-Sundvall M, Sandberg M, Hagberg H. Brain injury after hypoxia-ischemia in newborn rats: relationship to extracellular levels of excitatory amino acids and cysteine. Brain Res [Internet]. 1997;750(1-2):325–8. Available from: http://www.ncbi.nlm.nih.gov/pubmed/9098561

35. Sokolowska P, Passemard S, Mok a, Schwendimann L, Gozes I, Gressens P. Neuroprotective effects of NAP against excitotoxic brain damage in the newborn mice: implications for cerebral palsy. Neuroscience [Internet]. IBRO; 2011;173:156–68. Available from: http://www.ncbi.nlm.nih.gov/pubmed/21073926

36. Marret S, Mukendi R, Gadisseux J, Gressens P, Evrard P. Effect of ibotenate on brain development: an excitotoxic mouse model of microgyria and posthypoxic-like lesions. J Neuropathol Exp Neurol. 1995;54(3):358–70.

37. Hagberg H, Gilland E, Diemer NH AP. Hypoxia-Ischemia in the Neonatal Rat Brain: Histopathology after Post-Treatment with NMDA and Non-NMDA Receptor Antagonists. Biol Neonate [Internet]. 1994 [cited 2015 Nov

1];66(4):205–13. Available from: http://www.karger.com.libproxy.temple.edu/Article/Pdf/244109

38. Follett PL, Rosenberg P a, Volpe JJ, Jensen FE. NBQX attenuates excitotoxic injury in developing white matter. J Neurosci [Internet]. 2000;20(24):9235–41. Available from: http://www.ncbi.nlm.nih.gov/pubmed/11125001

39. Follett PL. Glutamate Receptor-Mediated Oligodendrocyte Toxicity in Periventricular Leukomalacia: A Protective Role for Topiramate. J Neurosci [Internet]. 2004;24(18):4412–20. Available from: http://www.jneurosci.org/cgi/doi/10.1523/JNEUROSCI.0477-04.2004

40. Rezaie P, Dean A. Periventricular leukomalacia, inflammation and white matter lesions within the developing nervous system. Neuropathology. 2002;22(3):106–32.

41. Eastman N, M D. The etiology of cerebral palsy. Am J Obstet Gynecol. 1955;69(5):950–61.

42. Grether JK, Nelson KB. Maternal infection and cerebral palsy in infants of normal birth weight. JAMA [Internet]. 1997;278(3):207–11. Available from: http://www.ncbi.nlm.nih.gov/pubmed/9218666

43. Wu CS, Pedersen LH, Miller JE, Sun Y, Streja E, Uldall P, et al. Risk of Cerebral Palsy and Childhood Epilepsy Related to Infections before or during Pregnancy. PLoS One. 2013;8(2):1–7.

44. Dammann O, Leviton A. Maternal Intrauterine Infection, Cytokines, and Brain Damage in the Preterm Newborn. Pediatr Res [Internet]. Nature Publishing Group; 1997 Jul 1 [cited 2015 Sep 26];42(1):1–8. Available from: http://www.nature.com.libproxy.temple.edu/pr/journal/v42/n1/full/pr19972261a.html

45. Bo Hyun Yoon, Romero R, Soon Ha Yang, Jong Kwan Jun, Kim IO, Choi - JH, et al. Interleukin-6 concentrations in umbilical cord plasma are elevated in neonates with white matter lesions associated with periventricular leukomalacia. Am J Obstet Gynecol. 1996;174(5):1433–40.

46. Yoon BH, Jun JK, Romero R, Park KH, Gomez R, Choi J-H, et al. Amniotic fluid inflammatory cytokines (interleukin-6, interleukin-1β, and tumor necrosis factor-α), neonatal brain white matter lesions, and cerebral palsy. Am J Obstet Gynecol [Internet]. 1997;177(1):19–26. Available from: http://www.sciencedirect.com/science/article/pii/S0002937897704320

47. Kadhim H, Tabarki B, De Prez C, Sébire G. Cytokine immunoreactivity in cortical and subcortical neurons in periventricular leukomalacia: are cytokines implicated in neuronal dysfunction in cerebral palsy? Acta Neuropathol [Internet]. 2003;105(3):209–16. Available from:

http://www.ncbi.nlm.nih.gov/pubmed/12557006

48. Kumral A, Baskin H, Yesilirmak DC, Ergur BU, Aykan S, Genc S, et al. Erythropoietin attenuates lipopolysaccharide-induced white matter injury in the neonatal rat brain. Neonatology [Internet]. 2007;92(4):269–78. Available from: http://www.ncbi.nlm.nih.gov/pubmed/17627093

49. Duncan JR, Cock ML, Scheerlinck JPY, Westcott KT, McLean C, Harding R, et al. White matter injury after repeated endotoxin exposure in the preterm ovine fetus. Pediatr Res. 2002;52(6):941–9.

50. Duncan J, Cock M, Suzuki K, Scheerlinck J, Harding R, REES S. Chronic Endotoxin Exposure Causes Brain Injury in the Ovine Fetus in the Absence of Hypoxemia. J Soc Gynecol Investig [Internet]. 2006;13(2):87–96. Available from: http://rsx.sagepub.com/cgi/doi/10.1016/j.jsgi.2005.12.003

51. Sofroniew M V., Vinters H V. Astrocytes: biology and pathology. Acta Neuropathol [Internet]. 2010;119(1):7–35. Available from: http://link.springer.com/10.1007/s00401-009-0619-8

52. Villapol S, Gelot A, Renolleau S, Charriaut-Marlangue C. Astrocyte responses after neonatal ischemia: the yin and the yang. Neuroscientist. 2008;14(July 2008):339–44.

53. Gelot A, Villapol S, Billette de Villemeur T, Renolleau S, Charriaut-Marlangue C. Astrocytic demise in the developing rat and human brain after hypoxic-ischemic damage. Dev Neurosci [Internet]. 2009;31(5):459–70. Available from: http://www.ncbi.nlm.nih.gov/pubmed/19672074

54. Garcia JH, Yoshida Y, Chen H, Li Y, Zhang ZG, Lian J, et al. Progression from ischemic injury to infarct following middle cerebral artery occlusion in the rat. Am J Pathol [Internet]. 1993;142(2):623–35. Available from: http://www.pubmedcentral.nih.gov/articlerender.fcgi?artid=1886726&tool=pmcentrez&rendertype=abstract

55. Liu D, Smith CL, Barone FC, Ellison JA, Lysko PG, Li K, et al. Astrocytic demise precedes delayed neuronal death in focal ischemic rat brain. Mol Brain Res. 1999;68:29–41.

56. Chen H, Chopp M, Schultz L, Bodzin G, Garcia JH. Sequential neuronal and astrocytic changes after transient middle cerebral artery occlusion in the rat. J Neurol Sci. 1993;118(2):109–16.

57. Liu W, Shen Y, Plane JM, Pleasure DE, Deng W. Neuroprotective potential of erythropoietin and its derivative carbamylated erythropoietin in periventricular leukomalacia. Exp Neurol [Internet]. Elsevier B.V.; 2011;230(2):227–39. Available from: http://www.pubmedcentral.nih.gov/articlerender.fcgi?artid=3114206&tool=pmcen

trez&rendertype=abstract

58. Shen Y, Liu X-B, Pleasure DE, Deng W. Axon-glia synapses are highly vulnerable to white matter injury in the developing brain. J Neurosci Res [Internet]. 2012;90(1):105–21. Available from: http://www.pubmedcentral.nih.gov/articlerender.fcgi?artid=3209489&tool=pmcentrez&rendertype=abstract

59. Schousboe A. Transport and metabolism of glutamate and GABA in neurons and glial cells. Int Rev Neurobiol. 1981;22:1–45.

60. Danbolt NC. Glutamate uptake. Prog Neurobiol. 2001;65:1–105.

61. Jensen FE. Role of glutamate receptors in periventricular leukomalacia. J Child Neurol. 2005;20(12):950–9.

62. Ribeiro F, Paquet M, Cregan S, Ferguson S. Group I metabotropic glutamate receptor signalling and its implication in neurological disease. CNS Neurol Disord Drug Targets. 2010;9(5):574–95.

63. Itoh T, Beesley J, Itoh A, Cohen AS, Kavanaugh B, Coulter DA, et al. AMPA glutamate receptor-mediated calcium signaling is transiently enhanced during development of oligodendrocytes. J Neurochem. 2002;81(2):390–402.

64. Insel TR, Miller LP, Gelhard RE. The ontogeny of excitatory amino acid receptors in the rat forebrain-I. N-methyl-D-aspartate and quisqualate receptors. Neuroscience. 1990;35(1):31–43.

65. Deng W, Pleasure J, Pleasure D. Progress in periventricular leukomalacia. Arch Neurol [Internet]. 2008;65(10):1291–5. Available from: http://www.ncbi.nlm.nih.gov/pubmed/18852342

66. Johnston M V., Hoon AH. Cerebral Palsy. Neuromolecular Med. 2006;8:435–50.

67. Van den Berg CJ, Garfinkel D. A stimulation study of brain compartments. Metabolism of glutamate and related substances in mouse brain. BiochemJ. 1971;123(0264-6021 (Print)):211–8.

68. Martinez-Hernandez AA, Bell KP, Norenberg MD. Glutamine Synthetase : Glial Localization in Brain. Science (80-). 1977;195(4284):1356–8.

69. Gjessing L, Gjesdahl P, Sjaastad O. The free amino acids in human cerebrospinal fluid. J Neurochem. 1972;19(February):1807–8.

70. Hamberger A, Nyström B. Extra- and intracellular amino acids in the hippocampus during development of hepatic encephalopathy. Neurochem Res [Internet]. 1984;9(9):1181–92. Available from: http://eutils.ncbi.nlm.nih.gov/entrez/eutils/elink.fcgi?dbfrom=pubmed&id=650423

4&retmode=ref&cmd=prlinks\npapers2://publication/uuid/0375343D-5D82-4127-B1BB-2F4F44F631E6

71. Albrecht J, Sidoryk-Węgrzynowicz M, Zielińska M, Aschner M. Roles of glutamine in neurotransmission. Neuron Glia Biol [Internet]. 2010;6(4):263–76. Available from: http://www.ncbi.nlm.nih.gov/pubmed/22018046

72. Varoqui H, Zhu H, Yao D, Ming H, Erickson JD. Cloning and functional identification of a neuronal glutamine transporter. J Biol Chem. 2000;275(6):4049–54.

73. Yao D, Mackenzie B, Ming H, Varoqui H, Zhu H, Hediger MA, et al. A novel system A isoform mediating Na+/neutral amino acid cotransport. J Biol Chem. 2000;275(30):22790–7.

74. Sugawara M, Nakanish T, Fei Y, Huang W, Ganapathy M, Leibach F, et al. Cloning of an Amino Acid Transporter with Functional Characteristics and Tissue Expression Pattern Identical to That of System A. J Biol Chem [Internet]. 2000;275(22):16473–7. Available from: http://www.jbc.org/cgi/doi/10.1074/jbc.C000205200

75. Rothstein JD, Martin L, Levey AI, Dykes-Hoberg M, Jin L, Wu D, et al. Localization of neuronal and glial glutamate transporters. Neuron. 1994;13(3):713–25.

76. Lehre KP, Danbolt NC. The Number of Glutamate Transporter Subtype Molecules at Glutamatergic Synapses : Chemical and Stereological Quantification in Young Adult Rat Brain. 1998;18(21):8751–7.

77. Tanaka K, Watase K, Manabe T, Yamada K, Watanabe M, Takahashi K, et al. Epilepsy and Exacerbation of Brain Injury in Mice Lacking the Glutamate Transporter GLT-1. Science (80-) [Internet]. 1997;276(5319):1699–702. Available from: http://www.sciencemag.org/cgi/doi/10.1126/science.276.5319.1699

78. Desilva TM, Kabakov AY, Goldhoff PE, Volpe JJ, Paul A. Regulation of Glutamate Transport in Developing Rat Oligodendrocytes. J Neurosci. 2009;29(24):7898–908.

79. Holmseth S, Dehnes Y, Huang YH, Follin-Arbelet V V., Grutle NJ, Mylonakou MN, et al. The Density of EAAC1 (EAAT3) Glutamate Transporters Expressed by Neurons in the Mammalian CNS. J Neurosci. 2012;32(17):6000–13.

80. Furuta a, Rothstein JD, Martin LJ. Glutamate transporter protein subtypes are expressed differentially during rat CNS development. J Neurosci. 1997;17(21):8363–75.

81. Bar-Peled O, Ben-Hur H, Biegon a, Groner Y, Dewhurst S, Furuta a, et al.

Distribution of glutamate transporter subtypes during human brain development. J Neurochem. 1997;69(6):2571–80.

82. Yamada K, Wantanabe M, Shibata T, Tanaka K, Wada K, Inoue Y. EAAT4 - EAAT4 is a post-synaptic glutamate transporter at Purkinji cell synapses. 1996. p. 2013–7.

83. Arriza JL, Eliasof S, Kavanaugh MP, Amara SG. Excitatory amino acid transporter 5, a retinal glutamate transporter coupled to a chloride conductance. Proc Natl Acad Sci U S A. 1997;94(8):4155–60.

84. Pow D V., Barnett NL. Developmental expression of excitatory amino acid transporter 5: A photoreceptor and bipolar cell glutamate transporter in rat retina. Neurosci Lett. 2000;280(1):21–4.

85. Levy LM, Warr O, Attwell D. Stoichiometry of the Glial Glutamate Transporter GLT-1 Expressed Inducibly in a Chinese Hamster Ovary Cell Line Selected for Low Endogenous Na ⁺ -Dependent Glutamate Uptake. 1998;18(23):9620–8.

86. Billups B, Rossi D, Oshima T, Warr O, Takahashi M, Sarantis M, et al. Physiological and pathological operation of glutamate transporters. Prog Brain Res. 1998;116:45–57.

87. Zerangue N, Kavanaugh M. Flux coupling in a neuronal glutamate transporter. Nature. 1996;383(6601):634–7.

88. Rose EM, Koo JCP, Antflick JE, Ahmed SM, Angers S, Hampson DR. Glutamate transporter coupling to Na,K-ATPase. J Neurosci [Internet]. 2009;29(25):8143–55. Available from: http://www.ncbi.nlm.nih.gov/pubmed/19553454

89. Danbolt NC, Furness DN, Zhou Y. Neuronal vs glial glutamate uptake: Resolving the conundrum. Neurochem Int [Internet]. Elsevier Ltd; 2016;98:29–45. Available from: http://linkinghub.elsevier.com/retrieve/pii/S0197018616301085

90. Wadiche JI, Arriza JL, Amara SG, Kavanaugh MP. Kinetics of a human glutamate transporter. Neuron. 1995;14:1019–27.

91. Otis TS, Jahr CE. Anion currents and predicted glutamate flux through a neuronal glutamate transporter. J Neurosci. 1998;18(18):7099–110.

92. Wadiche JI, Kavanaugh MP. Macroscopic and microscopic properties of a cloned glutamate transporter/chloride channel. J Neurosci. 1998;18(19):7650–61.

93. Otis TS, Kavanaugh MP. Isolation of current components and partial reaction cycles in the glial glutamate transporter EAAT2. J Neurosci. 2000;20(8):2749–57.

94. Petr GT, Sun Y, Frederick NM, Zhou Y, Dhamne SC, Hameed MQ, et al. Conditional deletion of the glutamate transporter GLT-1 reveals that astrocytic

GLT-1 protects against fatal epilepsy while neuronal GLT-1 contributes significantly to glutamate uptake into synaptosomes. J Neurosci [Internet]. 2015;35(13):5187–201. Available from: /pmc/articles/PMC4380995/?report=abstract

95. Watase K, Hashimoto K, Kano M, Yamada K, Watanabe M, Inoue Y, et al. Motor discoordination and increased susceptibility to cerebellar injury in GLAST mutant mice. 1998;10(June 1997):976–88.

96. Peghini P, Janzen J, Stoffel W. Glutamate transporter EAAC-1-deficient mice develop dicarboxylic aminoaciduria and behavioral abnormalities but no neurodegeneration. 1997;16(13):3822–32.

97. Rothstein J, Dykes-Hoberg M, Ca P, La B, Jin L, Rw K, et al. Antisense knockout of glutamate transporters reveals a predominant role for astroglial glutamate transport in excitotoxicity and clearance of extracellular glutamate. Neuron [Internet]. 1996;16:675–86. Available from: papers2://publication/uuid/327F682D-2D03-48C7-A0E6-A57E2CD92157

98. Pines G, Danbolt NC, Bjørås M, Zhang Y, Bendahan A, Eide L, Koepsell H, Storm-Mathisen J, Seeberg E KB. Cloning and expression of a rat brain L-glutamate transporter. Nature. 1992;360(6403):464–7.

99. Danbolt N, Storm-Mathisen J, Kanner BI. AN [Na+, K+] COUPLED L-GLUTAMATE TRANSPORTER PURIFIED FROM RAT BRAIN IS LOCATED IN GLIAL CELL PROCESSES. Neuroscience. 1992;51(2):295–310.

100. Levy LM, Lehre KP, Rolstad B, Danbolt NC. A monoclonal antibody raised against an [Na+ + K+] coupled L- glutamate transporter purified from rat brain confirms glial cell localization. FEBS Lett. 1993;317/1,2(1):79–84.

101. Robinson MB. The family of sodium-dependent glutamate transporters: a focus on the GLT-1/EAAT2 subtype. Neurochem Int [Internet]. 1998;33(6):479–91. Available from: http://www.ncbi.nlm.nih.gov/pubmed/10098717

102. Benediktsson A, Marrs G, Tu J, Worley P, Rothstein J, Bergles D, et al. NEURONAL ACTIVITY REGULATES GLUTAMATE TRANSPORTER DYNAMICS IN DEVELOPING ASTROCYTES A.M. Glia. 2012;60(2):175–88.

103. Yang Y, Gozen O, Watkins A, Lorenzini I, Lepore A, Gao Y, et al. Pre-synaptic regulation of astroglial excitatory neurotransmitter transporter GLT1. Neuron [Internet]. Elsevier Ltd; 2009;61(6):880–94. Available from: http://www.pubmedcentral.nih.gov/articlerender.fcgi?artid=2743171&tool=pmcentrez&rendertype=abstract

104. Ghosh M, Yang Y, Rothstein JD, Robinson MB. Nuclear factor-κB contributes to neuron-dependent induction of glutamate transporter-1 expression in astrocytes. J Neurosci [Internet]. 2011;31(25):9159–69. Available from:

http://www.pubmedcentral.nih.gov/articlerender.fcgi?artid=3138498&tool=pmcentrez&rendertype=abstract

105. Utsunomiya-tate N, Endou H, Kanai Y. Tissue specific variants of glutamate transporter GLT-1. FEBS Lett [Internet]. Federation of European Biochemical Societies; 1997;416(3):312–6. Available from: http://dx.doi.org/10.1016/S0014-5793(97)01232-5

106. Arriza JL, Fairman WA, Amara SG, Kavanaugh P, Wadiche I, Murdoch H. Functional Comparisons of Three Glutamate Cloned from Human Motor Cortex Transporter. 1994;14(September):5559–69.

107. Chen W, Aoki C, Mahadomrongkul V, Gruber CCE, Wang GJG, Blitzblau R, et al. Expression of a Variant Form of the Glutamate Transporter GLT1 in Neuronal Cultures and in Neurons and Astrocytes in the Rat Brain. J Neurosci. 2002;22(6):2142–52.

108. Schmitt A, Asan E, Lesch K-P, Kugler P. A splice variant of glutamate transporter GLT1/EAAT2 expressed in neurons: cloning and localization in rat nervous system. Neuroscience [Internet]. 2002;109(1):45–61. Available from: http://www.ncbi.nlm.nih.gov/pubmed/11784699

109. Pollard M, McGivan J. The rat hepatoma cell line H4-II-E-C3 expresses high activities of the high-affinity glutamate transporter GLT-1A. FEBS Lett. 2000;484(2):74–6.

110. Munch C, Ebstein M, Seefried U, Zhu B, Stamm S, Landwehrmeyer GB, et al. Alternative splicing of the 5'-sequences of the mouse EAAT2 glutamate transporter and expression in a transgenic model for amyotrophic lateral sclerosis. J Neurochem [Internet]. 2002;82(3):594–603. Available from: http://www.ncbi.nlm.nih.gov/entrez/query.fcgi?cmd=Retrieve&db=PubMed&dopt=Citation&list_uids=12153483

111. Rozyczka J, Engele J. Multiple 5′-splice variants of the rat glutamate transporter-1. Mol Brain Res. 2005;133(1):157–61.

112. Rauen T, Wießner M, Sullivan R, Lee A, Pow D V. A new GLT1 splice variant : cloning and immunolocalization of GLT1c in the mammalian retina and brain. 2004;45:1095–106.

113. Peacey E, Miller CCJ, Dunlop J, Rattray M. The Four Major N- and C-Terminal Splice Variants of the Excitatory Amino Acid Transporter GLT-1 Form Cell Surface Homomeric and Heteromeric Assemblies. Mol Pharmacol. 2009;75(5):1062–73.

114. Haugeto Ø, Ullensvang K, Levy LM, Chaudhry FA, Honore T, Nielsen M, et al. Brain Glutamate Transporter Proteins Form Homomultimers *. 1996;271(44):27715–22.

115. Yernool D, Boudker O, Jin Y, Gouaux E. Structure of a glutamate transporter homologue from Pyrococcus horikoshii. Nature. 2004;431:811–8.

116. Raunser S, Haase W, Bostina M, Parcej DN, Kühlbrandt W. High-yield expression, reconstitution and structure of the recombinant, fully functional glutamate transporter GLT-1 from Rattus norvegicus. J Mol Biol. 2005;351:598–613.

117. Gendreau S, Voswinkel S, Torres-Salazar D, Lang N, Heidtmann H, Detro-Dassent S, et al. A trimeric quaternary structure is conserved in bacterial and human glutamate transporters. J Biol Chem. 2004;279(38):39505–12.

118. Slotboom DJ, Lolkema JS, Konings N, Konings WN. Membranes and Bioenergetics : Membrane Topology of the C-terminal Half of the Neuronal , Glial , and Bacterial Glutamate Transporter Family Membrane Topology of the C-terminal Half of the Neuronal , Glial , and Bacterial Glutamate Transporter Family *. 1996;271(49):31317–21.

119. Wahle S, Stoffel W. Membrane topology of the high-affinity L-glutamate transporter (GLAST-1) of the central nervous system. J Cell Biol [Internet]. 1996;135(6 Pt 2):1867–77. Available from: http://www.pubmedcentral.nih.gov/articlerender.fcgi?artid=2133971&tool=pmcentrez&rendertype=abstract

120. Grunewald M, Bendahan A, Kanner BI. Biotinylation of single cysteine mutants of the glutamate transporter GLT-1 from rat brain reveals its unusual topology. Neuron. 1998;21(3):623–32.

121. Seal RP, Amara SG. A reentrant loop domain in the glutamate carrier EAAT1 participates in substrate binding and translocation. Neuron. 1998;21(6):1487–98.

122. Su Z, Leszczyniecka M, Kang D, Sarkar D, Chao W, Volsky DJ, et al. Insights into glutamate transport regulation in human astrocytes: cloning of the promoter for excitatory amino acid transporter 2 (EAAT2). Proc Natl Acad Sci U S A. 2003;100(4):1955–60.

123. Sitcheran R, Gupta P, Fisher PB, Baldwin AS. Positive and negative regulation of EAAT2 by NF-kappaB: a role for N-myc in TNFalpha-controlled repression. EMBO J [Internet]. 2005;24(3):510–20. Available from: http://www.pubmedcentral.nih.gov/articlerender.fcgi?artid=548660&tool=pmcentrez&rendertype=abstract

124. Lee E, Sidoryk-Wegrzynowicz M, Wang N, Webb A, Son DS, Lee K, et al. GPR30 regulates glutamate transporter GLT-1 expression in rat primary astrocytes. J Biol Chem. 2012;287(32):26817–28.

125. Karki P, Webb A, Smith K, Lee K, Son D-S, Aschner M, et al. cAMP response element-binding protein (CREB) and nuclear factor κB mediate the tamoxifen-

induced up-regulation of glutamate transporter 1 (GLT-1) in rat astrocytes. J Biol Chem [Internet]. 2013;288(40):28975–86. Available from: http://www.ncbi.nlm.nih.gov/pubmed/23955341

126. Kumar R, Prasad GS. Differential Regulation of GLT-1 / EAAT2 Gene Expression by NF- j B and N-myc in Male Mouse Brain During Postnatal Development. Neurochem Res. 2014;39:150–60.

127. Bartels DJ, Mitchell DA, Dong X, Deschenes RJ. Erf2, a novel gene product that affects the localization and palmitoylation of Ras2 in Saccharomyces cerevisiae. Mol Cell Biol [Internet]. 1999;19(10):6775–87. Available from: http://www.pubmedcentral.nih.gov/articlerender.fcgi?artid=84674&tool=pmcentrez&rendertype=abstract

128. Fukata M, Fukata Y, Adesnik H, Nicoll RA, Bredt DS, Francisco S. Identification of PSD-95 Palmitoylating Enzymes University of California at San Francisco. Neuron. 2004;44:987–96.

129. Yokoi N, Fukata Y, Sekiya A, Murakami T, Kobayashi K, Fukata M. Identification of PSD-95 Depalmitoylating Enzymes. J Neurosci. 2016;36(24):6431–44.

130. Lobo S, Greentree WK, Linder ME, Deschenes RJ. Identification of a Ras palmitoyltransferase in Saccharomyces cerevisiae. J Biol Chem. 2002;277(43):41268–73.

131. Roth AF, Feng Y, Chen L, Davis NG. The yeast DHHC cysteine-rich domain protein Akr1p is a palmitoyl transferase. J Cell Biol. 2002;159(1):23–8.

132. Fukata Y, Fukata M. Protein palmitoylation in neuronal development and synaptic plasticity. Nat Rev Neurosci [Internet]. Nature Publishing Group; 2010;11(3):161–75. Available from: http://www.ncbi.nlm.nih.gov/pubmed/20168314

133. Huang K, Kang MH, Askew C, Kang R, Sanders SS, Wan J, et al. Palmitoylation and function of glial glutamate transporter-1 is reduced in the YAC128 mouse model of Huntington disease. Neurobiol Dis [Internet]. Elsevier Inc.; 2010;40:207–15. Available from: http://dx.doi.org/10.1016/j.nbd.2010.05.027

134. Wan J, Savas JN, Roth AF, Sanders SS, Singaraja RR, Hayden MR, et al. Tracking brain palmitoylation change: Predominance of glial change in a mouse model of Huntington's disease. Chem Biol. 2013;20(11):1421–34.

135. Gibb SL, Boston-Howes W, Lavina ZS, Gustincich S, Brown RH, Pasinelli P, et al. A caspase-3-cleaved fragment of the glial glutamate transporter EAAT2 is sumoylated and targeted to promyelocytic leukemia nuclear bodies in mutant SOD1-linked amyotrophic lateral sclerosis. J Biol Chem. 2007;282(44):32480–90.

136. Foran E, Rosenblum L, Bogush A, Pasinelli P, Trotti D. Sumoylation of the

astroglial glutamate transporter EAAT2 governs its intracellular compartmentalization. Glia. 2014;62(8):1241–53.

137. Cimarosti H, Henley JM. Investigating the Mechanisms Underlying Neuronal Death in Ischemia Using In Vitro Oxygen-Glucose Deprivation : Potential Involvement of Protein SUMOylation Europe PMC Funders Author Manuscripts In Vivo Models of Ischemia. Neuroscientist. 2008;14(6):626–36.

138. Garcia-Tardon N, Gonzolez-Gonolez IM, Martinez-Villarreal J, Fernandez-Sanchez E, Gimenez C, Zafra F. Protein kinase C (PKC)-promoted endocytosis of glutamate transporter GLT-1 requires ubiquitin ligase Nedd4-2-dependent ubiquitination but not phosphorylation. J Biol Chem. 2012;287(23):19177–87.

139. Zhou J, Sutherland M. Glutamate Transporter Cluster Formation in Astrocytic Processes Regulates Glutamate Uptake Activity. J Neurosci [Internet]. 2004;24(28):6301–6. Available from: http://www.jneurosci.org/cgi/doi/10.1523/JNEUROSCI.1404-04.2004

140. Kalandadze A, Wu Y, Robinson MB. Protein kinase C activation decreases cell surface expression of the GLT-1 subtype of glutamate transporter: Requirement of a carboxyl-terminal domain and partial dependence on serine 486. J Biol Chem. 2002;277(48):45741–50.

141. González MI, Susarla BTS, Robinson MB. Evidence that protein kinase Cα interacts with and regulates the glial glutamate transporter GLT-1. J Neurochem. 2005;94(5):1180–8.

142. Guillet BA, Velly LJ, Canolle B, Masmejean FM, Nieoullon AL, Pisano P. Differential regulation by protein kinases of activity and cell surface expression of glutamate transporters in neuron-enriched cultures. Neurochem Int. 2005;46(4):337–46.

143. Matsumoto S, Shamloo M, Matsumoto E, Isshiki A, Wieloch T. Protein kinase C-gamma and calcium/calmodulin-dependent protein kinase II-alpha are persistently translocated to cell membranes of the rat brain during and after middle cerebral artery occlusion. J Cereb blood flow Metab. 2004;24:54–61.

144. McDonald JW, Silverstein FS, Johnston M V. MK-801 protects the neonatal brain from hypoxic-ischemic damage. Eur J Pharmacol. 1987;140(3):359–61.

145. Gilland E, Puka-Sundvall M, Hillered L, Hagberg H. Mitochondrial function and energy metabolism after hypoxia-ischemia in the immature rat brain: involvement of NMDA-receptors. J Cereb Blood Flow Metab [Internet]. 1998;18(3):297–304. Available from: http://jcb.sagepub.com/content/18/3/297.full

146. Hansen HH, Briem T, Dzietko M, Sifringer M, Voss A, Rzeski W, et al. Mechanisms leading to disseminated apoptosis following NMDA receptor blockade in the developing rat brain. Neurobiol Dis. 2004;16(2):440–53.

147. Ikonomidou C, Bosch F, Miksa M, Bittigau P, Vöckler J, Dikranian K, et al. Blockade of NMDA Receptors and Apoptotic Neurodegeneration in the Developing Brain. Science (80-). 1999;283(5398):70–4.

148. Soni N, Reddy BVK, Kumar P. GLT-1 transporter: An effective pharmacological target for various neurological disorders. Pharmacol Biochem Behav [Internet]. Elsevier Inc.; 2014;127:70–81. Available from: http://dx.doi.org/10.1016/j.pbb.2014.10.001

149. Rothstein JD, Patel S, Regan MR, Haenggeli C, Huang YH, Bergles DE, et al. Beta-lactam antibiotics offer neuroprotection by increasing glutamate transporter expression. Nature [Internet]. 2005;433(7021):73–7. Available from: http://www.ncbi.nlm.nih.gov/pubmed/15635412

150. World Health Organization. Second Meeting of the Subcommittee of the Expert Committee on the Selection and Use of Essential Medicines Geneva, 29 September to 3 October 2008. 2008;

151. Rasmussen BA, Baron DA, Kim JK, Unterwald EM, Scott M. β-Lactam antibiotic produces a sustained reduction in extracellular glutamate in the nucleus accumbens of rats. Amino Acids. 2011;40(2):761–4.

152. Mimura K, Tomimatsu T, Minato K, Jugder O, Kinugasa-Taniguchi Y, Kanagawa T, et al. Ceftriaxone preconditioning confers neuroprotection in neonatal rats through glutamate transporter 1 upregulation. Reprod Sci. 2011;18(12):1193–201.

153. Lai PC, Huang YT, Wu CC, Lai C, Wang PJ, Chiu TH. Ceftriaxone attenuates hypoxic-ischemic brain injury in neonatal rats. J Biomed Sci [Internet]. BioMed Central Ltd; 2011 Jan [cited 2015 Nov 1];18(1):69. Available from: http://www.jbiomedsci.com/content/18/1/69

154. Steadman E, Raisch DW, Bennett CL, Esterly JS, Becker T, Postelnick M, et al. Evaluation of a potential clinical interaction between ceftriaxone and calcium. Antimicrob Agents Chemother. 2010;54(4):1534–40.

155. Kim J, John J, Langford D, Walker E, Ward S, Rawls SM. Clavulanic acid enhances glutamate transporter subtype I (GLT - 1) expression and decreases reinforcing efficacy of cocaine in mice. Amino Acids [Internet]. Springer Vienna; 2015;48(3):689–96. Available from: "http://dx.doi.org/10.1007/s00726-015-2117-8

156. Kim DJ, King JA, Zuccarelli L, Ferris CF, Koppel GA, Snowdon CT, et al. Clavulanic acid: A competitive inhibitor of beta-lactamases with novel anxiolytic-like activity and minimal side effects. Pharmacol Biochem Behav [Internet]. Elsevier Inc.; 2009 [cited 2015 Nov 1];93(2):112–20. Available from: http://linkinghub.elsevier.com/retrieve/pii/S0091305709001336

157. GlaxoSmithKline. Highlights of Prescribing Information: AUGMENTIN. US

Food and Drug Administration.

158. Bolton GC, Allen GD, Davies BE, Filer CW, Jeffery DJ. The disposition of clavulanic acid in man. Xenobiotica fate foreign Compd Biol Syst. 1986;16(9):853–63.

159. Nakagawa H, Yamada M, Tokiyoshi K, Miyawaki Y KT. Penetration of potassium clavulanate/ticarcillin sodium into cerebrospinal fluid in neurosurgical patients. Jpn J Antibiot. 1994;47(1):93–101.

160. Huh Y, Ju MS, Park H, Han S, Bang YM, Ferris CF, et al. Clavulanic acid protects neurons in pharmacological models of neurodegenerative diseases. Drug Dev Res [Internet]. 2010;71(6):351–7. Available from: http://apps.isiknowledge.com/full_record.do?product=WOS&search_mode=Refine&qid=11&SID=S2mcK1@77dpaPIFo4kD&page=6&doc=255

161. Centers for Disease Control and Prevention. Cerebral Palsy (CP) [Internet]. [cited 2016 May 2]. Available from: http://www.cdc.gov/ncbddd/cp/

162. Kancherla V, Amendah DD, Grosse SD, Yeargin-Allsopp M, Van Naarden Braun K. Medical expenditures attributable to cerebral palsy and intellectual disability among Medicaid-enrolled children. Res Dev Disabil [Internet]. Elsevier Ltd; 2012;33(3):832–40. Available from: http://dx.doi.org/10.1016/j.ridd.2011.12.001

163. Shen Y, Plane JM, Deng W. Mouse models of periventricular leukomalacia. J Vis Exp. 2010;(May):1–4.

164. Clancy B, Darlington RB, Finlay BL. Translating developmental time across mammalian species. Neuroscience. 2001;105(1):7–17.

165. Girard S, Kadhim H, Beaudet N, Sarret P, S??bire G. Developmental motor deficits induced by combined fetal exposure to lipopolysaccharide and early neonatal hypoxia/ischemia: A novel animal model for cerebral palsy in very premature infants. Neuroscience. 2009;158(2):673–82.

166. Torp R, Lekieffre D, Levy LM, Haug FM, Danbolt NC, Meldrum BS, et al. Reduced postischemic expression of a glial glutamate transporter, GLT1, in the rat hippocampus. Exp brain Res [Internet]. 1995;103(1):51–8. Available from: http://www.ncbi.nlm.nih.gov/pubmed/7615037

167. Lehre KP, Levy LM, Storm-mathisen J, Ottersen OP, Danbolt NC. Differential Expression Rat Brain : Quantitative of Two Glial Glutamate and lmmunocytochemical Transporters in the Observations. 1995;(March).

168. Chaudhry FA, Lehre KP, Campagne MVL, Ottersen OP, Danbolt NC, Storm-mathisen J. Glutamate Transporters in Glial Plasma Membranes : Highly Differentiated Localizations Revealed by Quantitative Ultrastructural Immunocytochemistry. 1995;15:711–20.

169. Feather-Schussler DN, Ferguson TS. A Battery of Motor Tests in a Neonatal Mouse Model of Cerebral Palsy. J Vis Exp. 2016;(e53569).

170. Fox M. Reflex-ontogeny and behavioral development of the mouse. Anim Behav. 1965;13:234–41.

171. Heyser CJ. Assessment of developmental milestones in rodents. Curr Protoc Neurosci / Editor board, Jacqueline N Crawley [et al]. 2003;Chapter 8:Unit 8.18.

172. Wahlsten D. A developmental time scale for postnatal changes in brain and behavior of B6D2F2 mice. 1974;72:251–64.

173. Williams E, Scott JP. The Development of Social Behavior Patterns in the Mouse, in Relation to Natural Periods. Behaviour. 1953;6(1):35–65.

174. El-Khodor B. Behavioral Phenotyping for Neonates: Hind Limb Suspension Test (a.k.a. Tube Test). Treat-NMD. 2011;

175. Didonato C. Behavioral Phenotyping for neonates: Righting reflex. Treat-NMD. 2011;(2).

176. Hill J, Lim M, Stone M. Developmental milestones in the newborn mouse. In: Gozes I, editor. Neuropeptide Techniques. Totowa, NJ, USA: Human Press Inc.; 2007. p. 131–49.

177. Wahlsten D. Mouse Behavioral Testing. Elsevier Inc.; 2011.

178. Stanford Behavioral and Functional Neuroscience Laboratory [Internet]. Stanford Medicine. 2016 [cited 2011 Feb 10]. Available from: http://sbfnl.stanford.edu/

179. Lalonde R, Hayzoun K, Selimi F, Mariani J, Strazielle C. Motor coordination in mice with hotfoot, Lurcher, and double mutations of the Grid2 gene encoding the delta-2 excitatory amino acid receptor. Physiol Behav. 2003;80(2-3):333–9.

180. Buitrago MM, Schulz JB, Dichgans J, Luft AR. Short and long-term motor skill learning in an accelerated rotarod training paradigm. Neurobiol Learn Mem. 2004;81(3):211–6.

181. Brooks SP, Dunnett SB. Tests to assess motor phenotype in mice: a user's guide. Nat Rev Neurosci [Internet]. Nature Publishing Group; 2009;10(7):519–29. Available from: http://www.nature.com/doifinder/10.1038/nrn2652

182. Robinson MB. Examination of Glutamate Transporter Heterogeneity Using Synaptosomal Preparations. Methods Enzymol. 1998;296:189–202.

183. Schmued LC, Stowers CC, Scallet AC, Xu L. Fluoro-Jade C results in ultra high resolution and contrast labeling of degenerating neurons. Brain Res. 2005;1035(1):24–31.

184. Stain CV. Cresyl violet stain. 2013;1–4. Available from: neurosciencecourses.com

185. Pakkenberg B, Gundersen HJ. Total number of neurons and glial cells in human brain nuclei estimated by the disector and the fractionator. J Microsc [Internet]. 1988;150(Pt 1):1–20. Available from: http://www.ncbi.nlm.nih.gov/pubmed/3043005

186. COULIN C, DRAKEW A, FROTSCHER M, DELLER T. Stereological estimates of total neuron numbers in the hippocampus of adult reeler mutant mice: Evidence for an increased survival of Cajal-Retzius cells. J Comp Neurol. 2001;439(1):19–31.

187. Sanna F, Melis MR, Angioni L, Argiolas A. Clavulanic acid induces penile erection and yawning in male rats: Comparison with apomorphine. Pharmacol Biochem Behav [Internet]. Elsevier Inc.; 2013;103(4):750–5. Available from: http://dx.doi.org/10.1016/j.pbb.2012.12.001

188. Schroeder J, Tolman N, McKenna F, Watkins K, Passeri S, Hsu A, et al. Clavulanic acid reduces rewarding, hyperthermic and locomotor-sensitizing effects of morphine in rats: A new indication for an old drug? Drug Alcohol Depend. 2014;142:41–5.

189. Bax MC. Terminology and Classification of Cerebral Palsy. Dev Med Child Neurol. 1964;6:295–7.

190. Brogren E, Forssberg H, Hadders-Algra M. Influence of two different sitting positions on postural adjustments in children with spastic diplegia. Dev Med Child Neurol. 2001;43(8):534–46.

191. Liu W-Y, Zaino CA, McCoy SW. Anticipatory postural adjustments in children with cerebral palsy and children with typical development. Pediatr Phys Ther. 2007;19(3):188–95.

192. Heyrman L, Desloovere K, Molenaers G, Verheyden G, Klingels K, Monbaliu E, et al. Clinical characteristics of impaired trunk control in children with spastic cerebral palsy. Res Dev Disabil [Internet]. Elsevier Ltd; 2013;34(1):327–34. Available from: http://dx.doi.org/10.1016/j.ridd.2012.08.015

193. Uvebrant P. Hemiplegic Cerebral Palsy Aetiology and Outcome. J Chem Inf Model. 1988;53:1689–99.

194. Golomb MR, Garg BP, Saha C, Azzouz F, Williams LS. Cerebral Palsy After Perinatal Arterial Ischemic Stroke. J Child Neurol [Internet]. 2008;23(3):279–86. Available from: http://jcn.sagepub.com/cgi/doi/10.1177/0883073807309246

195. Damiano DL, Abel MF. Functional outcomes of strength training in spastic cerebral palsy. Arch Phys Med Rehabil. 1998;79(2):119–25.

196. Bulman-Fleming MB, Bryden MP, Rogers TT. Mouse paw preference: Effects of variations in testing protocol. Behav Brain Res. 1997;86:79–87.

197. Ostensjø S, Carlberg EB, Vøllestad NK. Everyday functioning in young children with cerebral palsy: functional skills, caregiver assistance, and modifications of the environment. Dev Med Child Neurol. 2003;45(9):603–12.

198. Huang Z, Liu J, Cheung PY, Chen C. Long-term cognitive impairment and myelination deficiency in a rat model of perinatal hypoxic-ischemic brain injury. Brain Res [Internet]. Elsevier B.V.; 2009;1301:100–9. Available from: http://dx.doi.org/10.1016/j.brainres.2009.09.006

199. Toomela A. Short-term memory in young adults with spastic diplegic cerebral palsy. Dev Neuropsychol [Internet]. 2012;37(4):317–32. Available from: http://www.ncbi.nlm.nih.gov/pubmed/22612544

200. Holck P, Nettelbladt U, Sandberg AD. Children with cerebral palsy, spina bifida and pragmatic language impairment: Differences and similarities in pragmatic ability. Res Dev Disabil [Internet]. Elsevier Ltd; 2009;30(5):942–51. Available from: http://dx.doi.org/10.1016/j.ridd.2009.01.008

201. Nashner L, Shumway-Cook A, Marin O. Stance Posture Control in Select Groups of Children with Cerebral Palsy: Deficits in Sensory Organization and Muscular Coordination. Exp Brain Res. 1983;49:393–409.

202. Santamaria V, Rachwani J, Saavedra S, Woollacott M. Effect of Segmental Trunk Support on Posture and Reaching in Children With Cerebral Palsy. Pediatr Phys Ther [Internet]. 2016;28(3):285–93. Available from: http://content.wkhealth.com/linkback/openurl?sid=WKPTLP:landingpage&an=00001577-201628030-00006

203. Heyrman L, Feys H, Molenaers G, Jaspers E, Monari D, Meyns P, et al. Three-dimensional head and trunk movement characteristics during gait in children with spastic diplegia. Gait Posture [Internet]. Elsevier B.V.; 2013;38(4):770–6. Available from: http://dx.doi.org/10.1016/j.gaitpost.2013.03.019

204. Nichol P, Corliss R, Yamada S, Shiota K, Saijoh Y. Muscle Patterning in Mouse and Human Abdominal Wall Development and Omphalocele Specimens of Humans. Anat Rec. 2012;295(12):2129–40.

205. Brossard-Racine M, Hall N, Majnemer A, Shevell MI, Law M, Poulin C, et al. Behavioural problems in school age children with cerebral palsy. Eur J Paediatr Neurol [Internet]. Elsevier Ltd; 2012;16(1):35–41. Available from: http://dx.doi.org/10.1016/j.ejpn.2011.10.001

206. Weber P, Bolli P, Heimgartner N, Merlo P, Zehnder T, Kätterer C. Behavioral and emotional problems in children and adults with cerebral palsy. Eur J Paediatr Neurol [Internet]. 2016;0:2–6. Available from:

http://www.ncbi.nlm.nih.gov/pubmed/26748599

207. Almeida a, gado-Esteban M, Bolanos JP, Medina JM. Oxygen and glucose deprivation induces mitochondrial dysfunction and oxidative stress in neurones but not in astrocytes in primary culture. J Neurochem [Internet]. 2002;81(2):207–17. Available from: http://dx.doi.org/10.1046/j.1471-4159.2002.00827.x\nhttp://onlinelibrary.wiley.com/store/10.1046/j.1471-4159.2002.00827.x/asset/j.1471-4159.2002.00827.x.pdf?v=1&t=hz2hhcai&s=075957bd677ae5e8dd93797c9e2764b0d9b36c2f

208. Lukaszevicz A-C, Sampaïo N, Guégan C, Benchoua A, Couriaud C, Chevalier E, et al. High sensitivity of protoplasmic cortical astroglia to focal ischemia. J Cereb Blood Flow Metab. 2002;22:289–98.

209. Raghavendra Rao VL, Dogan A, Todd KG, Bowen KK, Kim BT, Rothstein JD, et al. Antisense knockdown of the glial glutamate transporter GLT-1, but not the neuronal glutamate transporter EAAC1, exacerbates transient focal cerebral ischemia-induced neuronal damage in rat brain. J Neurosci. 2001;21(6):1876–83.

210. Chen J, Hsu-chou H, Lu J, Chiang Y, Huang H, Wang H, et al. Down-regulation of the glial glutamate transporter GLT-1 in rat hippocampus and striatum and its modulation by a group III metabotropic glutamate receptor antagonist following transient global forebrain ischemia. Neuropharmacology. 2005;49:703–14.

211. Raghavendra Rao VL, Muralikrishna A, Dogan A, Bowen KK, Hatcher J, Rothstein D, et al. Glial glutamate transporter GLT-1 down-regulation precedes delayed neuronal death in gerbil hippocampus following transient global cerebral ischemia. Neurochem Int. 2000;36:531–7.

212. Martin LJ, Brambrink AM, Lehmann C, Portera-Cailliau C, Koehler R, Rothstein J, et al. Hypoxia-ischemia causes abnormalities in glutamate transporters and death of astroglia and neurons in newborn striatum. Ann Neurol [Internet]. 1997 Sep [cited 2015 Nov 1];42(3):335–48. Available from: http://www.ncbi.nlm.nih.gov/pubmed/9307255

213. Nagae LM, Hoon Jr. AH, Stashinko E, Lin D, Zhang W, Levey E, et al. Diffusion tensor imaging in children with periventricular leukomalacia: variability of injuries to white matter tracts. AJNR Am J Neuroradiol [Internet]. 2007;28(7):1213–22. Available from: http://www.ncbi.nlm.nih.gov/pubmed/17698519

214. Yang Y, Rothstein J. Astrocytes in (Patho)Physiology of the Nervous System: Specialized Neurotransmitter Transporters in Astrocytes. Vladimir P, Haydon P, editors. New York: Springer Science+Business Media LLC; 2009. 69-105 p.

215. DANILOV CA, FISKUM G. Hyperoxia Promotes Astrocyte Cell Death After Oxygen and Glucose Deprivation. Glia. 2008;56(7):801–8.

216. Ouyang Y-B, Voloboueva LA, Xu L-J, Giffard RG. Selective Dysfunction of Hippocampal CA1 Astrocytes Contributes to Delayed Neuronal Damage after Transient Forebrain Ischemia. J Neurosci [Internet]. 2007;27(16):4253–60. Available from: http://www.jneurosci.org/cgi/doi/10.1523/JNEUROSCI.0211-07.2007

217. Henn FA, Anderson DJ, Rustad DG. Glial contamination of synaptosomal fractions. Brain Res. 1976;101:341–4.

218. Weller ML, Stone IM, Goss A, Rau T, Rova C, Poulsen DJ. Selective Over Expression Of EAAT2 In Astrocytes Enhances Neuroprotection From Moderate But Not Severe Hypoxia- Ischemia. Neuroscience. 2008;15(10):1203–14.

219. Rimmele TS, Rosenberg PA. GLT-1: The elusive presynaptic glutamate transporter. Neurochem Int [Internet]. Elsevier Ltd; 2016; Available from: http://www.ncbi.nlm.nih.gov/pubmed/27129805

220. Gundersen V, Danbolt NC, Ottersen OP. Demonstration of glutamate/aspartate uptake activity in nerve endings by use of antibodies recognizing exogenous D-aspartate. 1993;57(1):97–111.

221. Williams S., Macnab LT, Pow DV. Cryptic expression of functional glutamate transporters in the developing rodent brain. Neuron Glia Biol. 2006;2:199–215.

222. Yeh T-H, Hwang H-M, Chen J-J, Wu T, Li AH, Wang H-L. Glutamate transporter function of rat hippocampal astrocytes is impaired following the global ischemia. Neurobiol Dis [Internet]. 2005;18(3):476–83. Available from: http://www.sciencedirect.com/science/article/pii/S0969996104003225

223. Ketheeswaranathan P, Turner NA, Spary EJ, Batten TFC, McColl BW, Saha S. Changes in glutamate transporter expression in mouse forebrain areas following focal ischemia. Brain Res [Internet]. Elsevier B.V.; 2011;1418:93–103. Available from: http://dx.doi.org/10.1016/j.brainres.2011.08.029

224. Bruhn T, Levy LM, Nielsen M, Christensen T, Johansen FF, Diemer NH. Ischemia induced changes in expression of the astrocyte glutamate transporter GLT1 in hippocampus of the rat. Neurochem Int [Internet]. 2000;37(2-3):277–85. Available from: http://www.ncbi.nlm.nih.gov/pubmed/10812213

225. Zelenaia OA, Robinson MB. Degradation of Glial Glutamate Transporter mRNAs Is Selectively Blocked by Inhibition of Cellular Transcription. 2000;1:2252–8.

226. Thöne-Reineke C, Neumann C, Namsolleck P, Schmerbach K, Krikov M, Schefe JH, et al. The beta-lactam antibiotic, ceftriaxone, dramatically improves survival, increases glutamate uptake and induces neurotrophins in stroke. J Hypertens [Internet]. 2008;26(12):2426–35. Available from: http://www.ncbi.nlm.nih.gov/pubmed/19008722

227. Lipski J, Wan CK, Bai JZ, Pi R, Li D, Donnelly D. Neuroprotective potential of ceftriaxone in in vitro models of stroke. Neuroscience [Internet]. 2007 [cited 2015 Nov 1];146:617–29. Available from: http://ac.els-cdn.com.libproxy.temple.edu/S0306452207001583/1-s2.0-S0306452207001583-main.pdf?_tid=963ed71c-80f2-11e5-acf3-00000aab0f02&acdnat=1446421689_e8cfa1a98a11d182fe48137d82e7af52

228. Lee S, Su Z-Z, Emdad L, Gupta P, Sarkar D, Borjabad A, et al. Mechanism of ceftriaxone induction of excitatory amino acid transporter-2 expression and glutamate uptake in primary human astrocytes. J Biol Chem [Internet]. 2008;283(19):13116–23. Available from: http://www.pubmedcentral.nih.gov/articlerender.fcgi?artid=2442320&tool=pmcentrez&rendertype=abstract

229. Feng D, Wang W, Dong Y, Wu L, Huang J, Ma Y, et al. Ceftriaxone alleviates early brain injury after subarachnoid hemorrhage by increasing excitatory amino acid transporter 2 expression via the PI3K/Akt/NF-kB signaling pathway. Neuroscience. 2014;268:21–32.

230. Dugan L, Choi D. Excitotoxic injury in Hypoxia-Ischemia. In: iegel GJ, Agranoff BW, Albers RW, et al. E, editor. Basic Neurochemistry: Molecular, Cellular and Medical Aspects [Internet]. 6th editio. Philadelphia: Lippincott-Raven; 1999. Available from: http://www.ncbi.nlm.nih.gov/books/NBK27972/

231. Kost G, Selvaraj S, Lee Y, Kim D, Ahn C, Singh B. Clavulanic acid inhibits MPP+-induced ROS generation and subsequent loss of dopaminergic cells. Brain Res. 2012;1469:129–35.

232. Sarco DP, Becker J, Palmer C, Sheldon RA, Ferriero DM. The neuroprotective effect of deferoxamine in the hypoxic-ischemic immature mouse brain. Neurosci Lett. 2000;282(1-2):113–6.

233. Ji HF, Shen L, Zhang HY. Beta-Lactam antibiotics are multipotent agents to combat neurological diseases. Biochem Biophys Res Commun. 2005;333(3):661–3.

234. Mesters JR, Barinka C, Li W, Tsukamoto T, Majer P, Slusher BS, et al. Structure of glutamate carboxypeptidase II, a drug target in neuronal damage and prostate cancer. EMBO J. 2006;25(6):1375–84.

235. Luthi-Carter R, Berger U V, Barczak a K, Enna M, Coyle JT. Isolation and expression of a rat brain cDNA encoding glutamate carboxypeptidase II. Proc Natl Acad Sci U S A [Internet]. 1998;95(6):3215–20. Available from: http://www.pubmedcentral.nih.gov/articlerender.fcgi?artid=19722&tool=pmcentrez&rendertype=abstract

236. Bzdega T, Turi T, Wroblewska B, She D, Chung HS, Kim H, et al. Molecular Cloning of a Peptidase Against N-Acetylaspartylglutamate from a Rat

Hippocampal cDNA Library. J Neurochem [Internet]. 2002;69(6):2270–7. Available from: http://doi.wiley.com/10.1046/j.1471-4159.1997.69062270.x

237. Luthi-Carter R, Barczak a K, Speno H, Coyle JT. Molecular characterization of human brain N-acetylated alpha-linked acidic dipeptidase (NAALADase). J Pharmacol Exp Ther. 1998;286(2):1020–5.

238. Slusher BS, Vornov JJ, Thomas a G, Hurn PD, Harukuni I, Bhardwaj a, et al. Selective Inhibition of NAALADase, which Converts NAAG to Glutamate, Reduces Ischemic Brain Injury. Nat Med. 1999;5(12):1396–402.

239. Bacich DJ, Wozniak KM, Lu XCM, O'Keefe DS, Callizot N, Heston WDW, et al. Mice lacking glutamate carboxypeptidase II are protected from peripheral neuropathy and ischemic brain injury. J Neurochem. 2005;95(2):314–23.

240. Banani A, Maleki-Dizaji N, Garjani A, Mostafalou S, Ziaee M. Clavulanic acid exhibits anti-inflammatory effects on carrageenan-induced paw edema model of inflammation in rats. Ann Biol Res. 2012;3(7):3312–20.

241. Pasparakis M, Luedde T, Schmidt-Supprian M. Dissection of the NF-kappaB signalling cascade in transgenic and knockout mice. Cell Death Differ [Internet]. 2006;13(5):861–72. Available from: http://www.ncbi.nlm.nih.gov/pubmed/16470223

242. Justicia C, Ramos-Cabrer P, Hoehn M. MRI detection of secondary damage after stroke: Chronic iron accumulation in the thalamus of the rat brain. Stroke. 2008;39(5):1541–7.

243. Sapolsky R, Pulsinelli W. Glucocorticoids Potentiate Ischemic Injury to Neurons: Therapeutic Implications. Science (80-). 1985;229(4720):1397–400.

244. Aronowski J, Zhao X. Molecular pathophysiology of cerebral hemorrhage: Secondary brain injury. Stroke. 2011;42(6):1781–6.

245. Thornton C, Rousset CI, Kichev A, Miyakuni Y, Vontell R, Baburamani AA, et al. Molecular mechanisms of neonatal brain injury. Neurol Res Int. 2012;2012.

246. Cirstea M, Levin M. Compensatory strategies for reaching in stroke. Brain [Internet]. 2000;123:940–53. Available from: http://brain.oxfordjournals.org/content/123/5/940.abstract

247. Frost SB, Barbay S, Friel KM, Plautz EJ, Nudo RJ, Frost SB, et al. Reorganization of Remote Cortical Regions After Ischemic Brain Injury : A Potential Substrate for Stroke Recovery Reorganization of Remote Cortical Regions After Ischemic Brain Injury : A Potential Substrate for Stroke Recovery. J Neurophysiol. 2003;89:3205–14.

248. Donoghue JP, Suner S, Sanes JN. Dynamic organization of primary motor cortex

output to target muscles in\nadult rats. I. Long-term patterns of reorganization following motor or mixed\nperipheral nerve lesions. Exp Brain Res. 1990;79:492–503.

249. Matthews P, Phil D. Functional Brain Reorganization and Recovery after Injury to White Matter. In: Waxman S, editor. Multiple Sclerosis As A Neuronal Disease. Elsevier Academic Press; 2005. p. 451–66.

250. Brigidi G, Bamji S. Detection of Protein Palmitoylation in Cultured Hippocampal Neurons by Immunoprecipitation and Acyl-Biotin Exchange (ABE). J Vis Exp. 2013;72:e50031.

251. Barkovich AJ. The encephalopathic neonate: Choosing the proper imaging technique. Am J Neuroradiol. 1997;18(10):1816–20.

252. Di Battista AP, Buonora JE, Rhind SG, Hutchison MG, Baker AJ, Rizoli SB, et al. Blood Biomarkers in Moderate-To-Severe Traumatic Brain Injury: Potential Utility of a Multi-Marker Approach in Characterizing Outcome. Front Neurol [Internet]. 2015;6(May):110. Available from: http://www.pubmedcentral.nih.gov/articlerender.fcgi?artid=4443732&tool=pmcentrez&rendertype=abstract

253. Gazzolo D, Marinoni E, Di Iorio R, Lituania M, Marras M, Bruschettini M, et al. High maternal blood S100B concentrations in pregnancies complicated by intrauterine growth restriction and intraventricular hemorrhage. Clin Chem [Internet]. 2006 May 1 [cited 2015 Nov 1];52(5):819–26. Available from: http://www.clinchem.org/content/52/5/819.long

254. Di Battista AP, Rhind SG, Baker AJ. Application of blood-based biomarkers in human mild traumatic brain injury. Front Neurol [Internet]. 2013 Jan [cited 2015 Oct 24];4:44. Available from: http://www.pubmedcentral.nih.gov/articlerender.fcgi?artid=3640204&tool=pmcentrez&rendertype=abstract